การสังเคราะห์อนุพันธ์แมนโซโนนเพื่อเป็นสารต้านแบคทีเรีย

นางสาวริตา ฮิรานี

วิทยานิพนธ์นี้เป็นส่วนหนึ่งของการศึกษาตามหลักสูตรปริญญาวิทยาศาสตรมหาบัณฑิต
สาขาวิชาเคมี ภาควิชาเคมี
คณะวิทยาศาสตร์ จุฬาลงกรณ์มหาวิทยาลัย
ปีการศึกษา 2559

SYNTHESIS OF MANSONONE DERIVATIVES AS ANTIBACTERIAL AGENTS

Miss Rita Hairani

A Thesis Submitted in Partial Fulfillment of the Requirements
for the Degree of Master of Science Program in Chemistry
Department of Chemistry
Faculty of Science
Chulalongkorn University
Academic Year 2016

Thesis Title	SYNTHESIS OF MANSONONE DERIVATIVES AS ANTIBACTERIAL AGENTS
By	Miss Rita Hairani
Field of Study	Chemistry
Thesis Advisor	Assistant Professor Warinthorn Chavasiri, Ph.D.

Accepted by the Faculty of Science, Chulalongkorn University in Partial Fulfillment of the Requirements for the Master's Degree

.....Dean of the Faculty of Science
(Associate Professor Polkit Sangvanich, Ph.D.)

THESIS COMMITTEE

.....Chairman
(Associate Professor Vudhichai Parasuk, Ph.D.)

.....Thesis Advisor
(Assistant Professor Warinthorn Chavasiri, Ph.D.)

.....Examiner
(Assistant Professor Pattara Thiraphibundet, Ph.D.)

.....External Examiner
(Assistant Professor Veena Nukoolkarn, Ph.D.)

ริตา ฮิรานี : การสังเคราะห์อนุพันธ์แมนโซโนนเพื่อเป็นสารต้านแบคทีเรีย (SYNTHESIS OF MANSONONE DERIVATIVES AS ANTIBACTERIAL AGENTS) อ.ที่ปรึกษาวิทยานิพนธ์หลัก: ผศ. ดร.วรินทร ชวศิริ, 151 หน้า.

ได้ทดสอบฤทธิ์ต้านแบคทีเรียของสาร 7 ชนิดที่แยกจากสิ่งสกัดหยาบไดคลอโรมีเทนของแก่นไม้จันทน์ชะมด *Mansonia gagei* Drumm. คือ mansorin A (1), mansorin B (2), mansorin C (3), mansonone C (4), mansonone E (5), mansonone G (6), และ mansonone H (7) ต่อเชื้อ *Staphylococcus aureus* ATCC 25923, *Streptococcus mutans* ATCC 25175, *Streptococcus sobrinus* KCCM 11898, *Propionibacterium acnes* KCCM 41747 และ *Salmonella typhi* ATCC 422 พบว่า 6 แสดงฤทธิ์ที่ดี และเนื่องจากพบในปริมาณมากจึงได้สังเคราะห์อนุพันธ์ของ mansonone G (G01 – G20) โดยดัดแปรหมู่ไฮดรอกซีที่ตำแหน่ง C6 และนำไปทดสอบฤทธิ์การต้านแบคทีเรีย ทั้งนี้อนุพันธ์ G02 – G20 ได้ถูกสังเคราะห์ขึ้นเป็นครั้งแรก อนุพันธ์ของ mansonone G ส่วนใหญ่มีฤทธิ์ต้านแบคทีเรียดีกว่า 6 ซึ่งได้จากธรรมชาติ อนุพันธ์ G07 และ G08 ให้ค่า MIC ต่ำกว่า 6 ถึง 64 เท่า นอกจากนี้ได้ทดสอบฤทธิ์ต้านกระบวนการสร้างไขมัน พบว่า 4 และ 6 สามารถยับยั้งกระบวนการสร้างเซลล์ไขมันชนิด 3T3-L1 pre-adipocytes และเมื่อนำอนุพันธ์ G15, G16 และ G17 มาทดสอบและศึกษากลไก พบว่าอนุพันธ์เหล่านี้มีฤทธิ์ต้านกระบวนการสร้างไขมันเนื่องจากสามารถยับยั้งการผลิตสาร adiponectin.

ภาควิชา เคมี ลายมือชื่อนิสิต .....

สาขาวิชา เคมี ลายมือชื่อ อ.ที่ปรึกษาหลัก .....

ปีการศึกษา 2559

5672207423 : MAJOR CHEMISTRY
KEYWORDS: MANSONIA GAGEI DRUMM. / MANSONONES / MANSONONE DERIVATIVES / ANTIBACTERIAL ACTIVITY / ANTI-ADIPOGENIC ACTIVITY

RITA HAIRANI: SYNTHESIS OF MANSONONE DERIVATIVES AS ANTIBACTERIAL AGENTS. ADVISOR: ASST. PROF. WARINTHORN CHAVASIRI, Ph.D., 151 pp.

Seven compounds isolated from the CH_2Cl_2 extract of *Mansonia gagei* Drumm. heartwoods, *i.e.* mansorin A (1), mansorin B (2), mansorin C (3), mansonone C (4), mansonone E (5), mansonone G (6), and mansonone H (7), were evaluated for their antibacterial activities towards *Staphylococcus aureus* ATCC 25923, *Streptococcus mutans* ATCC 25175, *Streptococcus sobrinus* KCCM 11898, *Propionibacterium acnes* KCCM 41747, and *Salmonella typhi* ATCC 422. 6 displayed good activity and was obtained in large amount among other mansonones, therefore some derivatives of mansonone G were carried out and their antibacterial activity were evaluated. Twenty mansonone G derivatives (G01 – G20) were obtained by modified the hydroxyl group at C6 of 6. Among these derivatives, G02 – G20 were identified as new semisynthetic compounds. In antibacterial activity, most of mansonone G derivatives showed better activity than 6. G07 and G08 displayed sixty-four times lower in MIC than its natural 6. Moreover, anti-adipogenic activity was also performed to all compounds. 4 and 6 possessed the suppression in 3T3-L1 pre-adipocytes differentiation. The suppression were also observed by G15, G16, and G17. Further investigation on their mechanism indicated that G15, G16, and G17 had potential activity in adipogenesis by suppressing the production of adiponectin.

Department: Chemistry Student's Signature .....
Field of Study: Chemistry Advisor's Signature .....
Academic Year: 2016

ACKNOWLEDGEMENTS

The author would like to express her gratitude towards Allah the almighty for all the grace and wonderful life that she got. She also would like to express appreciation to her advisor Assistant Professor Warinthorn Chavasiri Ph.D. for his advice, guidance and encouragement throughout the course of this research.

Appreciations were given to Asean Scholarship Chulalongkorn University 2013 which was supported her financially, throughout the course and Beasiswa Kaltim Cemerlang 2015 for supporting her financially at the end of her course time. The author also thankful for the experience that has been given to her for conducted research experience at Ewha Womans University which was financially supported by Overseas Research Experience Scholarship from Graduate School Chulalongkorn University. Appreciation was given to Thesis Grant Scholarship, for its funding support to author thesis research.

Author would extend her gratitude to Professor Eun Sook Hwang, from College of Pharmacy & Graduate School of Pharmaceutical Sciences at Ewha Womans University for her guidance while author doing her research experience in South Korea. Furthermore, author appreciation has been given to the Head of Department of Chemistry Associate Professor Vudichai Parasuk, Ph.D. Chulalongkorn University for his kindness and help. Author would also like to thank to all of committee members for their time and suggestion during final presentation.

Appreciation was given by author to Department of Chemistry staff member, for their assistance during the course time. To all members in Natural Product Research Unit and WC laboratory member, author are grateful for the experience and help that given to her during the research time. Respect and love to author family for their support and love during this course. Lastly, author would like to express her gratitude towards all of her friends for their endless support during her study in Chulalongkorn University.

CONTENTS

Page

Page

Page

Page

List of Tables

Table Page

List of Figures

Figure Page

Figure Page

Figure Page

List of Schemes

List of Abbreviations

AA	=	acrylamide
ADW	=	autoclaved deionized water
APS	=	ammonium persulfate
ATCC	=	American Type Culture Collection
β	=	beta
$BaCl_2$	=	barium chloride
BCS	=	Bovine Calf Serum
BSA	=	Bovine Serum Albumin
δ	=	delta
℃	=	degree celcius
CFU	=	colony-forming unit
$CDCl_3$	=	chloroform-d
CH_2Cl_2	=	dichloromethane
CH_3I	=	methyl iodide
C_2H_5Br	=	ethyl bromide
C_4H_9Br	=	1-bromobutane
$C_8H_{17}Br$	=	1-bromooctane
$C_{12}H_{25}Br$	=	1-bromododecane
CO_2	=	carbondioxide
d	=	doublet
dd	=	doublet of doublet
DMSO	=	dimethylsulfoxide
DMEM	=	Dulbecco's Modified Eagle's Medium
DTT	=	dithiothreitol
DW	=	deionized water
ECL	=	enhanced chemiluminescence
ESI	=	electron spray ionization
EtOAc	=	ethyl acetate

EtOH = ethanol

FBS = Fetal Bovine Serum

g = gram

h = hour

HCl = hydrochloric acid

HRMS = high resolution mass spectra

H_2SO_4 = sulphuric acid

Hz = hertz

kg = kilogram

K_2CO_3 = potassium carbonate

KCCM = Korean Culture Center of Microorganisms

L = Liter

m = multiplet

mA = milli ampere

MeI = methyl iodide

MeOH = methanol

mg = milligram

µg = microgram

min = minute/minutes

mL = milliliter

µL = microliter

mm = millimeter

mmol = millimol

mM = millimolar

µM = micromolar

MF = Mac Farland

MHz = megahertz

MIC = minimum inhibitory concentration

MS = Mass Spectrophotometry

$NaHCO_3$ = sodium bicarbonate

NaOH = sodium hydroxide

Na_2SO_4 = sodium sulfate

Na_3VO_4 = sodium orthovanadate

NC = nitrocellulose

nm = nanometer

NMR = Nuclear Magnetic Resonance

ORO = oil red O

PAGE = polyacrylamide gel

PBS = Phosphate Buffer Saline

PMSF = phenylmethylsulfonyl fluoride

PPh_3 = triphenylphospine

rpm = revolution per minute

s = singlet

sec = second

SDS = sodium dodecyl sulfate

TBST = Tris-buffered saline, 0.1% Tween 20

TEMED = tetramethylethylenediamine

TLC = Thin Layer Chromatography

V = voltage

CHAPTER I
INTRODUCTION

Nature has provided many things for humankind, including a source of therapeutic agents for thousands of years, which could obtain from plants, lichens, fungi, bacteria, algae, and animals. More than 50% of all the drugs in clinical use in the world are derived from natural products and their derivatives.[1] The term of natural products refers to secondary metabolites which are derived and isolated from natural sources.[2] Secondary metabolites are defined as chemical constituents which have a much more limited distribution in nature and can be obtained in only specific organisms or groups of organisms.[3] These metabolites are produced within the organisms and can be presumed as products of biochemical "side tracks" in the cells of organism and not required for daily functioning of the organism.[4] In consequence, secondary metabolites have many biological activities, thus, they have been used in traditional medicine treatment for centuries, and currently in cosmetics, fine chemicals, nutraceuticals, and pharmaceuticals.[5]

Plants, as one of natural products sources, have established the foundation of sophisticated traditional medicine systems and according to the earliest records from around 2900-2600 BCE, there were approximately 1000 plant-derived substances used in traditional medicine systems.[6] Moreover, the great civilizations of the ancient Chinese, Indians, and North Africans had documented the written evidence of the use of plants in wide variety of diseases treatments.[7] Up to now, the enormous majority of people still rely on their traditional medicinal plants for their daily healthcare needs.[8] Medicinal plants continue to be the main source of medication in developing countries.[9]

1.1 Naturally Occurring Naphthoquinones

One of secondary metabolites groups which widely can be found in nature are naphthoquinones. These compounds are known to have many biological activities and can be produced by many types of higher plants, fungi, animals, and microorganisms.[10, 11] Several pharmacological properties of naphthoquinones such as anticancer, antifungal, antimicrobial, antiviral, and antimalarial have been investigated.[12-16] The concern in these compounds has been expanded in recent years due to their pharmacological properties and the variety of their structural.[17]

Naphthoquinones are simple compounds having C_6–C_4 skeleton or naphthalene nucleus with two carbonyl groups on one nucleus and highly relative small molecules which have a diverse distribution in nature.[18, 19] There are two types of naphthoquinones *i.e.* 1,2-naphthoquinone (naphthalene skeleton substitute in position C1 and C2) and 1,4-naphthoquinone (naphthalene skeleton substitute in position C1 and C4).[18, 20]

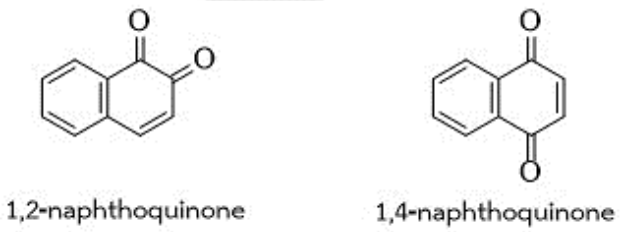

Figure 1.1 Core structures of 1,2 and 1,4-naphthoquinones

As well as their monomers, typical 1,2-naphthoquinones (*ortho*-naphthoquinones) and 1,4-naphthoquinones (*para*-naphthoquinones) were isolated from natural products as dimer, trimer, and tetramer.[21-23] In addition, their furano and pyrano derivatives could also be obtained from natural products.[18]

Mostly, naphthoquinones are colored compounds (yellow, orange, and brown), and hence, they are important in dye pigmentation. In addition, they are usually soluble in acetic acid, acetone, alcohol, benzene, chloroform, and dimethyl sulfoxide, while some others are slightly soluble in hot water.[20]

In nature, mainly naphthoquinones can be found in plants in which the biosynthesis can occur *via* variety of pathways including the acetate-malonate pathway, shikimate-succinyl CoA combined pathway and the shikimate-mevalonate pathway.[20] Some naphthoquinones are derived from pentaketides, hexaketides, and heptaketides.[19].

Naturally occurring naphthoquinones which have been determined in some families of plants such as Avicenniaceae, Bignoniaceae, Boraginaceae, Droseraceae, Ebenaceae, Juglandaceae, Nephentaceae, and Plumbaginaceae, mostly are typical 1,4-naphthoquinones such as plumbagin, juglone, and lawsone.[20] The biological activities of these compounds have been investigated.

Plumbagin (5-hydroxy-2-methyl-1,4-naphthoquinone) is a naturally occurring yellow pigment isolated from the plants in Plumbaginaceae, Drosceraceae, Ancistrocladaceae, and Dioncophyllaceae families.[24] According to de Paiva and coworkers, plumbagin isolated from *Plumbago scandens*, exhibited relatively specific activity against *Staphylococcus aureus*.[25] In addition, another study also reported that plumbagin isolated from *P. zeylanica* displayed activity as a drug for various bacterial infectious diseases.[26] This compound also has been reported exerted anticancer activity on non-small cell lung cancer, antidepressant-like activity in unstressed and stressed mice.[27, 28] Another pharmacological properties of this compound such as anti-inflammatory and anti-fibrotic activities have also been evaluated.[24, 29, 30]

Juglone (5-hydroxy-1,4-naphthoquinone), obtained from the red wood (*Caesalpinia sappan*), was found to exhibit strong inhibition against some oral pathogens such as *Porphyromonas sp.*, *Streptococcus mutans*, *Actinobacillus viscosus*, *Streptococcus sobrinus*, and *Streptococcus salivarius.*[31] Another study reported that juglone isolated from *Juglans mandschurica* Maxim possessed antiproliferative and antitumor effects.[32, 33]

Lawsone (2-hydroxy-1,4-naphthoquinone), a natural pigment present in *Lawsonia inermis* or henna leaves, has been used since the Bronze Age for dying fingernails, hair, skin (including body art), leather, silk, and wool.[34] The antibacterial activity of this compound has been reported showing good antibacterial activity against two Gram-positive bacteria.[35] In addition, lawsone also reported to display remarkable inhibitory activity on the oxidative burst response of the whole blood, polymorphonuclear cells.[36]

Lapachol (2-hydroxy-3-(3'-methyl-2'-butenyl)-1,4-naphthoquinone) is a natural pigment isolated from *Tabebuia spp.*, Bignoniaceae family, has been investigated for its antimicrobial activity.[37, 38] This compound also can be found in other plant families such as Verbenaceae, Proteaceae, Leguminosae, and Sapotaceae.[39] It was known that lapachol exhibited anti-inflammatory effect, anthelmintic activity against *Toxocara canis* larvae, and anticancer activity.[40-42]

Shikonin, another typical 1,4-naphthoquinone, is a major bioactive compound isolated from Zicao (purple gromwell) or the dried root of *Lithospermum erythrorhizon* which usually used as a component of Chinese herbal medicine.[43] The antibacterial of shikonin has been evaluated and it showed that this compound exhibits greatest antibacterial activity towards *Pseudomonas aeruginosa*, *Escherichia coli*, *Staphylococcus aureus*, and *Klebsiella pneumonia*. This compound has been investigated for its anti-HIV therapeutic agent, anticancer agent.[43] Its anti-adipogenic activity was also been investigated and found that shikonin inhibits fat accumulation in 3T3-L1 adipocytes.[44] Moreover its mechanism study was also investigated and resulted that shikonin can inhibits adipogenesis by the modulation of WNT/β-catenin pathway, by blocking the mir-34a-FKBP1B pathway which signifies a promising potential agent to prevent obesity, by suppression of ERK 1/2 phosphorylation during the early stages of adipocyte differentiation in 3T3-L1 cells.[45-47] Other study also reported its anti-adipogenic mechanism study *via* the modulation of adipogenesis, lipogenesis, and β-oxidation *in vivo*.[48]

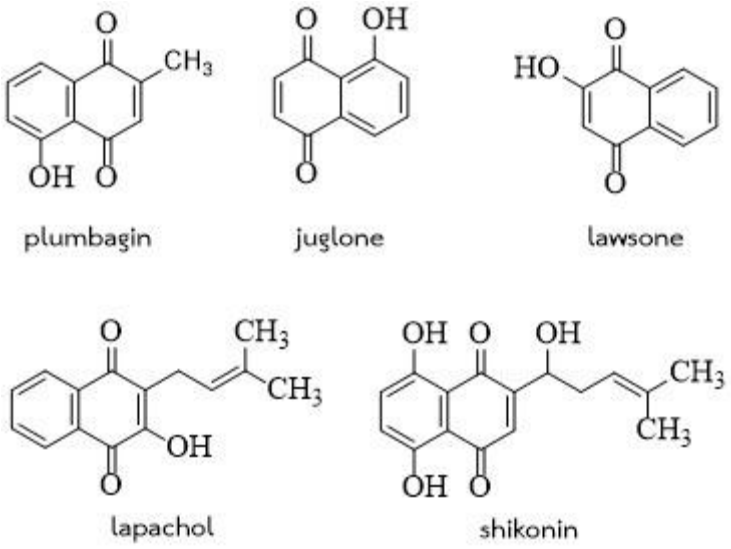

Figure 1.2 Some natural 1,4-naphthoquinones

Several typical 1,2-napthoquinones have also been isolated from various plant families. A natural tetrahydropyran-fused 1,2-naphthoquinone named β-lapachone (3,4-dihydro-2,2-dimethyl-2H-naphthol[1,2-b]pyran-5,6-dione) could be attained from the heartwood of Bignoniaceae and Verbanaceae families.[49] β-lapachone was known as a natural derivative of lapachol which presented in a small amount in the woods of Lapacho tree or *Tabebuia* spp. (Bignoniaceae family) and also can be obtained from the synthesis of lapachol through the cyclization of the prenyl side chain of lapachol.[40] This compound is known to have antimicrobial activity and possess the most effective against *S. aureus* strains.[50] Other studies also reported that this compound exhibited potential anti-anthelmintic, anticancer, antitumor, anti-inflammatory, antiplasmodial, and anti-*Trypanosoma cruzi* activities.[40, 51-55]

Another compound which has similar structure with β-lapachone is named biflorin (6,9-dimethyl-3-(4-methyl-3-pentenyl)naphtha[1,8-bc]pyran-7,8-dione).[56] This compound is known as a prenylated 1,2-naphthoquinone, isolated from the roots of *Capraria biflora* L., a perennial shrub belonging to Schophulariaceae family.[56-59] In addition, a dimer of biflorin (bisflorin) was also obtained from this species.[59] The antibacterial activity of biflorin has been investigated using the microdilution method for evaluating the minimum inhibitory concentration (MIC) against six bacterial strains

including Gram-positive and Gram-negative bacteria.[17] Moreover, some biological activities of this compound have also been investigated such as antitumor, cytotoxicity, and antimutagenic activities.[58, 60, 61]

Dunnione, a natural dehydrofuran-fused 1,2-naphthoquinone, was first isolated from the leaves of *Streptocarpus dunnii* Mast., along with dehydrodunnione, 7-hydroxydunnione, and 8-hydroxydunnione.[62, 63] This compound exhibited an unusually broad spectrum antifungal activity.[64]

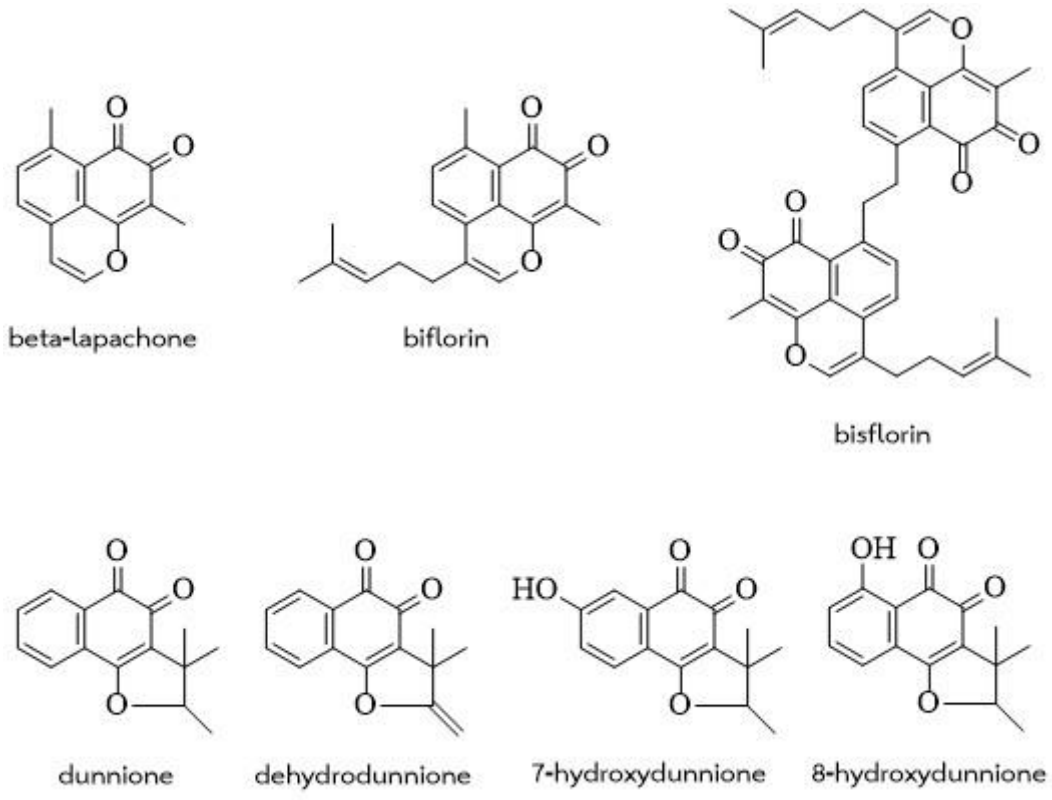

Figure 1.3 Some natural 1,2-naphthoquinones

Naphthofuranone phytoalexins such as naphtho[1,2-b]furan-4,5-dione (**a**), 3-hydroxy-naphtho[1,2-b]furan-4,5-dione (**b**), and 2-[2′-(2′-hydroxy)propyl]-naphtho[l,2-b]furan-4,5-dione (**c**), isolated from *Avicennia marina* which is infected by a fungus *Phytophthora*, belong to typical 1,2-naphthoquinones.[65] These compounds are

known as phytoalexins because of the compounds are formed after the infection of wound tissue of *Avicennia marina* seedlings by this fungus.

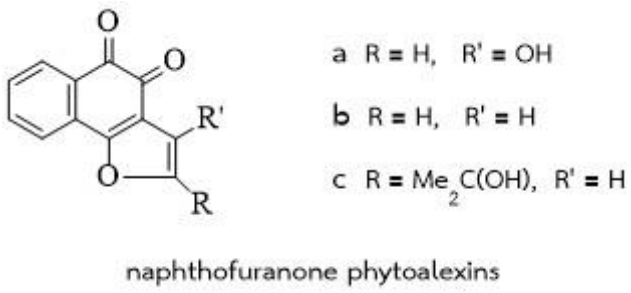

Figure 1.4 Naphthofuranone phytoalexins from *A. marina*

Another typical 1,2-naphthoquinones can be isolated from *Mansonia gagei* Drumm. heartwoods (Sterculaceae family) which is used as a material plant in this study.

1.2 Typical 1,2-Naphthoquinones from *Mansonia gagei* Drumm.

Thailand is a tropical country with a large variety of plants which can be found in the southern and northern parts of Thailand. Evergreen forest can be found in the southern part, while in the northern part is known as one of the richest areas of plants in the world.[9] This country has a long history of using medicinal plants which are known as *samunphrai*.[66] Many medicinal plants in Thailand have offered the basis for modern pharmaceuticals.[67] Recently, there has been a rising of interest in Thai medicinal plants due to their effectiveness and affordability.[66] In addition there is a consideration that utilization of traditional medicine is generally safer than modern medicine.

One of plants which are used as medicinal plants in Thailand is *M. gagei*. The extract of this plant yielded several mansonones belonging typical 1,2-naphthoquinones. This plant is a local plant growing in Thailand and belonging to Sterculaceae family.[68, 69] This plant (Figure 1.5) is known for its local name as *chan-cha-mod*, *chan-hom*, *chan-khao*, or *chan-pha-ma*.[68]

Figure 1.5 *Mansonia gagei* Drumm.

The characteristics of this plant *i.e.* the color of flower is white and cluster, the bark is white-grey and quite smooth, and the leaf has oblong-lanceolate shape about 3-6 cm wide and 8-14 cm long.[70] Based on folklore beliefs in Thailand, the heartwood of this plant can be used as antidepressant, antiemetic, cardiac stimulant, onilivertigo and refreshment agent.[68, 69]

According to some literatures, the biological activities and chemical constituents of *M. gagei* extract have been investigated. In 2002, Tiew reported that the CH_2Cl_2 extract of *M. gagei* heartwoods revealed good preliminary screening assays in cytotoxicity, antifungal, antioxidant, antithrombin, and anticancer properties.[71] Further investigation, several bioactive compounds were isolated from this extract such as dehydrooxopirezinone, mansorins (A, B, and C), mansonones (C, E, G, H, N, O, P and Q). In addition, four additional compounds together with some compounds isolated from the CH_2Cl_2 extract were isolated from EtOAc and MeOH extracts of this plant, 3-methoxy-4,5-dihydroxybenzaldehyde, mansoxetane, mansonones R and S. Moreover, all isolated compounds were evaluated for their biological activities. It can be concluded that mansonones (1,2-naphthoquinones) displayed higher activity than mansorins (coumarins) in cytotoxic and anticancer activities.

At the same year, Tiew and coworkers reported that the hexane and CH_2Cl_2 crude extracts of *M. gagei* were more biologically active than others in cytotoxicity against brine shrimp with LC_{50} values were 23.69 and 22.83 μg/mL, respectively.

According to the biological activity study, mansorin B and mansonone C gave promising results in the cytotoxicity test against brine shrimp.[69]

Moreover, in 2003, Tiew and coworkers also reported that mansonones C and E isolated from the CH_2Cl_2 extract of *M. gagei* heartwoods are the only active compounds against *Candida albicans* and *Cladosporium cucumerinum* with a minimal inhibitory amount of 0.15 and 2.5 µg, 0.6 and 0.6 µg, respectively. In addition, mansorins A and B were active against *C. cucumerinum* with a minimal inhibitory amount of 2.5 and 0.6 µg, respectively. On the other hand, mansonone C was found to be the only isolated compound against the larvae *Aedes aegypti* at 50 ppm and mansonone N was found to be the only isolated compound that exhibited the radical scavenging properties in DPPH.[68]

In 2004, Tiangthem studied the antihistamic activity of this plant and the results revealed that the CH_2Cl_2 extracts from the roots and leaves displayed high antihistamic activity with inhibition values are 96 and 81%, respectively.[70]

Furthermore, in 2007, El-Halawany and coworkers reported that the $CHCl_3$-soluble fraction from the MeOH extract of heartwood of *M. gagei* showed potency as anti-estrogenic. Fourteen compounds including mansorins A and C, mansonones F, G, H, N, O, S, I, mansorins I, II and III, and acetovanilone were isolated. Mansorins I-III and mansonone I were new isolated compounds. Based on biological activity test, mansonones F and S displayed the most potent anti-estrogenic.[72]

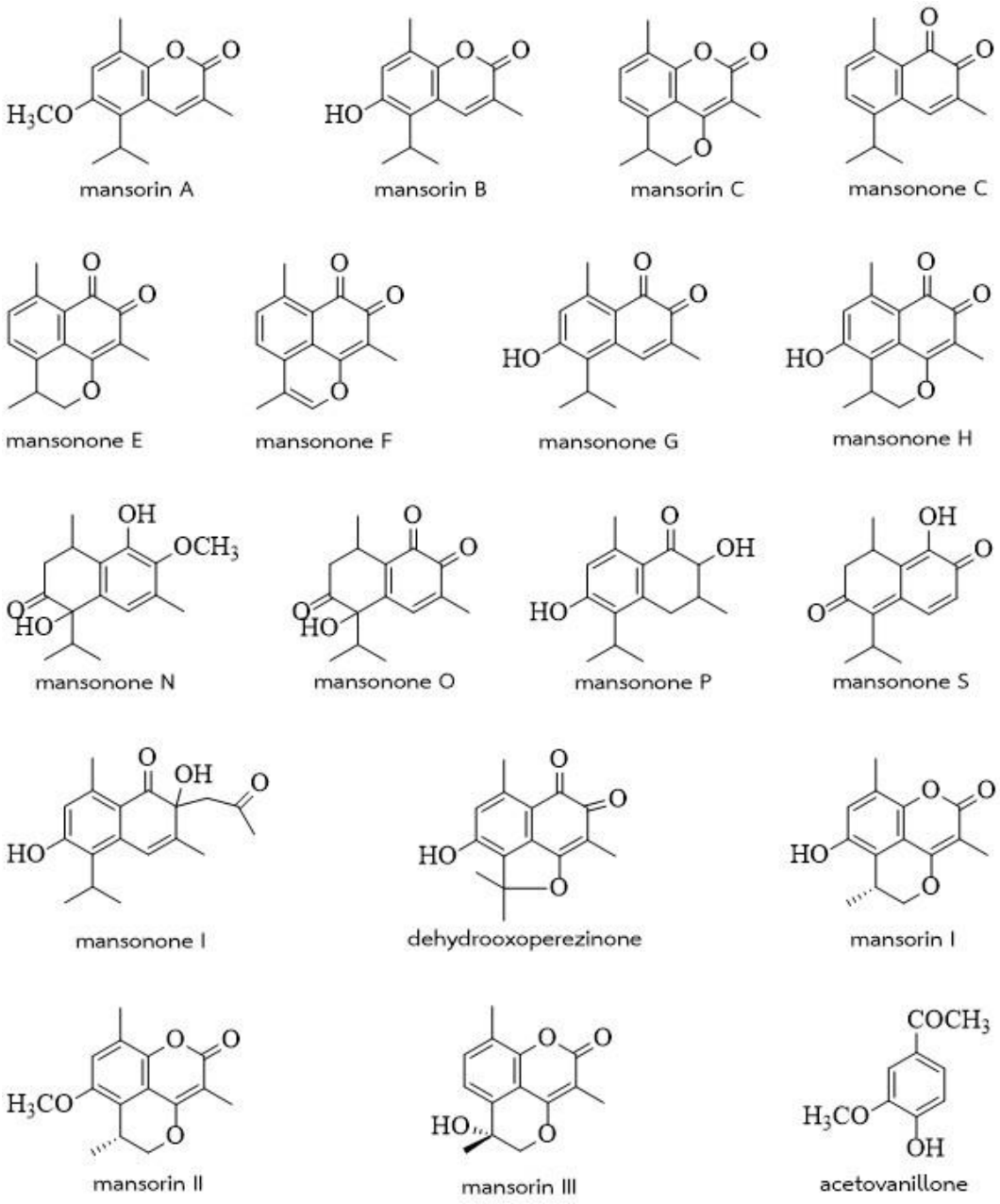

Figure 1.6 Chemical constituents from *M. gagei* heartwoods

1.3 Mansonones, Typical 1,2-Naphthoquinones Derived from Other Plants

Naturally occurring typical 1,2-naphthoquinones (mansonones) can also be found in other species of plants. Bettolo and coworkers in 1965 have recognized several 1,2-naphthoquinones along with 1,4-naphthoquinones which designed as mansonones A-F, from the heartwoods of *M. altissima*.[73] Moreover, Tanaka and

coworkers in 1966 investigated mansonones A, C, E, F, G, and H together with β-sitosterol and β-sitosteryl palmitate from the acetone extract of *M. altissima* heartwood.[74] Following investigation, Galeffi and coworkers in 1969 discovered mansonone L together with mansonones C, E, F, G, H, and I.[75]

These compounds could also be found in other plant families such as Malvaceae and Ulmaceae. Mansonones D, E, F, G, and H were reported to be isolated from *Thespesia populnea* (Malvaceae family) by Puckhaber and Stipanovic in 2004.[76] Mansonone C, orange yellow rods, was isolated from *Ulmus glabra* heartwood (Ulmaceae family).[77] Mansonones E and F were also isolated from the dried root bark of *U. pumila*.[78]

1.4 Synthesis of Mansonones and Their Biological Activities

Several studies involved the synthesis of mansonone derivatives from both natural and synthesis procedures. El-Halawany and coworkers in 2007 derivertized mansonone G together with mansorin A from their natural compounds isolated from *M. gagei* heartwood extract.[79] The result showed that the phenolic hydroxyl group in mansonone G and mansorin A was not essential in anti-estrogenic acitivity. Furthermore, the result also indicated that acetyl mansonone G gave a promising potential for the synthesis of anti-estrogenic agents.

In 2004, Shin and coworkers synthesized mansonone F derivatives by varying its substituent at C3 and investigated their anti-MRSA (anti-methicillin resistance *Staphylococcus aereus*) activity.[80] The results revealed that 1,2-quinone and tricyclic systems of mansonone F played important role in anti-MRSA activity. In addition, there was no significantly effect on antibacterial activity by derivatives containing alkyl and electron-withdrawing groups at C3 of mansonone F derivatives and the polar substituents at C3 eliminated the activity.

Another investigation continued to synthesize C6 and C9 analogues of mansonone F as well as evaluated the anti-MRSA activity by Suh and coworkers in

2006.[81] Most of these analogues displayed good or excellent anti-MRSA activity and specifically the 6-*n*-butyl mansonone F exhibited four times higher than that of vancomycin.

Moreover, mansonone F derivatives were further synthesized as topoisomerase inhibitors by Wu and coworkers in 2011.[82] Based on the evaluation, these derivatives were found to have strong activity as topoisomerase inhibitors, with much more significant inhibitions on topoisomerase II rather than topoisomerase I.

Another kind of mansonone, *i.e*. mansonone E, was synthesized as its derivatives by Huang and coworkers in 2013, which were prepared *via* copper-catalyzed azide-alkyne cycloaddition (CuAAC) click chemistry and evaluated their activity as topoisomerase inhibitors.[83] The results indicated that compounds with the substituents of the triazole showed important role for cytotoxicity.

1.5 Bacteria

Bacteria are single-cell microorganisms without chlorophyll having both DNA and RNA, as well as capable to exhibit all of fundamental life processes, such as growth, metabolism and reproduction.[84] They can be found in, on, and around most living and nonliving things.[85] They are neither plants nor animals and their cells differ somewhat from the cells of plants or animals. The bacteria cell walls are stronger per unit thickness than the cell wall of higher plants due to the chemical structure of the unit parts of bacteria cell wall which has covalent bond forming a strong networks.[86]

Bacteria belong to prokaryote organisms and has no real nucleus in cell, different with eukaryote organisms such as plants, animals, and fungi (including yeasts).[85, 87] The outer layer of bacteria cell is composed of two components, *i.e.* a rigid cell wall (containing muramic acid) and plasma membrane. While, the protoplasm is encountered at inside of outer layer, which consists of cytoplasm and cytoplasmic inclusions such as ribosomes, mesosomes, granules, vacuoles, and nuclear matter.[84] The structural features of bacterial cell are described in Figure 1.7.

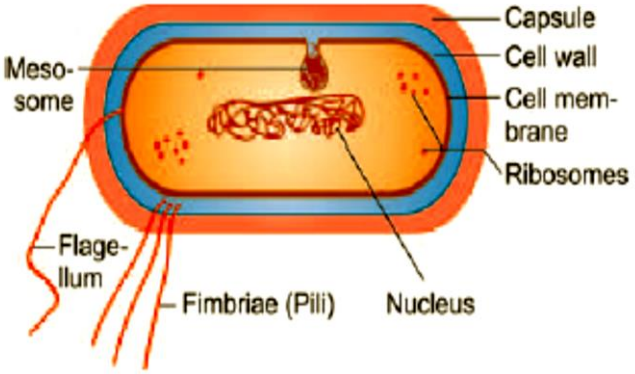

Figure 1.7 Structure of bacterial cell

In microbiology, bacteria are classified based on the clinical laboratories finding, such as:

1. The energy that the bacteria uses for surviving[88]
    a. Photosynthetic bacteria (bacteria that use light energy)
    b. Chemotrophic bacteria (bacteria that use energy from chemical reactions)
2. The shape of bacteria, scientists divide the bacteria into some groups[84, 85]
    a. spherical cells, which are labeled as cocci (coccus) and they are described as staphylococci, streptococci, and diplococci.
    b. cylindrical or rod-shaped cells, called bacilli (bacillus).
    c. curved rods, known as vibrio which has vibratory motility as their characteristic.
    d. spiral-shaped bacteria.
3. The oxygen demand for sustaining its life[88]
    a. Aerobic bacteria (bacteria that need oxygen)
    b. Anaerobic bacteria (bacteria that can grow without oxygen)
    c. Bacteria that can life in a little oxygen condition
    d. Facultative bacteria (bacteria that can life with and without oxygen condition)
4. The staining of the cell wall

Most of bacteria are colorless and have small size which measured in terms of micron,[84] therefore it is difficult to distinguish between groups of bacteria under microscope. There is a technique for distinguishing bacteria, *i.e.* the Gram staining, described by Hans Christian Joachim Gram in 1884.[84, 87] This technique is used for studying the morphologic appearance of bacteria in which the bacteria are divided into

two groups, *i.e.* Gram positive bacteria and Gram negative bacteria.[84] Gram positive bacteria being stained dark purple or violet when treated with Gentian violet then iodine/potassium iodide, while Gram negative bacteria can be visualized by eosin or fuschin being red.[87]

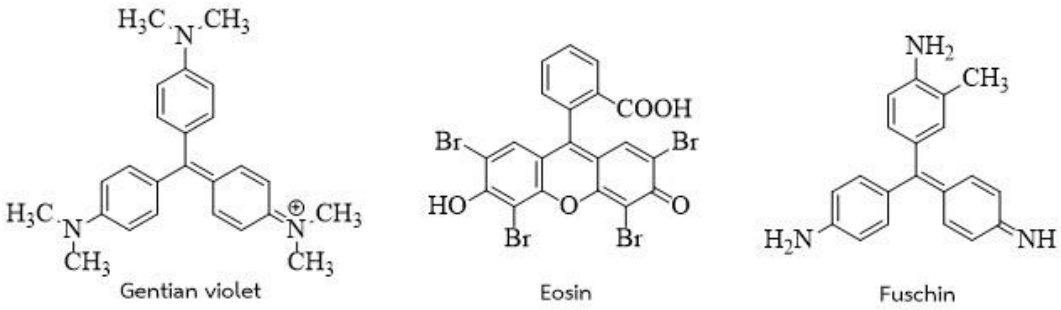

Figure 1.8 Staining agents for bacterial

The difference between Gram positive and Gram negative bacteria lies on their cell wall characteristics.[84] Gram positive bacteria have a cytoplasmic membrane surrounded by a tough and rigid mesh while Gram negative bacteria have a cytoplasmic membrane surrounded by a thin cell wall that is itself surrounded by a second lipid membrane called the outer membrane, which contains large amounts of lipopolysaccharide (LPS).[89]

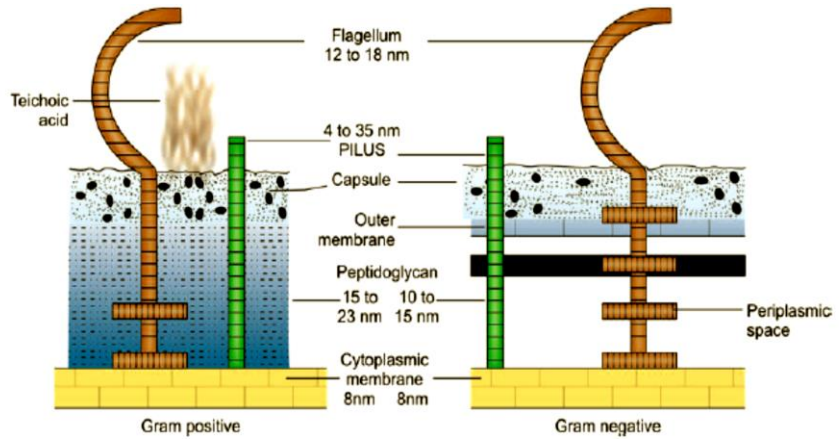

Figure 1.9. The differences of cell walls of Gram positive and Gram negative bacteria

As comparison, the cell wall of Gram negative bacteria has a complex structure than Gram positive bacteria. The peptidoglycan layer of Gram positive bacteria is thicker than that in Gram negative bacteria. Gram negative bacteria cell wall contains higher lipids amount than that in Gram positive bacteria. The teichoic acids only present in Gram positive bacteria, in which this component constitute major surface antigens of this kind bacteria.[84] The comparisons of cell walls of Gram positive and Gram negative bacteria are presented in Table 1.1.

Table 1.1 Comparisons of Gram positive and Gram negative bacteria cell walls

	Gram positive	Gram negative
Structure	Monolayer	Multilayer/complex
Thickness of peptidoglycan layer	15-25 nm	10-15 nm
Variety of amino acid	Few	Several
Aromatic and sulfur containing amino acids	Absent	Present
Lipids	Low (2-4%)	High (15-20%)
Teichoic acids	Present	Absent
Periplasmic space	Absent	Present
Result of enzyme digestion	Protoplast	Spheroplast

In this study, Gram positive and Gram negative bacteria were used as microorganisms tested, *i.e. Staphylococcus aureus* ATCC 25923, *Streptococcus sobrinus* KCCM 11898, *Streptococcus mutans* ATCC 25175, *Propionibacterium acnes* KCCM 41747, and *Salmonella typhi* ATCC 422.

a. Staphylococcus aureus

S. aureus (Figure 1.10) is an ovoid or spherical, non-motile, rarely capsulated, can produce golden yellow colonies, pathogenic, and belongs to Gram positive bacteria. It is known as aerob bacterium and can grow on simple media at optimum temperature 37°C and pH 7.4. This bacterium produces hemolysin which may cause a hemolysis. In addition, it can also produce a toxin which may cause nausea, vomiting and diarrhea.[84]

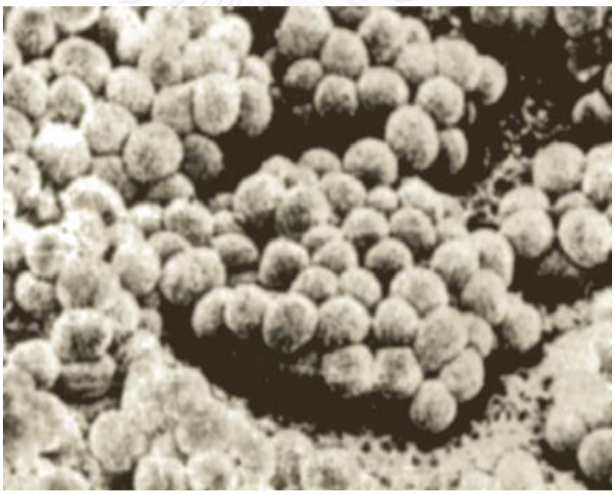

Figure 1.10. Colonies of *Staphylococcus aureus*

b. Streptococcus sobrinus

S. sobrinus belonging to Gram positive bacteria is one of phylogenetic mutans group which commonly associated with caries dental teeth.[90] *S. sobrinus* is also known as the most acidogenic bacteria among other oral streptococci.[91]

c. *Streptococcus mutans*

S. mutans (Figure 1.11) belongs to Gram positive bacteria, facultatively anaerobic, and non-capsulated coccus. In 1924, Clarke isolated *S. mutans* from human carious lesions and discovered that this bacterium has a significant contributor to

human dental caries.[92] *S. mutans* is known to be the main cariogenic organism in plaque due to its acid tolerant and also its ability in becoming numerically valuable in the total plaque population.[93] The acid tolerant of *S. mutans* was investigated by Belli in 1991, and found that *S. mutans* was able to develop the adaptive tolerance during prolonged growth at low pH which distinguished it from organisms not commonly associated with dental caries.[94]

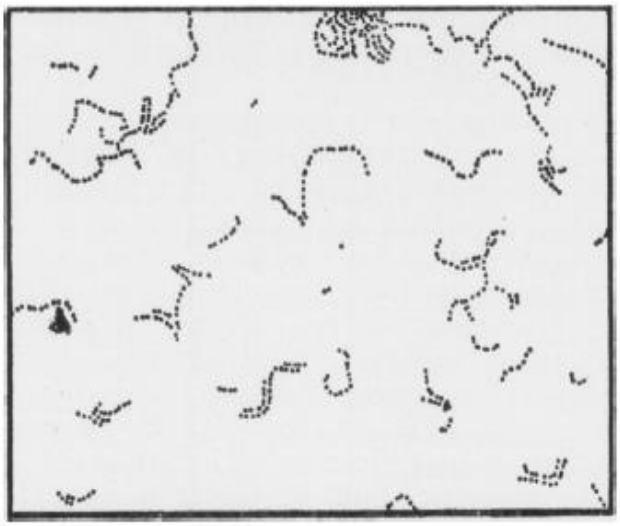

Figure 1.11 The morphology of *Streptococcus mutans* (24 hours broth culture)

d. *Propionibacterium acnes*

P. acnes belongs to an anaerobic, non-spore-forming, Gram-positive, and pleomorphic rod whose end products of fermentation include propionic acid.[95, 96] This bacteria is known to cause human skin commensal and involves in the pathogenesis of acne.[97] Chronic inflammatory acne cannot be classified as an infectious disease due to this bacteria are normally present on the skin of a vast majority individuals.[98]

e. *Salmonella typhi*

S. typhi is a Gram negative and facultative anaerobe bacterium belonging to Enterobacteriaceae family.[99] This bacterium can cause typhoid fever in humans.[100] Typhoid fever is a systemic febrile illness and transmitted by fecal-oral route which mainly *via* contaminated food and water.[101]

1.6 Chloramphenicol as One of Broad Spectrum Antibiotic

Antibiotics produced by bacteria or fungi are small molecules that used for killing bacteria without harming the person or animal being treated. Antibiotics can be divided into whether they are capable to kill bacteria (bactericidal) or merely suppress the growth of bacteria (bacteriostatic).[89, 102] Moreover, they can also be classified according to the cellular component or system they affect.[102]

In this study, the antibiotic used as positive control was chloramphenicol. Chloramphenicol or D-(*threo*-2-dichloroacetamido-1-*p*-nitrophenyl-1,3-propanediol is one of the oldest and most potent of antibiotics used in chemotherapy.[103, 104]

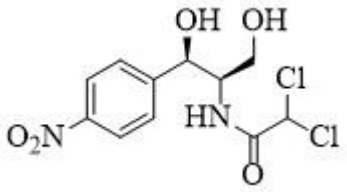

At the beginning of finding this antibiotic, chloramphenicol was known as chloromycetin (contained both nitrogen and non-ionic chlorine) and isolated from filtrates of submerged aerated cultures of *Streptomyces* sp.[105] In addition, this antibiotic has a broad spectrum (can suppresses some Gram positive and Gram negative bacterial) and acts as a bacteriostatic agent. The target and pathway affected by chloramphenicol are presented in Table 1.2.[102]

Table 1.2 Chloramphenicol target and pathway

Antibiotic type	Derivation	Species range	Primary target	Pathway affected
Phenicols	from *S. venezuelae*	Some Gram positive and Gram negative species	50S ribosome	Protein translation

1.7 Resistance of Antibiotics and Bacteria

The invention of antibiotics which can cure infection diseases caused by bacteria, have helped humans to treat this disease. But over the past several decades, numerous species of bacteria have become increasingly resistant to antibiotics. In fact, this phenomenon has been a recognized reality almost since the antibiotic discovery era, but only within the past twenty years has the emergence of dangerous.[106]

1.8 Adipose Tissue

Adipose tissue is known as a metabolic organ which is important for whole–body insulin sensitivity and energy homeostatis.[107] It is characterized as fat storage depots with widely varying function, size, and structure.[108] There are two hormones produced exclusively in adipocytes *i.e*. leptin and adiponectin, which have several functions including the modulation of sensitivity to insulin and regulation of food intake.[109]

Indeed, there are two kinds of adipose tissues with different functions coexist in humans, *i.e*. white and brown adipose tissues (Figure 1.12). White adipose tissue (WAT) is mainly involved in energy storage and mobilization, whereas brown adipose tissue (BAT) is specialized in energy expenditure.[110] The relative amounts of both adipose tissues are genetically distinguished and rely on many factors such as age, sex, environmental temperature, and nutritional status.[111]

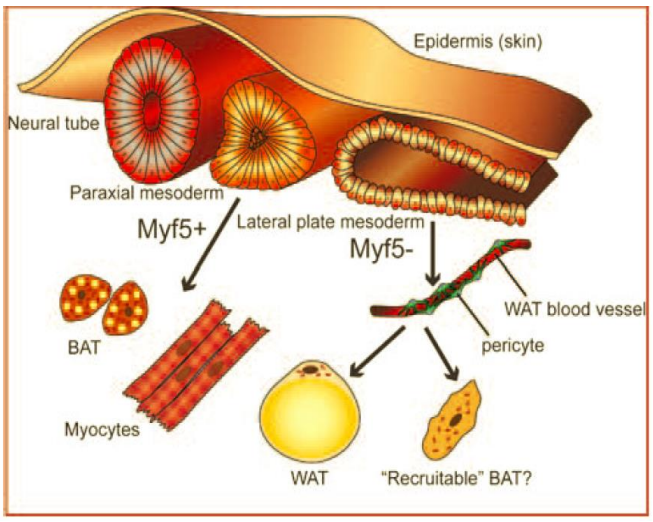

Figure 1.12 The different origins of white and brown adipose tissues [112]

The characteristics of white and brown adipose tissues summarized by Saely and coworkers (2012) are shown in Table 1.3.[113] White adipocytes are spherical cells which their sizes depending on the size of the singlet lipid droplet (consists of triglycerides). In addition, white adipocytes have a thin and elongated mitochondria which is variable in amount. While, brown adipocytes are multiple small vacuoles and contain abundant of mitochondria.

Table 1.3 The characteristics of white and brown adipose tissues

	White adipose tissue	Brown adipose tissue
Function	The storage of energy	The production of heat
Morphology	As single lipid droplet, and contains variable amount of mitochondria	As multiple small molecule, and contains abundant of mitochondria
Human data	Large amount are associated with increased risk of obesity-related disorders	Large amount are associated with decreased risk of obesity-related disorders
Impact of aging	Increases with age relative to total body weight	Decreases with age

1.9 Adipogenesis

Adipose tissue expands by the increasing of the number and size of adipocytes and these adipocytes reach maturity and become functional *via* adipogenesis.[114] Adipogenesis (Figure 1.13) is defined as a specific differentiation process by which fat cells (adipocytes) are formed from their pre-adipocyte precursor cells.[45] This process is regulated by a number of transcriptions factors, such as peroxisome proliferator-activated receptor **γ** (PPAR**γ**) and CCAAT/enhancer binding proteins (CEBPs).[47]

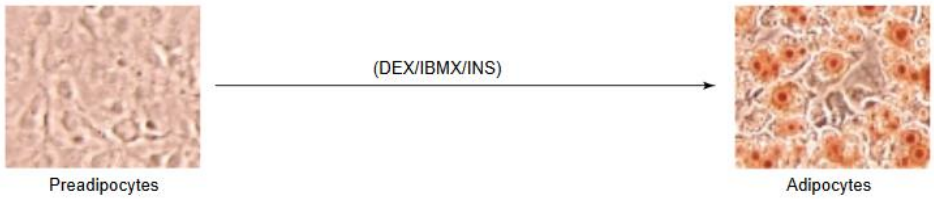

Figure 1.13 Adipogenesis (differentiation process) [115]

1.10 Adipose Tissue Dysfunction

The metabolism of adipose tissue is closely linked to obesity. The obese state defined as a body mass index (BMI) ≥30 kg/m^2) is described by an excessive growth of adipose tissue mass, which displays in increased size (adipocyte hypertrophy), increased number (adipocyte hyperplasia), and increased intracellular lipids.[108] White adipose tissue is important for maintaining the energy homeostasis and highly influences obesity.[47]

It is also known that the obesity significantly contributes the risk of developing type 2 diabetes mellitus, hypertension, cardiovascular disease, stroke, fatty liver diseases, dementia, obstructive sleep apnea, and several types of cancer.[116, 117] In order to decrease the obesity, the substances that can inhibit adipogenesis are needed. Controlling adipogenesis is a potential strategy to prevent obesity. These substances are called as anti-adipogenic agents.

In laboratory study, 3T3-L1 cell lines have been widely used as *in vitro* models on anti-adipogenic assay. This cell lines is originally derived from mouse embryos which can be differentiated into adipocytes which stimulated by dexamethasone, IBM, and insulin.[44]

1.11 The Aim of This Research

Nowadays, the discovery of new antibacterial agents is considerably as an important research due to some antibiotic resistance effect towards bacterial strains. In addition, since the number of studies in the field of adipose tissue has increased exponentially over the last decade due to the rising of obesity prevalence and its metabolic disorders caused the anti-adipogenic activity is also consider as an important study. One of well-known secondary metabolites with good antibacterial and anti-adipogenic activities is naphthoquinone groups.

According to the previous literature review, it seemed that mansonones isolated from *M. gagei* heartwoods were interesting for further investigation as well as their derivatives in antibacterial and anti-adipogenic activities. Previous studies reported that mansonones as well as their synthetic derivatives displayed antibacterial activity but no report before on antibacterial activity from mansonone G derivatives. Moreover, there is no report on anti-adipogenic activity of mansonones as well as their derivatives. Therefore, the aims of this research were summarized as follows:

- To isolate mansonones from *M. gagei* heartwoods.
- To synthesize mansonone derivatives.
- To determine their antibacterial and anti-adipogenic activities.

CHAPTER II

EXPERIMENTAL

2.1 Plant Material

The dried heartwoods of *Mansonia gagei* Drumm. was bought from Tai Hua Chan, the herbal drug store in Bangkok, Thailand in December 2014.

Figure 2.1 Dried heartwoods of *M. gagei*

2.2 Equipments and Instruments

^{1}H and ^{13}C NMR spectra were recorded in $CDCl_3$ or acetone-d_6 or otherwise stated and were analyzed by using a Bruker Ultrashield 400 Plus NMR spectrometer or a Varian Mercury NMR spectrometer with an Oxford YH400 magnet operating at 400 MHz for ^{1}H and 100 MHz for ^{13}C. High resolution mass spectra (HRMS) were recorded on a Bruker Daltonics microTOF using electron spray ionization (ESI).

2.3 Chemicals

All solvents used in this research were distilled prior to use except those which were reagent grades. Thin layer chromatography (TLC) was performed on aluminium sheets precoated with silica gel (Merck Kieselgel 60 PF_{254}). Silica gel (No. 7729, 7734, and 9385, Merck) was used as stationary phase on quick column chromatography and open column chromatography.

2.4 Extraction of Plant Material

The dried-powdered *M. gagei* heartwoods (10 kg) were extracted by maceration method, where sample soaked in CH_2Cl_2 for 3 days at room temperature and was repeated three times. Then, the extract was filtered and evaporated under vacuum to obtain dark-brown CH_2Cl_2 extract (276 g, 2.8% yield of the dried heartwood).

2.5 Separation and Purification of Chemical Constituents

The CH_2Cl_2 extract (200 g) was fractionated by silica gel quick column (No. 7729, Merck). A stepwise elution was conducted by hexane and followed by increasing the polarity with EtOAc and final with 10% MeOH in EtOAc. The fractions were combined according to TLC profiles to give 8 fractions (MGD1-MGD8).

MGD3, MGD4 and MGD5 were further separated on silica gel column (No. 7734, Merck) using stepwise system of hexane–CH_2Cl_2, CH_2Cl_2-EtOAc and EtOAc-MeOH of increasing polarity. Further separation of MGD3 yielded three compounds, *i.e*. mansorin A (**1**, 0.72 g), mansorin C (**3**, 0.03 g) and mansonone C (**4**, 0.08 g). While, mansorin B (**2**, 0.06 g) and mansonone E (**5**, 0.20 g) were obtained from MGD4. Mansonone H (**7**, 0.19 g) was isolated from MGD5. Mansonone G (**6**, 10.00 g) as a major compound was isolated from both MGD4 and MGD5. The structural identification of these compounds (Figure 2.2) were conducted by comparing spectroscopic data with previous reports.

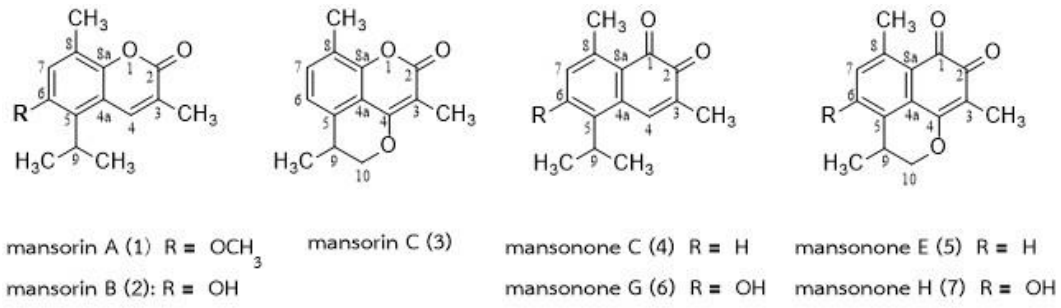

Figure 2.2 Isolated compounds from the CH_2Cl_2 extract of *M. gagei* heartwoods

Mansorin A (**1**) ^{1}H NMR (400 MHz, $CDCl_3$): δ (ppm) 7.90 (s, 1H), 6.90 (s, 1H), 3.83 (s, 3H), 3.55 (m, 1H), 2.42 (s, 3H), 2.23 (s, 3H), and 1.37 (d, *J* = 7.1 Hz, 6H).

Mansorin B (**2**) ^{1}H NMR (400 MHz, $CDCl_3$): δ (ppm) 7.90 (s, 1H), 6.77 (s, 1H), 5.19 (s, 1H), 3.53 (m, 1H), 2.35 (s, 3H), 2.24 (s, 3H), and 1.42 (d, *J* = 7.0 Hz, 6H).

Mansorin C (**3**) ^{1}H NMR (400 MHz, $CDCl_3$): δ (ppm) 7.31 (d, *J* = 7.6 Hz, 1H), 7.00 (d, *J* = 7.6 Hz, 1H), 4.41 (dd, *J* = 10.7, 4.1 Hz, 1H), 4.13 (dd, *J* = 10.8, 6.7 Hz, 1H), 3.17 (m, 1H), 2.43 (s, 3H), 2.07 (s, 3H), and 1.33 (d, *J* = 7.0 Hz, 3H).

Mansonone C (**4**) ^{1}H NMR (400 MHz, $CDCl_3$): δ (ppm) 7.65 (s, 1H), 7.43 (d, *J* = 8.1 Hz, 1H), 7.19 (d, *J* = 8.0 Hz, 1H), 3.38 (m, 1H), 2.63 (s, 3H), 2.08 (d, *J* = 1.8 Hz, 3H), and 1.29 (d, *J* = 7.0 Hz, 1H).

Mansonone E (**5**) ^{1}H NMR (400 MHz, $CDCl_3$) : δ (ppm) 7.34 (d, *J* = 8.5 Hz, 1H), 7.00 (d, *J* = 7.6 Hz, 1H), 3.17 (m, 1H), 4.40 (dd, *J* = 10.1, 3.4 Hz, 1H), 4.22 (dd, *J* = 10.1, 4.3 Hz, 1H), 2.65 (s, 3H), 1.95 (s, 3H), and 1.36 (d, *J* = 7.1 Hz, 3H).

Mansonone G (**6**) ^{1}H NMR (400 MHz, acetone-d_6): δ (ppm) 7.87 (s, 1H), 6.64 (s, 1H), 3.63 (m, 1H), 2.45 (s, 3H), 1.95 (s, 3H), and 1.34 (d, *J* = 7.0 Hz, 6H).

Mansonone H (**7**) ^{1}H NMR (400 MHz, acetone-d_6): δ (ppm) 6.84 (s, 1H), 4.48 (d, *J* = 10.9 Hz, 1H), 4.36 (dd, *J* = 10.9, 3.3 Hz, 1H), 3.32 (m, 1H), 2.52 (s, 3H), 1.86 (s, 3H), and 1.32 (d, *J* = 7.0 Hz, 3H).

2.6 Synthesis of Mansonone Derivatives

2.6.1 The Derivatization of Mansonone G into Its Ether Analogues

The derivatization of mansonone G into its ether analogues was performed using El-Halawany, *et al.* method.[79] Mansonone G (**6**, 122 mg, 0.5 mmol) was dissolved in acetone (15 mL), then K_2CO_3 (700 mg, 5 mmol) was added into the solution. CH_3I (0.75 mL, 12 mmol) was added while stirring and the mixture was refluxed for 5–8 h. The progress of the reaction was followed by TLC. After the reaction

was completed, the reaction mixture was extracted with EtOAc (15 mL, three times). The organic layer was dried over anhydrous Na_2SO_4, filtered the drying agent, evaporated the solvent, and purified by silica gel column (No. 9385, Merck) using hexane:EtOAc (4:1) to yield compound **G01** as orange powder (100 mg, 82% yield). The same procedure was conducted by changing CH_3I with C_2H_5Br (0.89 mL), C_4H_9Br (1.30 mL), $C_8H_{17}Br$ (2.07 mL), $C_{12}H_{25}Br$ (2.88 mL), benzyl bromide (1.43 mL), allyl bromide (1.04 mL), 3,3-dimethylallyl bromide (1.39 mL), geranyl bromide (2.4 mL), and cinnamyl bromide (to yield compounds **G02** (98 mg, 80%yield), **G03** (96 mg, 79% yield), **G04** (93 mg, 76% yield), **G05** (119 mg, 98%yield), **G06** (20.4 mg, 16.7%yield), **G07** (43 mg, 35.3%yield), **G08** (27 mg, 22.1%yield), **G09 (**75.4 mg, 61.8% yield), and **G10** (84.1 mg, 68.9% yield), respectively. Compounds **G07** and **G08** were purified by hexane:CH_2Cl_2:EtOAc (5:2.5:0.5), while compound **G09** was purified using hexane:CH_2Cl_2:EtOAc (7:2.5:0.5). The structures of these ether analogues (Figure 2.3) were elucidated using NMR and MS analysis. Nine compounds were identified as new semisynthetic ether analogues, *i.e*. compounds **G02** – **G10**.

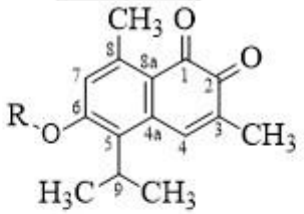

G01 R = CH_3
G02 R = C_2H_5
G03 R = C_4H_9
G04 R = C_8H_9
G05 R = $C_{12}H_{25}$
G06 R = benzyl
G07 R = allyl
G08 R = 3,3-dimethylallyl
G09 R = geranyl
G10 R = cinnamyl

Figure 2.3 The structures of ether analogues of mansonone G

G01 (methyl ether mansonone G). ^{1}H NMR (400 MHz, $CDCl_3$): δ (ppm) 7.70 (s, 1H), 6.60 (s, 1H), 3.90 (3H), 3.58 (m, 1H), 2.62 (s, 3H), 2.04 (s, 3H), and 1.35 (d, *J* = 7.0 Hz, 6H). ^{13}C NMR: δ (ppm) 182.4, 180.4, 163.0, 146.3, 138.3, 134.9, 134.3, 122.8, 114.8, 55.3, 29.5, 23.5, 21.2, and 15.9.

G02 (ethyl ether mansonone G). ^{1}H NMR (400 MHz, $CDCl_3$): δ (ppm) 7.70 (s, 1H), 6.58 (s, 1H), 4.13 (q, *J* = 6.96 Hz, 2H), 3.58 (m, 1H), 2.62 (s, 3H), 2.05 (s, 3H), 1.49 (t, *J* = 6.96 Hz, 3H), and 1.38 (d, *J* = 7.04 Hz, 6H). ^{13}C NMR: δ (ppm) 182.4, 180.4, 162.5, 146.3, 138.2, 134.9, 134.3, 134.2, 122.7, 115.3, 63.9, 29.5, 23.5, 21.2, 15.9, and 14.4. HRMS (ESI): calcd for $C_{17}H_{21}O_3$ $[M+Na]^+$: 295.1310, found 295.1309.

G03 (butyl ether mansonone G). ^{1}H NMR (400 MHz, $CDCl_3$) : δ (ppm) 7.69 (s, 1H), 6.58 (s, 1H), 4.04 (t, *J* = 6.32 Hz, 2H), 3.57 (m, 1H), 2.59 (s, 3H), 2.02 (s, 3H), 1.83 (m, 2H), 1.50 (m, 2H), 1.36 (d, *J* = 6.96 Hz, 6H), and 0.98 (t, *J* = 7.32 Hz, 3H). ^{13}C NMR: δ (ppm) 182.4, 180.2, 162.6, 146.2, 138.2, 134.7, 134.2, 134.1, 122.5, 115.2, 68.0, 30.9, 26.7, 23.4, 21.1, 19.2, 15.8, and 13.5. HRMS (ESI): calcd for $C_{19}H_{24}O_3$ $[M+Na]^+$: 323.1623, found 323.1621.

G04 (octyl ether mansonone G). ^{1}H NMR (400 MHz, $CDCl_3$): δ (ppm) 7.71 (s, 1H), 6.59 (s, 1H), 4.04 (t, *J* = 6.44 Hz, 2H), 3.59 (m, 1H), 2.62 (s, 3H), 2.05 (s, 3H), 1.86 (m, 2H), 1.50 (m, 2H), 1.41 (d, *J* = 6.20 Hz, 6H), 1.32 (m, 8H), and 0.89 (t, *J* = 6.12 Hz, 3H). ^{13}C NMR: δ (ppm) 182.5, 180.3, 162.6, 146.3, 138.2, 134.9, 134.3, 134.2, 122.6, 115.3, 68.4, 31.6, 29.0, 28.9, 26.8, 26.0, 23.6, 22.5, 21.2, 15.9, and 13.9. HRMS (ESI): calcd for $C_{23}H_{32}O_3$ $[M+Na]^+$: 379.2249, found 379.2254.

G05 (dodecyl ether mansonone G). ^{1}H NMR (400 MHz, $CDCl_3$) : δ (ppm) 7.70 (s, 1H), 6.58 (s, 1H), 4.03 (t, *J* = 6.40 Hz, 3H), 3.59 (m, 1H), 2.60 (s, 3H), 2.03 (s, 3H), 1.84 (m, 2H), 1.48 (m, 2H), 1.37 (d, *J* = 7.00 Hz, 6H), 1.26 (m, 16H), 0.86 (t, *J* = 6.00 Hz, 3H). ^{13}C NMR: δ (ppm) 182.3, 180.2, 162.6, 146.3, 138.2, 134.8, 134.2, 134.1, 122.5, 115.2, 68.0, 31.7, 29.4, 29.3, 29.1, 29.0, 28.8, 25.9, 23.5, 22.4, 21.2, 15.8, and 13.8. HRMS (ESI): calcd for $C_{27}H_{40}O_3$ $[M+Na]^+$: 435.2875, found 435.2881.

G06 (benzyl ether mansonone G) ^{1}H NMR (400 MHz, $CDCl_3$): δ (ppm) 7.72 (s, 1H), 7.42 (m, 5H), 6.70 (s, 1H), 5.16 (s, 2H), 3.63 (m, 1H), 2.62, (s, 3H), 2.06 (s, 3H), and 1.38 (d, *J* = 7.08 Hz, 6H). ^{13}C NMR: δ (ppm) 182.6, 180.7, 162.4, 146.5, 138.5, 135.9, 135.3, 134.8, 134.7, 128.9, 128.5, 127.7, 123.4, 116.2, 70.8, 27.0, 23.8, 21.6, and 16.2. HRMS (ESI): calcd for $C_{23}H_{32}O_3$ $[M+Na]^+$: 357.1467, found 357.1464.

G07 (allyl ether mansonone G) ^{1}H NMR (400 MHz, $CDCl_3$): δ (ppm) 7.71 (s, 1H), 6.59 (s, 1H), 6.07 (m, 1H), 5.44 (m, 1H), 5.34 (m, 1H), 4.63 (d, *J* = 5.20 Hz, 2H), 3.60 (m, 1H), 2.61 (s, 3H), 2.05 (s, 3H), 1.39 (d, *J* = 7.08 Hz, 6H). ^{13}C NMR (400 MHz, $CDCl_3$): δ (ppm) 182.6, 180.7, 162.3, 146.5, 138.5, 135.2, 134.6, 132.3, 123.2, 122.4, 118.4, 116.1, 69.3, 27.0, 23.8, 21.4, and 16.2. HRMS (ESI): calcd for $C_{23}H_{32}O_3$ $[M+Na]^+$: 307.1310, found 307.1293.

G08 (3,3-dimethylallyl ether mansonone G) ^{1}H NMR (400 MHz, $CDCl_3$): δ (ppm) 7.71 (s, 1H), 6.59 (s, 1H), 5.48 (t, *J* = 5.44 Hz, 1H), 4.60 (d, *J* = 6.64 Hz, 2H), 3.58 (m, 1H), 2.62 (s, 3H), 2.05 (s, 3H), 1.82 (s, 3H), 1.76 (s, 3H), and 1.36 (d, *J* = 7.04 Hz, 6H). ^{13}C NMR: δ (ppm) 182.8, 180.7, 162.8, 146.6, 138.9, 138.6, 135.1, 134.8, 134.7, 123.0, 116.0, 65.5, 27.1, 25.9, 23.9, 23.8, 21.5, 18.5, and 16.2. HRMS (ESI): calcd for $C_{23}H_{32}O_3$ $[M+Na]^+$: 335.1623, found 335.1624.

G09 (geranyl ether mansonone G) ^{1}H NMR (400 MHz, $CDCl_3$): δ (ppm) 7.71 (s, 1H), 6.60 (s, 1H), 5.49 (t, *J* = 6.32 Hz, 1H), 5.09 (t, *J* = 5.80 Hz, 1H), 4.62 (d, *J* = 6.60 Hz, 2H), 3.57 (m, 1H), 2.63 (s, 3H), 2.05 (s, 3H), 2.12 (m, 2H), 1.75 (s, 3H), 1.67 (s, 3H), 1.61 (s, 3H), 1.37 (d, *J* = 6.96 Hz, 6H), and 1.25 (m, 2H). ^{13}C NMR: δ (ppm) 182.5, 180.4, 162.4, 146.3, 141.9, 138.3, 134.9, 131.8, 128.3, 123.4, 122.2, 119.6, 118.5, 115.7, 65.2, 39.3, 29.5, 26.1, 25.5, 23.6, 21.2, 17.6, 16.5, and 15.9. HRMS (ESI): calcd for $C_{23}H_{32}O_3$ $[M+Na]^+$: 403.2249, found 403.2252.

G10 (cinnamyl ether mansonone G) ^{1}H NMR (400 MHz, $CDCl_3$): δ (ppm) 7.72 (s, 1H), 7.37 (m, 5H), 6.66 (s, 1H), 6.76 (m, 2H), 6.42 (m, 1H), 3.63 (m, 1H), 2.64 (s, 3H), 2.06 (s, 3H), 1.42 (d, *J* = 7.04 Hz, 6H). ^{13}C NMR: δ (ppm) 182.7, 180.7, 162.2, 146.5, 138.5, 135.3, 134.8, 134.7, 134.1, 128.8, 128.4, 126.8, 123.3, 116.1, 69.3, 27.2, 23.9, 21.6, and 16.2. HRMS (ESI): calcd for $C_{23}H_{32}O_3$ $[M+Na]^+$: 383,1623, found 383.1638.

2.6.2 The Derivatization of Mansonone G into Its Ester Analogues

The derivatization of mansonone G into its ester analogues was performed into two steps.[118] Firstly, PPh_3 0.52 g (2 mmol) in CH_2Cl_2 (3 mL) was added into a mixture of *n*-butyric acid (1.05 mL, 1 mmol) and trichloroacetonitrile 0.37 g (2 mmol) in CH_2Cl_2 (3 mL) at room temperature. Then, the mixture was stirred for approximately 1 h.

The second step, mansonone G (**6**) 0.122 g (0.5 mmol) in CH_2Cl_2 (10 mL) and *4*-picoline 0.3 mL (3 mmol) were added to the previous mixture (in step 1). The mixture was refluxed and stirred at 38–40 °C for 3 h or until the reaction occurred completely (confirmed by TLC). After that, the organic layer was extracted with 10% HCl and saturated aqueous $NaHCO_3$, respectively. Furthermore, the organic layer was dried over anhydrous Na_2SO_4, filtered, and evaporated using rotatory vacuum evaporator. The product was purified by subjecting to silica gel column and eluted with hexane:EtOAc (4:1) to yield compound **G11** as orange powder (84 mg, 69%yield). The same procedure was conducted by changing *n*-butyric acid with caproic acid, caprylic acid, capric acid, benzoic acid, 2-chlorobenzoic acid, 2-methoxybenzoic acid, and 4-methoxybenzoic acid to yield compounds **G12** (15 mg, 12.3 %yield), **G13** (14 mg, 11.5 %yield), and **G14** (34 mg, 27.9 %yield), **G15** (84.4 mg, 69.2 %yield), **G16** (77.9 mg, 63.9 %yield), **G17** (34.1 mg, 27.9 %yield), and **G18** (42.6 mg, 34.9 %yield), respectively. All of these ester analogues were recognized as new semisynthetic compounds (**G11**–**G18**).

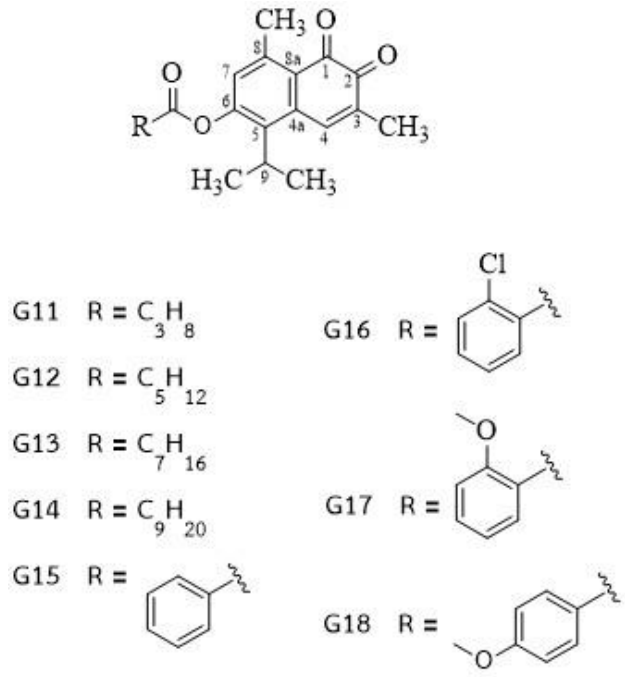

Figure 2.4 The structures of ester analogues of mansonone G

G11 (mansonone G butanoate). ^{1}H NMR (400 MHz, $CDCl_3$) : δ (ppm) 7.72 (s, 1H), 6.86 (s, 1H), 3.47 (m, 1H), 2.61 (s, 3H), 2.61 (t, *J* = 7.28 Hz, 2H), 2.07 (s, 3H), 1.82 (m, 2H), 1.36 (d, *J* = 6.72 Hz, 6H), and 1.07 (t, *J* = 7.40 Hz, 3H). ^{13}C NMR: δ (ppm) 181.7, 181.3, 171.4, 154.0, 144.5, 138.0, 137.0, 135.5, 135.2, 128.2, 127.7, 36.4, 26.8, 22.8, 21.9, 18.2, 16.0, and 13.6. HRMS (ESI): calcd for $C_{23}H_{32}O_3$ $[M+Na]^+$: 337.1416, found 337.1431.

G12 (mansonone G hexanoate). ^{1}H NMR (400 MHz, $CDCl_3$) : δ (ppm) 7.63 (s, 1H), 6.78 (s, 1H), 3.39 (m, 1H), 2.54 (s, 3H), 2.54 (t, *J* = 7.28 Hz, 2H), 2.00 (s, 3H), 1.72 (m, 2H), 1.35 (m, 2H), 1.29 (d, *J* = 7.16 Hz, 6H), 1.14 (m, 2H), and 0.87 (t, *J* = 6.84 Hz, 3H). ^{13}C NMR: δ (ppm) 181.7, 181.3, 171.6, 154.0, 144.6, 138.0, 137.0, 135.5, 135.3, 128.2, 127.8, 34.5, 31.3, 26.8, 24.3, 22.2, 22.3, 22.0, 16.0, and 13.9. HRMS (ESI): calcd for $C_{23}H_{32}O_3$ $[M+Na]^+$: 365.1729, found 365.1731.

G13 (mansonone G octanoate). ^{1}H-NMR (400 MHz, $CDCl_3$) : δ (ppm) 7.64 (s, 1H), 6.78 (s, 1H), 3.39 (m, 1H), 2.54 (t, *J* = 7.24 Hz, 2H), 2.53 (s, 3H), 2.00 (s, 3H), 1.71 (m, 2H), 1.35 (m, 2H), 1.29 (d, *J*=7.08 Hz, 6H), 1,22 (m, 6H), 0.83 (t, *J* = 5.60 Hz, 3H). ^{13}C-NMR: (ppm) 181.7, 181.3, 171.6, 154.0, 144.6, 138.0, 137.0, 135.5, 135.2, 128.2, 127.8, 34.6, 31.6, 29.0,

28.9, 26.8, 24.7, 22.8, 22.6, 22.0, 16.0, and 14.0. HRMS (ESI): calcd for $C_{23}H_{32}O_3$ [M+Na]$^+$: 393.2042, found 393.2045.

G14 (mansonone G decanoate). ^{1}H-NMR (400 MHz, $CDCl_3$) : δ (ppm) 7.70 (s, 1H), 6.85 (s, 1H), 3.46 (m, 1H), 2.62 (t, *J* = 7.60 Hz, 2H), 2.60 (s, 3H), 2.07 (s, 3H), 1.75 (m, 2H), 1.40 (m, 2H), 1.35 (d, *J* = 7.08 Hz, 6H), and 1.29 (m, 10H), 0.87 (t, *J* = 6.08 Hz, 3H). ^{13}C-NMR: δ (ppm) 181.8, 181.3, 171.6, 154.0, 144.6, 138.0, 136.9, 135.5, 135.3, 128.2, 127.8, 34.6, 31.8, 29.7, 29.4, 29.2, 29.1, 26.8, 24.7, 22.8, 22.6, 22.0, 16.0, and 14.1. HRMS (ESI): calcd for $C_{17}H_{21}O_3$ [M+Na]$^+$: 421.2355, found 421.2359.

G15 (mansonone G benzoate). ^{1}H-NMR (400 MHz, $CDCl_3$) : δ (ppm) 8.21 (d, *J* = 7.12 Hz, 2H), 7.70 (s,1H), 7.69 (t, *J* = 7.48 Hz, 1H), 7.56 (m, 2H), 6.98 (s, 1H), 3.53 (m, 1H), 2.63 (s, 3H), 2.09 (s, 3H), and 1.39 (d, *J* = 7.08 Hz, 6H). ^{13}C-NMR: δ (ppm) 181.9, 181.5, 164.8, 154.4, 144.8, 138.0, 137.4, 135.7, 135.5, 134.3, 130.5, 129.0, 128.6, 27.1, 23.0, 22.1, and 16.2. HRMS (ESI): calcd for $C_{17}H_{21}O_3$ [M+Na]$^+$: 371.1259, found 371.1262.

G16 (mansonone G 2-chloro benzoate). ^{1}H NMR (400 MHz, $CDCl_3$) : δ (ppm) 8.06 (d, *J* = 8.48 Hz, 1H), 7.74 (s, 1H), 7.55 (m, 2H),), 7.44 (m, 2H), 7.00 (s, 1H), 3.53 (m, 1H), 2.64 (s, 3H), 2.08 (s, 3H), and 1.38 (d, *J* = 7.20 Hz, 6H). ^{13}C NMR: δ (ppm) 181.8, 181.5, 163.6, 154.0, 144.8, 138.0, 137.4, 135.9, 134.9, 133.9, 131.8, 128.6, 128.2, 127.1, 27.0, 23.0, 22.2, and 16.2. HRMS (ESI): calcd for $C_{17}H_{21}O_3$ [M+Na]$^+$: 405.0870, found 405.0860.

G17 (mansonone G 2-methoxy benzoate). ^{1}H NMR (400 MHz, $CDCl_3$): δ (ppm) 7.71 (s, 1H), 6.56 (s, 1H), 6.06 (m, 1H), 5.42 (m, 1H), 5.30 (m, 1H), 4.58 (d, *J* = 5.08 Hz, 2H), 3.46 (m, 1H), 2.52 (s, 3H), 2.14 (s, 3H), 1.39 (d, *J* = 7.08 Hz, 6H). ^{13}C NMR (400 MHz, $CDCl_3$): δ (ppm) 182.6, 180.6, 161.4, 143.3, 140.3, 132.9, 132.3, 129.9, 119.3, 117.8, 114.1, 69.1, 32.4, 21.1, 18.1, and 16.1. HRMS (ESI): calcd for $C_{23}H_{32}O_3$ [M+Na]$^+$: 307.1310, found 307.1293.

G18 (mansonone G 4-methoxy benzoate). ^{1}H NMR (400 MHz, $CDCl_3$) : δ (ppm) 8.15 (d, *J* = 8.76 Hz, 2H), 7.73 (s, 1H), 7.02 (d, *J* = 2.00 Hz, 2H), 6.96 (s, 1H), 3.91 (-OCH_3), 3.52 (m, 1H), 2.63 (s, 3H), 2.08 (s, 3H), and 1.38 (d, *J* = 7.08 Hz, 6H). ^{13}C-NMR: δ (ppm) 182.0,

181.5, 164.5, 154.6, 144.7, 138.1, 137.5, 135.7, 135.4, 134.7, 133.8, 133.7, 132.7, 129.8, 129.6, 128.8, 121.2, 114.3, 55.7, 27.1, 23.0, 22.1, and 16.2. HRMS (ESI): calcd for $C_{17}H_{21}O_3$ $[M+Na]^+$: 401.1365, found 401.1370.

2.6.3 The Derivatization of Mansonone G with Epichlorohydrin

The derivatization of mansonone G (**6**) with epichlorohydrin into its mansonone G epoxide was performed using Nouailhas, *et al*. method.[119] Mansonone G (**6**, 122 mg, 0.5 mmol) was dissolved in epichlorohydrin (4 mL) and refluxed until 98°C using two-neck round-bottomed flask. At this point temperature, an ethanolic solution of NaOH (10 mg, 0.25 mmol) in 95% EtOH (1 mL) was added dropwise using a dropping funnel. The progress of the reaction was monitored by TLC. After 2 h, the reaction mixture was cooled at room temperature and added 15 mL of acetone. The white salts released as by-products were filtered out. The acetone and non-reacted excess of epichlorohydrin were evaporated using a rotatory vacuum evaporator at 80°C. The reaction product was then redissolved in 15 mL of acetone, filtered, and the filtrate was evaporated at 80°C. This last step was repeated twice. Then, the reaction product was purified by silica gel column (No. 9385, Merck) using hexane:CH_2Cl_2:EtOAc (3:2.5:0.5) to obtain **G19** (63.2 mg, 51.8% yield) and **G20** (30 mg, 24.6% yield).

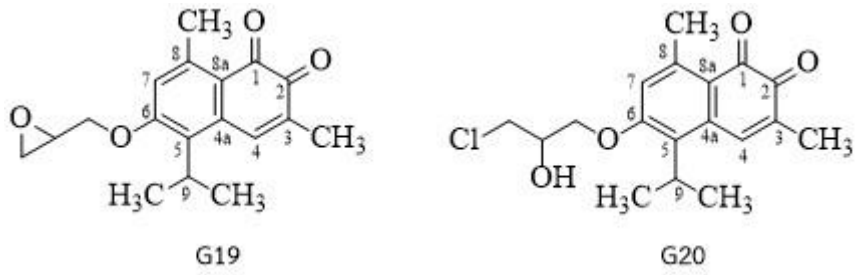

Figure 2.5 The structures of analogues of mansonone G with epichlorohydrin

G19. ^{1}H NMR (400 MHz, $CDCl_3$) : δ (ppm) 7.71 (s, 1H), 6.59 (s, 1H), 4.37 (dd, *J* = 2.8, 2.8 Hz, 1H), 3.99 (dd, *J* = 6.08, 6.08 Hz, 1H), 3.60 (m, 1H), 3.42 (m, 1H), 2.62 (s, 3H), 2.06 (s, 3H), and 1.38 (dd, *J* = 7.08 Hz, 6H). ^{13}C NMR: δ (ppm) 182.6, 180.7, 162.1, 146.5, 138.4,

135.4, 134.6, 123.6, 115.9, 69.5, 49.9, 44.7, 29.8, 27.7, 23.8, 21.5, and 16.2. HRMS (ESI): calcd for $C_{18}H_{20}O_4$ $[M+Na]^+$: 323.1259, found 323.1257.

G20. ^{1}H NMR (400 MHz, DMSO): δ (ppm) 7.76 (1H, s), 6.76 (1H, s), 5.58 (1H, s), 3.99 (t, *J* = 9.16 Hz, 4H), 2.39 (s, 3H), 1.81 (s, 3H), and 1.19 (d, *J* = 6.88 Hz, 6H). ^{13}C NMR: δ (ppm) 181.7, 180.1, 162.1, 145.3, 138.0, 135.0, 134.2, 133.8 122.7, 116.0, 69.7, 68.6, 46.6, 26.3, 23.1, 21.2, 18.2, and 15.5. HRMS (ESI): calcd for $C_{18}H_{21}ClO_4$ $[M+H]^+$: 336.1128, found 337.1237.

2.7 The Evaluation of Antibacterial Activity

2.7.1 Test Microorganisms

The test microorganisms belong to both Gram positive and Gram negative bacteria. Gram positive bacteria including *Staphylococcus aureus* ATCC 25923, *Streptococcus mutans* ATCC 25175, *Streptococcus sobrinus* KCCM 11898, and *Propionibacterium acnes* KCCM 41747 were employed in this bioassay, while *Salmonella typhi* ATCC 422 was used as representative for Gram negative bacteria. The bacteria were periodically sub-cultured and maintained in nutrient agar medium.

2.7.2 Preparation of Microbial Inoculum

Some colonies of each test organism were inoculated into nutrient broth (NB) and incubated at 37°C for 18-24 h. Then, the turbidity produced was adjusted to match Mc Farland 0.5 standard (99.5 mL of 1% H_2SO_4 and 0.5 mL of 1.175% $BaCl_2$). Then this suspension of bacteria was used for antibacterial activity.

2.7.3 Antibacterial Activity Test

Antibacterial activity was determined by agar well diffusion method as described by Karuppiah and Mustaffa method with some modification.[120] Nutrient agar which contains 8 g nutrient broth and 20 g agar powder in 1 L distilled water, was

autoclaved at 121°C for 15 min. Then 25 mL nutrient agar was poured into a sterilized petri dish (9 mm diameter). The plates were left at room temperature for solidification. Tested bacterial suspension (0.5 MF, 100 µL) was swabbed onto the agar surface. Wells (diameter 6 mm) were then punched in the agar using a sterile cork-borer. About 30 µL of 1 mM compound was placed into the well. The clear zone was measured in mm after 18 – 24 h incubation at 37°C. All experiments were done in triplication and the results were expressed as average values. Chloramphenicol (0.5 mM) was used as a positive control and acetone (sample solvent) as a negative control.

2.7.4 Determination of Minimum Inhibitory Concentration (MIC) Value

Minimum inhibitory concentration (MIC) value of compound was determined by the method as described by Sawasdee with some modification.[121] The tested compound was dissolved in DMSO to prepare stock solutions of 1000 µM. From this stock solution, the concentrations of compound were varied and prepared by using nutrient broth. Triplicate 50 µL compounds each concentrations were placed into sterile 96-well plates. The suspension of bacteria (0.5 MF) were diluted 1:200 (~10^6 CFU/Ml) using nutrient broth and 50 µL added to the top well in each row. Plates were incubated at 37°C for 15 h, then 10 µL of resazurin indicator (0.18%) was added to each well and determined after incubation for 2–3 h. Chloramphenicol was used as positive control.

2.8 The Evaluation of Anti-adipogenic Activity

2.8.1 Cell Culture

3T3-L1 cells were maintained in DMEM which supplemented with 10% of BCS. These cells (1x10^5 cells/10 mL) were maintained every two days in petridish (diameter 100 mm) and incubated in incubator at 37°C supplemented with constant 5% CO_2.

2.8.2 Differentiation of 3T3-L1 Cells in 24-Wells Plate

In second day, 3T3-L1 cells were then seeding into 24-wells plate using DMEM supplemented with 10% of FBS. Each well contained $2x10^4$ cells/0.5 mL. After cells grown to confluence for 48 h, the medium was changed to 10% FBS/DMEM containing dexamethasone (1 µM), insulin (5 µg/mL), and rosiglitazone (10 µM), to differentiate adipocytes (day 0). Medium was then replaced with 10% FBS/DMEM containing insulin (5 µg/mL) after 48 h and refreshed with 10% FBS/DMEM every other day during differentiation. In order to investigate the effect of all isolated compounds (mansorins and mansonones) and several mansonone derivatives on adipogenesis, cells were treated with 10 µM of compounds (dissolved in DMSO) and/or by varying the concentrations as 0, 1, 5, 10, 20, and 50 µM for several candidate compounds, in differentiation day 0, day 2, day 4, and day 6. Cells were incubated in incubator at 37°C supplemented with constant 5% CO_2.

2.8.3 Oil Red O Staining

At differentiation day 7, cells were taken from incubator and washed with PBS, then followed by adding 10% formalin (1 mL) into each well at room temperature. The plates were wrapped with transparent plastic and aluminium foil. After a couple days of incubation, the formalin was discarded and washed the cells with 60% isopropanol. Then removed isopropanol and left the wells dried completely. Into dried wells, Oil Red O working solution was added and incubated for 10 min at room temperature. Stained cells were washed with distilled water 2 or 3 times and dissolved in 100% isopropanol for measuring the absorbance at 500 nm.

2.8.4 Preparation for Western Blot Analysis

2.8.4.1 Differentiation of 3T3-L1 Cells in 6-Wells Plate

In general, the procedure was the same as the differentiation of 3T3-L1 cells in 24-wells plate. For 6-well plate, the 3T3-L1 were seeding with the density of cells

$1x10^5$ cells/2 mL/well. The cells were treated by compounds with various concentrations as 0, 1, 5, 10, 20, and 50 μM, in differentiation day 0, day 2, day 4, and day 6. Cells were incubated in incubator at 37°C supplemented with constant 5% CO_2.

2.8.4.2 Preparation for Protein Extraction

At day 7, cells in 6-well plates were taken from incubator and followed by protein preparation procedure. For harvesting the detachment of cells, gently scrapped the cells using a plastic cell scrapper and then collected the cells into 15 mL centrifuge tube. These cells were then centrifuged at 1000 rpm, room temperature, for 3 min. After centrifugation finished, the supernatants were discarded and cold PBS (1 mL) was added into each tube, homogenized by pipetting 2 until 3 times. Remove the solution of cells into Eppendorf tubes completely and centrifuge at 5000 rpm, 4°C, for 3 min. Removed all PBS using pipet (in ice). These pellets can be stored in -70°C deep freezer before continued for the next step.

2.8.4.3 Cells Lysis for Protein Extraction

The pellets from deep freezer were moved into ice and added 50 μL of lysis buffer containing DTT (1 mM), PMSF (1 mM), Na_3VO_4 (1 mM), and protease inhibitor. Incubate for 20 min in ice and vortex the tubes every 5 min for 5 sec. Then centrifuged at 12.000 rpm, 4°C, for 10 min.

2.8.4.4 Determination of Protein Concentration by Bradford Protein Assay

In order to determine the concentration of protein, a protein quantification assay was performed by using Bradford protein assay. Some Eppendorf tubes were prepared and pipetted 1 mL of Bradford reagent into each tube. A small volume (1 μL) of lysate was used to perform this protein quantification assay. BSA (10 mg/mL) was added as 0, 1, 2, 4, and 8 μL, for standard in this assay. After that measured the absorbance at 595 nm.

2.8.4.5 Preparation of PAGE Gel

7.5% polyacrylamide gel (running gel) was prepared by mixing 2400 µL of ADW, 1250 µL of 1.5 M Tris (pH 8.8), 1250 µL of 30% AA, 50 µL of 10% SDS, 50 µL of 10% APS, and 5 µL of TEMED, in a conical flask and shake. Put this mixture using pipet between the glass plates which already set up at the casting frame and casting stand (Figure 2.6) to about ¾ inch below the short plate. A small layer of ADW was added on top of the gel. Incubation for 20 min to let it become gel.

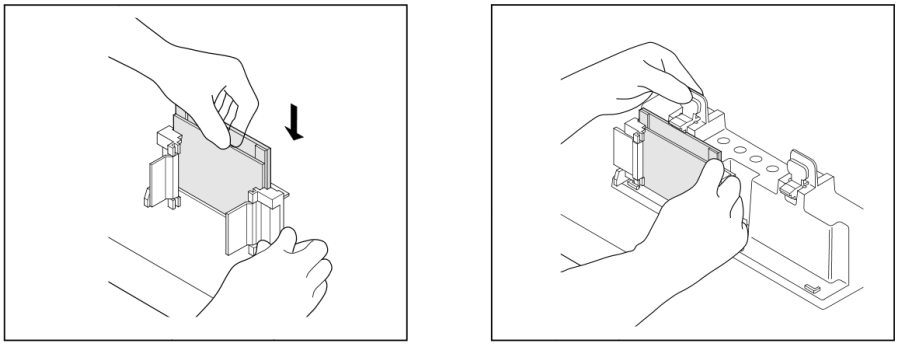

Figure 2.6 Gel casting frame and casting stand [122]

While waiting the running gel become gel, the stacking gel was prepared by mixing 1400 µL of ADW, 250 µL of 1 M Tris (pH 6.8), 330 µL of 30% AA, 20 µL of 10% SDS, 20 µL of 10% APS, and 2 µL of TEMED, in a conical flask and shake. After running gel polymerized, then absorb the DW using filter paper and pipet stacking gel until overflow. Insert the well forming comb into the opening between the glass plates and incubate for 10 min.

2.8.4.6 Sample Preparation

The amount of protein sample according to protein quantification assay was mixed with sample buffer containing 2x Laemmli sample buffer and β-mercaptoethanol. Boiled the protein sample in 100°C water bath for 3 min and put in ice directly before pipet into gel.

2.8.4.7 SDS-PAGE Electrophoresis

The gel cassette from the casting stand was removed and placed in the electrophoresis tank with the short plate inside. Take out the well forming comb and pour enough running buffer into the tank as well as into the wells. Slowly loaded samples and protein marker into each well using pipet. Cover the top of tank with the lid aligning the electrodes (black or red) appropriately. Connect the electrophoresis tank to the power supply and allowed the samples to run at 15–20 mA, 180 V, for 1.5 h.

2.8.4.8 Protein Transfer

After SDS-PAGE electrophoresis finished, prepared transfer tank for protein transfer process which already filled with TBST. In addition, also prepared cassette, sponge, filter papers (2 pieces per gel), and NC membrane, which soaked in TBST for 15 min.

The gel from electrophoresis tank was taken carefully from the cassette. Remove the stacking gel buy cutting this gel and then covered with filter paper. At the opposite side of gel, cover with NC membrane, afterwards put filter paper on this membrane. Put this component between the sponges in the cassette and set to the clamp. Cover the top of tank with the lid aligning the electrodes (black or red) appropriately. Connect the transfer tank to the power supply and allowed the samples to run at 200 mA, 300 V, for 1 h.

2.8.4.9 Western Blot Analysis

The NC membrane was taken from the cassette carefully and mark the band showed by pencil or pen. Put this membrane into 10 – 15 mL of blotting buffer (3 % BSA in TBST containing 0.1% Tween 20) and shake for 30 min at room temperature. After discard BSA, 10 mL of adiponectin (1:1000 dilution) as primary antibody was added and incubated by shaking overnight at 4°C in cold room.

Subsequently, removed the primary antibody and washed membrane with 10–15 mL of 0.1% Tween 20/TBST, shake for 10 min at room temperature, and discard the solution. This step was repeated three times. After that rabbit antibody was added as secondary antibody and incubated for 1 h by shaking at room temperature. Then, washed the membrane with 10–15 mL of 0.1% Tween 20/TBST, shake for 10 min at room temperature, and discard the solution. This step was also repeated three times.

After that, put the membrane into developer cassette on transparent plastic, spread the ECL solution containing ECL1 and ECL2 onto the membrane, and covered the membrane with other transparent plastic. Then, developed the images on film in dark room.

CHAPTER III

RESULTS AND DISCUSSION

3.1 Extraction of *Mansonia gagei* Heartwoods

About 10 kg of dried powder of *M. gagei* heartwoods was extracted by soaking in CH_2Cl_2 at room temperature, leaving for three days, filtering, and evaporating. This step was repeated three times with fresh solvent. The crude CH_2Cl_2 extract was obtained as dark-brown (276 g, 2.76% yield of dried-powdered heartwoods).

3.2 Separation of the CH_2Cl_2 Extract of *Mansonia gagei* Heartwoods

A part of the CH_2Cl_2 extract of *M. gagei* heartwoods (200 g) was subjected to silica gel quick column. The column was initially eluted with hexane 100%, then followed by increasing polarity with a mixture of EtOAc in hexane (5–80%), EtOAc 100%, and final with a mixture of MeOH in EtOAc (5–10%). Approximately 1 L of solvent was collected for each fraction and then evaporated the solvent using vacuum rotary evaporator. The fractions were collected and combined based on TLC results, eight fractions (MGD1-MGD8) were obtained. The results of fractionation of the CH_2Cl_2 extract are shown in Table 3.1.

Table 3.1 The fractionation of the CH_2Cl_2 extract of *M. gagei* heartwoods by quick column

Eluent (% volume by volume)	Fraction	Remarks	Weight (g)
Hexane – 5% EtOAc/hexane	MGD1	Yellow oil	0.77
5% EtOAc/hexane	MGD2	Yellow-brown solid	2.37
5% – 20% EtOAc/hexane	MGD3	Red-brown solid	6.06
20% EtOAc/hexane	MGD4	Red-brown solid	11.33
20% – 60% EtOAc/hexane	MGD5	Brown solid	64.50
60% – 80%EtOAc /hexane	MGD6	Brown solid	16.70
80% EtOAc	MGD7	Brown solid	6.77
EtOAc – 10% MeOH/EtOAc	MGD8	Brown solid	29.34

Fractions MGD3, MGD4 and MGD5 were further separated using silica gel column. The columns were eluted with step gradient of hexane-EtOAc and EtOAc-MeOH as solvent systems. There were seven isolated compounds obtained after further separation of fractions on silica gel column. Mansorin A (**1**, 716 mg), mansorin C (**3**, 32 mg) and mansonone C (**4**, 77 mg) were isolated from MGD3. The separation of MGD4 furnished mansorin B (**2**, 64 mg) and mansonone E (**5**, 207 mg). Mansonone G (**6**, 9.9 g) as a major compound of this extract was obtained from the precipitate formed by quick column and also from further separation of both MGD4 and MGD5. Mansonone H (**7**, 196 mg) was isolated from MGD5. In brief, the separation and purification of chemical constituents from the CH_2Cl_2 extract of *M. gagei* heartwoods are summarized in Scheme 3.1.

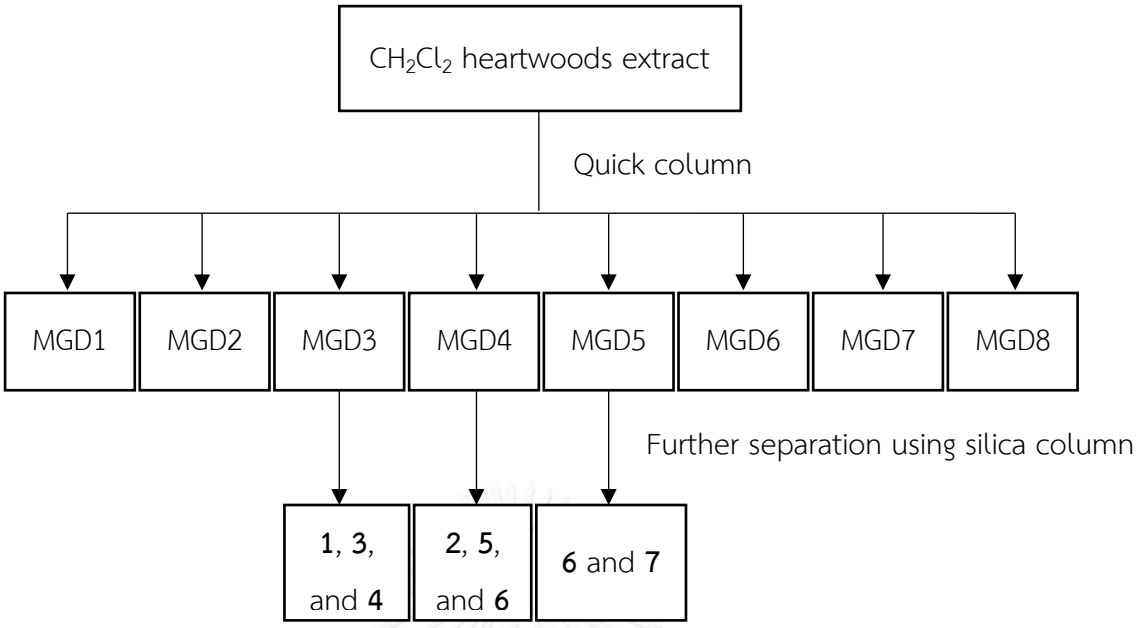

Scheme 3.1 Separation and purification of chemical constituents from the CH_2Cl_2 extract of *M. gagei* heartwoods

3.3 Structural Elucidation of Isolated Compounds

The structural identification of these compounds were conducted by comparing spectroscopic data with previous studies.[69, 71] The NMR spectral data of compounds **1**–**3** and compounds **4**–**7** are presented in Tables 3.2 and 3.3, respectively.

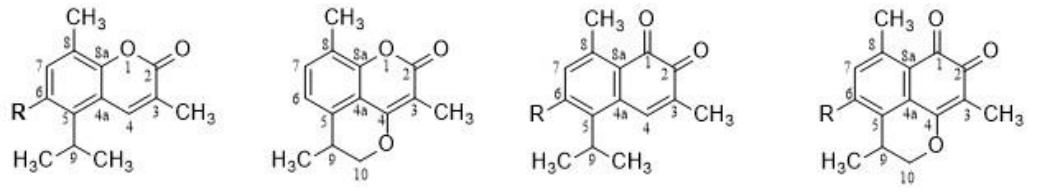

mansorin A (1) R = OCH_3
mansorin B (2): R = OH

mansorin C (3)

mansonone C (4) R = H
mansonone G (6) R = OH

mansonone E (5) R = H
mansonone H (7) R = OH

Table 3.2 Tentative ^{1}H NMR chemical shifts assignment of compounds **1**–**3**

Position	Chemical shift (ppm)		
	Compound **1**	Compound **2**	Compound **3**
4	7.90 (s, 1H)	7.90 (s, 1H)	-
6	-	-	7.00 (d, *J* = 7.6 Hz, 1H)
7	6.90 (s, 1H)	6.77 (s, 1H)	7.31 (d, *J* = 7.6 Hz, 1H)
9	3.55 (m, 1H)	3.53 (m, 1H)	3.17 (m, 1H)
10	-	-	4.13 (dd, *J* = 6.7, 10.8 Hz, 1H) 4.41 (dd, *J* = 4.1, 10.7 Hz, 1H)
3-CH_3	2.23 (s, 3H)	2.24 (s, 3H)	2.07 (s, 3H)
6-OCH_3	3.83 (s, 3H)	-	-
6-OH	-	5.19 (s, 1H)	-
8-CH_3	2.42 (s, 3H)	2.35 (s, 3H)	2.43 (s, 3H)
9-$(CH_3)_2$	1.37 (d, *J* = 7.1 Hz, 6H)	1.42 (d, *J* = 7.0 Hz, 6H)	1.33 (d, *J* = 7.0 Hz, 3H)

Table 3.3 Tentative ^{1}H NMR chemical shift assignments of compounds **4**–7

Position	Chemical shift (ppm)			
	Compound **4**	Compound **5**	Compound **6**	Compound **7**
4	7.65 (s, 1H)	-	7.87 (s, 1H)	-
6	7.19 (d, *J* = 8.0 Hz, 1H)	7.34 (d, J = 8.5 Hz, 1H)	-	-
7	7.43 (d, *J* = 8.1 Hz, 1H)	7.00 (d, *J* = 7.6 Hz, 1H)	6.64 (s, 1H)	6.84 (s, 1H)
9	3.38 (m, 1H)	3.17 (m, 1H)	3.63 (m, 1H)	3.32 (m, 1H)
10	-	4.22 (dd, *J* = 10.1, 4.3 Hz, 1H)	-	4.48 (d, *J* = 10.9 Hz, 1H)
		4.40 (dd, *J* = 10.1, 3.4 Hz, 1H)		4.36 (dd, *J* = 10.9, 3.3 Hz, 1H)
3-CH_3	2.08 (d, *J* = 1.8 Hz, 3H)	1.95 (s, 3H)	1.95 (s, 3H)	1.86 (s, 3H)
8-CH_3	2.63 (s, 3H)	2.65 (s, 3H)	2.45 (s, 3H)	2.52 (s, 3H)
9-$(CH_3)_2$	1.29 (d, *J* = 7.0 Hz, 1H)	1.36 (d, *J* = 7.1 Hz, 3H)	1.34 (d, *J* = 7.0 Hz, 6H)	1.32 (d, *J* = 7.0 Hz, 3H)

3.4 Preliminary Antibacterial Activity of Isolated Compounds

All isolated compounds were examined for their antibacterial activity which was performed using agar well diffusion method. This protocol is one of common techniques to determine antibacterial activity. Four Gram positive bacteria (*Staphylococcus aureus* ATCC 25923, *Streptococcus mutans* ATCC 25175, *Streptococcus sobrinus* KCCM 11898, and *Propionibacterium acne* KCCM 41747) and a Gram negative bacteria (*Salmonella typhi* ATCC 422) were employed. All isolated compounds except for mansorin C (**3**) were prepared in acetone as 1 mM. Mansorin C (**3**) was not evaluated for its antibacterial activity due to its small quantity obtained. Chloramphenicol (0.5 mM) and acetone were used as positive and negative control, respectively. The results of antibacterial activity of isolated compounds are presented in Table 3.4.

Table 3.4 Inhibition zone of isolated compounds

Compound (1 mM)	Diameter of inhibition zone (mm)				
	S. aureus ATCC 25923	*S. mutans* ATCC 25175	*S. sobrinus* KCCM 11898	*P. acnes* KCCM 41747	*S. typhi* ATCC 422
Mansorin A (**1**)	9.0±0.82	8.7±0.47	7.8±0.94	7.2±0.58	7.0±1.47
Mansorin B (**2**)	12.0±0.00	9.8±0.47	8.3±0.82	10.4±0.38	8.5±0.82
Mansonone C (**4**)	12.7±0.58	13.7±1.15	9.3±0.58	13.3±0.38	11.3±1.89
Mansonone E (**4**)	19.7±0.58	20.3±1.15	16.7±0.58	13.5±0.43	11.6±0.38
Mansonone G (**5**)	13.7±1.15	14.7±0.58	10.0±0.00	15.6±1.23	11.9±1.18
Mansonone H (**6**)	12.0±1.00	10.3±1.53	8.3±0.58	11.9±1.13	11.0±0.25
Chloramphenicol (0.5 mM)	20.7±0.58	20.7± 0.58	20.3±0.58	17.0±1.23	21.7±0.58

Values are presented as mean ±SD of triplicate experiments

Diameter of inhibition zone including diameter of well (6 mm)

Note: 6.0 = No activity, 6.1 – 8.0 = Weak, 8.1 – 10.0 = Moderate, 10.1 – 13.0 = Good, 13.1 – 15.0 = Very good, >15 = Excellent

There were two kinds of secondary metabolites isolated from the CH_2Cl_2 heartwoods extract of *M. gagei, i.e.* coumarins and 1,2-naphthoquinones. As shown in Table 3.9, mansorins A (**1**) and B (**2**) as representative of coumarins displayed weak to good antibacterial activity against all bacteria, with diameter of inhibition zone (mm) ranging from 9.0 – 12.0 against *S. aureus*, 8.7 – 9.8 against *S. mutans*, 7.8 – 8.3 against *S. sobrinus*, 7.2 – 10.4 against *P. acnes*, and 7.0 – 9.5 against *S. typhi*. While mansonones exhibited moderate to excellent antibacterial activity with diameter of inhibition zone (mm) ranging from 12.0–19.7 against *S. aureus*, 10.3 – 20.3 against *S. mutans*, 8.0 – 15.7 against *S. sobrinus*, 11.9 – 15.6 against *P. acnes*, and 1.0 – 11.9 against *S. typhi*.

According to these results, mansonones exhibited relatively more effective activity than mansorins. Previous studies also reported the same trend of these two groups in other activities. It visualized that mansonones resulted better activity than mansorins in Brine Shrimp Lethality test, as well as in anticancer, antifungal, antithrombin, and anti-estrogenic.[71, 72] This result indicated that the quinone moiety (pharmacophoric element) in typical 1,2-naphthoquiones played significant role in biological activity. In addition, quinone-containing compounds have been well known to possess important physiological functions in animals and plants.[83]

Moreover, the results also showed that *S. typhi*, which was rather difficult to be inhibited. Previous studies reported that Gram-positive bacteria were easier to inhibit than Gram-negative bacteria.[123, 124] The difference of the cell wall structure and cell wall membrane properties of both Gram-positive and negative bacteria may be as the reason for this behavior. Gram-positive bacteria is known to have an outer peptidoglycan layer which could not be as an effective permeability barrier.[123] While the outer cell membrane of Gram-negative bacteria contains lipopolysaccharides (LPS) which can facilitate in creating a permeability barrier and protect the cells of bacteria.[124]

Among mansonones, it showed that mansonones E (**5**) and G (**6**) displayed higher activity than other mansonones with inhibition zone of 19.7 and 13.7 for *S. aureus*, 20.3 and 14.7 for *S. mutans*, 16.7 and 10.0 for *S. sobrinus*, 13.5 and 15.6 for *P.*

acnes, 11.6 and 11.9 for *S. typhi,* respectively. As described previously, it was known that the structures between mansonones C (**4**) and G (**6**), as well as between mansonones E (**5**) and H (**7**) were similar except for having the difference substituent only at C6. The different substituent attached to the structures of mansonones C (**4**) and G (**6**) as well as mansonones E (**5**) and H (**7**), contributed the different results in antibacterial activity. The substituents on the parent compounds were found to have great influence on bioactivity.

In comparison with the structures between mansonones C (**4**) and G (**6**), it was found that mansonone G (**6**) having an –OH group provided better activity than that having H, mansonone C (**4**). The presence of –OH group in mansonone G (**6**) made this compound more polar than mansonone C (**4**), and hence mansonone G (**6**) could be easier to disturb the permeability of membrane cell wall of bacteria. In contrast to mansonones E (**5**) and H (**7**), the presence of –OH group in mansonone H (**7**) did not promise to give better activity because it made mansonone H (**7**) being too polar and resulted rather difficult to diffuse to the membrane of bacteria cell wall. The comparison of polarity of these compounds are figured in Figure 3.1. In this case, it can be assumed that the polarity of compound gave the influence to the cell wall membrane permeability. The compound which was not too polar and not too nonpolar was required for disturbing the permeability of cell wall membrane of bacteria.

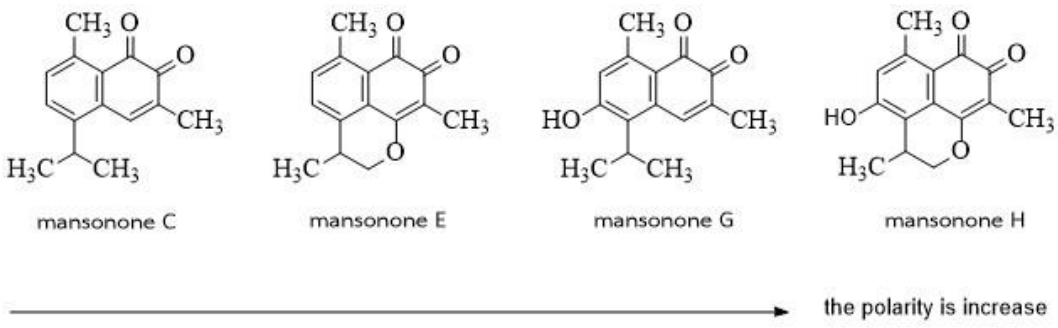

Figure 3.1 The comparison of the polarity of mansonones C, E, G, and H

3.5 Synthesis of Mansonone G Derivatives

Due to mansonone G showing good antibacterial activity against some bacteria, some derivatives were synthesized. In brief, the synthetic procedure for mansonone G derivatives is summarized in Scheme 3.2.

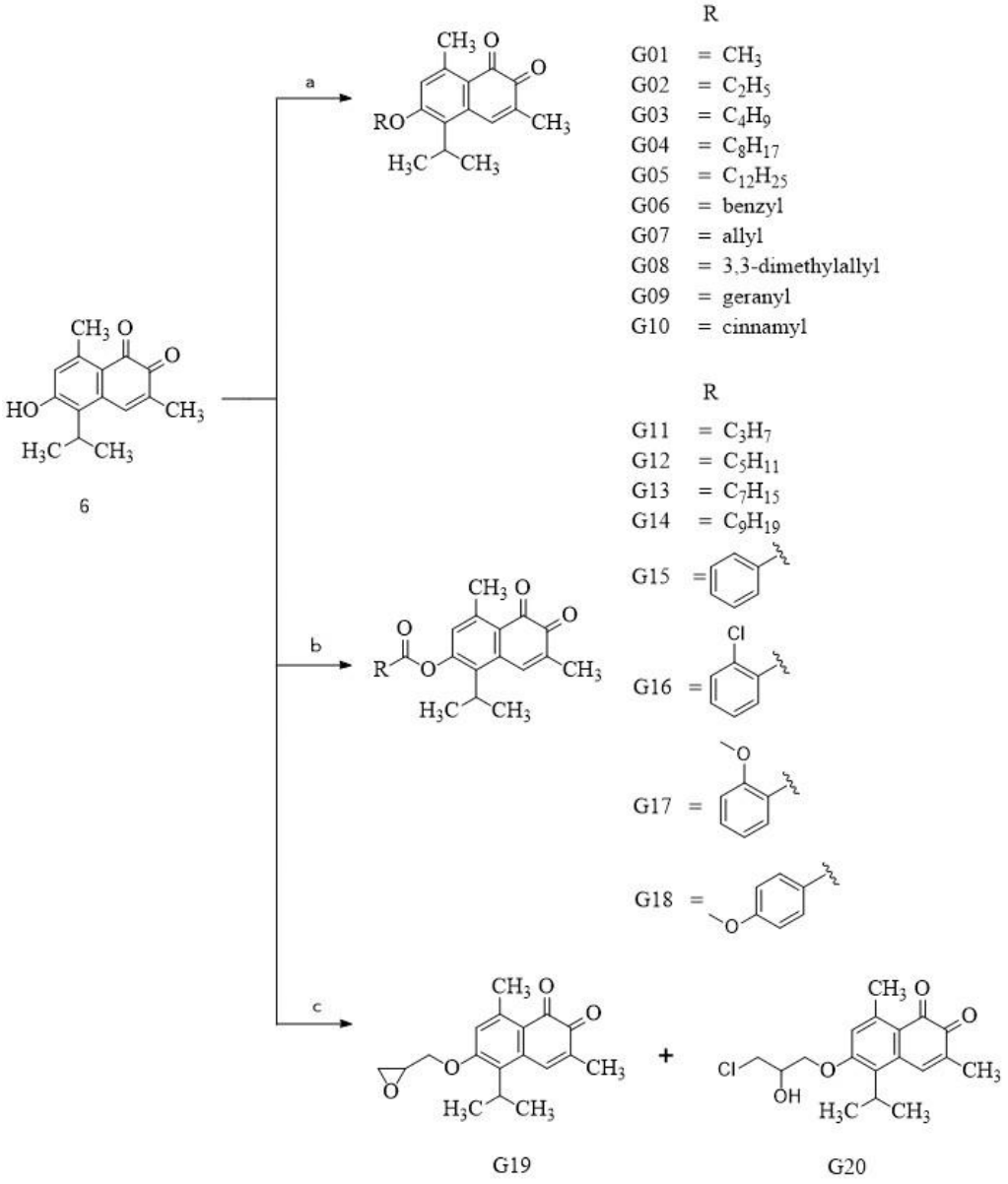

Reagents and conditions: a. alkyl halide, K_2CO_3, acetone, reflux at 78°C, 5 – 8 h; b. Carboxylic acid, trichloroacetonitrile, CH_2Cl_2, 4-picoline, reflux at 30°C for 2 h; c. Epichlorohydrin, NaOH in EtOH, reflux at 90°C for 2 h.

Scheme 3.2 General procedure for the synthesis of mansonone G derivatives

3.5.1 Ether Analogues of Mansonone G

According to Scheme 3.2, ten ether analogues of mansonone G (**G01** – **G10**) were synthesized using El-Halawany, *et al*. method.[79] Several reagents such as K_2CO_3, aliphatic alkyl and allyl halides in acetone were employed in the reaction under reflux condition at 78°C for 5 – 8 h.

The alkylation was performed using several alkyl or allyl halides, including methyl iodide, ethyl bromide, *n*-butyl bromide, octyl bromide, dodecyl bromide, allyl bromide, 3,3-dimethylallyl bromide, geranyl bromide, benzyl bromide, and cinnamyl bromide). After refluxed and further purification by silica gel column, the desired products were obtained as shown in Table 3.5.

Table 3.5 The yields and characteristics of ether analogues of mansonone G (G01–G10)

Ether analogues	Appearance	Weight (mg)	Yield (%)	Remarks
G01	Orange powder	100	82	Known
G02	Orange needle	98	80	New
G03	Orange powder	96	79	New
G04	Orange powder	93	76	New
G05	Orange powder	119	98	New
G06	Orange powder	62	50	New
G07	Orange powder	47	39	New
G08	Orange powder	61	50	New
G09	Orange powder	72	62	New
G10	Orange powder	49	40	New

As presented in Table 3.5, the derivatives synthesized from the alkylation of mansonone G (**6**) with aliphatic alkyl halides could be achieved in good to excellent yields (**G01**–**G05**, 76–98%). While the reaction of mansonone G (**6**) with allyl halides provided the poor production (**G07** and **G08**, 39 and 50%, respectively) and geranyl

bromide in moderate yield (**G09**, 62%). For compounds **G06** and **G10** were obtained in poor yield (50 and 40%, respectively).

3.5.2 Structural Elucidation of Ether Analogues of Mansonone G

The structural identification of these compounds were conducted by NMR and MS analysis. Amongst these ether analogues, **G02**–**G10** were identified as new semisynthetic compounds, while **G01** was a known compound.

G01 (methyl ether mansonone G) was obtained as an orange powder from the methylation of mansonone G (**6**) by MeI in the presence of K_2CO_3. The ^{1}H NMR spectrum (Figure 3.2) of this compound exhibited the signals of an isopropyl group at δ_H 3.58 and 1.35 ppm, two singlets of methyl groups at δ_H 2.0 4 and 2.62 ppm, an aromatic proton at δ_H 6.60 ppm and an olefinic proton at δ_H 7.70 ppm. The presence of O-CH_3 signal was assigned at δ_H 3.83 ppm which replaced the hydroxyl group in mansonone G. Moreover, according to its ^{13}C NMR spectrum (Figure 3.3), O-CH_3 group was assigned at δ_C 55.3 ppm. The comparison of ^{1}H NMR spectra of **G01** with methyl ether mansonone of G is depicted in Table 3.6. According to the spectral data from previous study, it can be concluded that **G01** was methyl ether mansonone G.

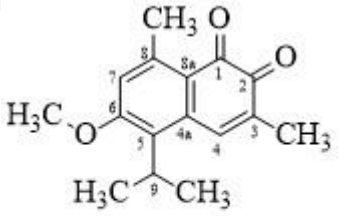

G01

Table 3.6 Tentative NMR chemical shift assignment of methyl ether mansonone G and **G01**

Position	Chemical shift (ppm)		
	Methyl ether mansonone G [79]	**G01**	
	δ_H	δ_H	δ_C
1	-	-	182.4
2	-	-	180.4
3	-	-	134.9
4	7.71 (s, 1H)	7.70 (s, 1H)	146.3
4a	-	-	134.3
5	-	-	134.3
6	-	-	163.0
7	6.60 (s, 1H)	6.60 (s, 1H)	114.8
8	-	-	138.3
8a	-	-	122.8
O-CH_3	3.91	3.90	55.3
9	3.59 (m, 1H)	3.58 (m, 1H)	26.6
3-CH_3	2.06 (s, 3H)	2.04 (s, 3H)	15.9
8-CH_3	2.64 (s, 3H)	2.62 (s, 3H)	21.2
9-$(CH_3)_2$	1.37 (d, *J* = 6.9 Hz, 6H)	1.35 (d, *J* = 7.0 Hz, 6H)	23.5

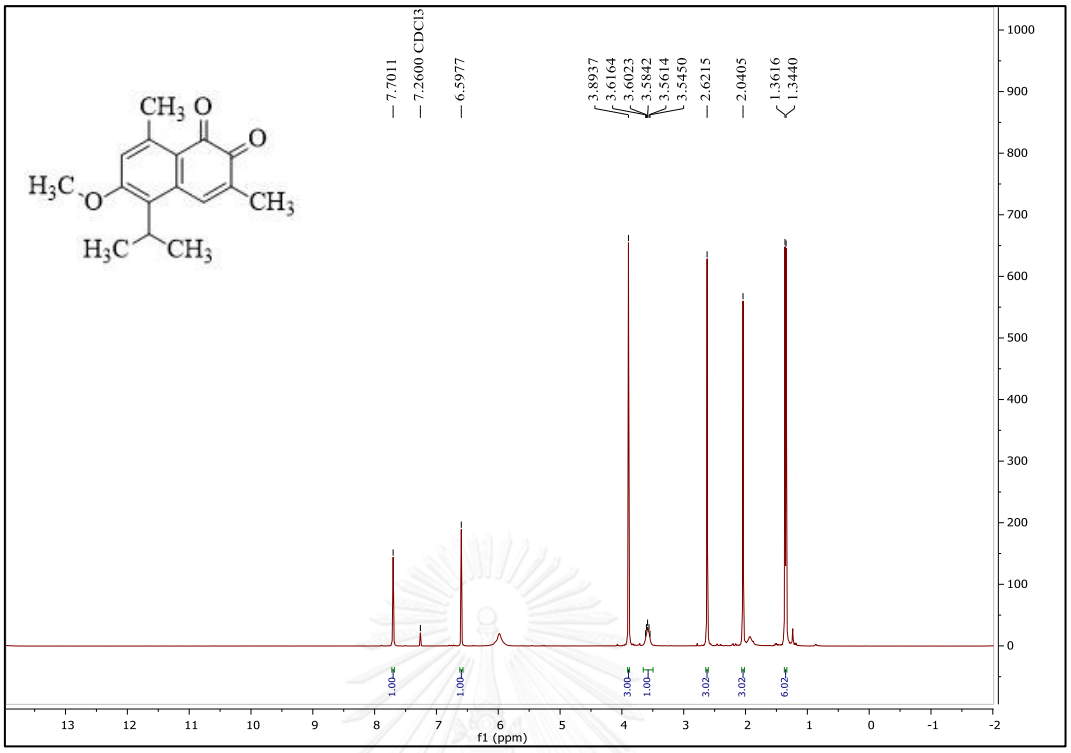

Figure 3.2 The ^{1}H NMR spectrum of **G01**

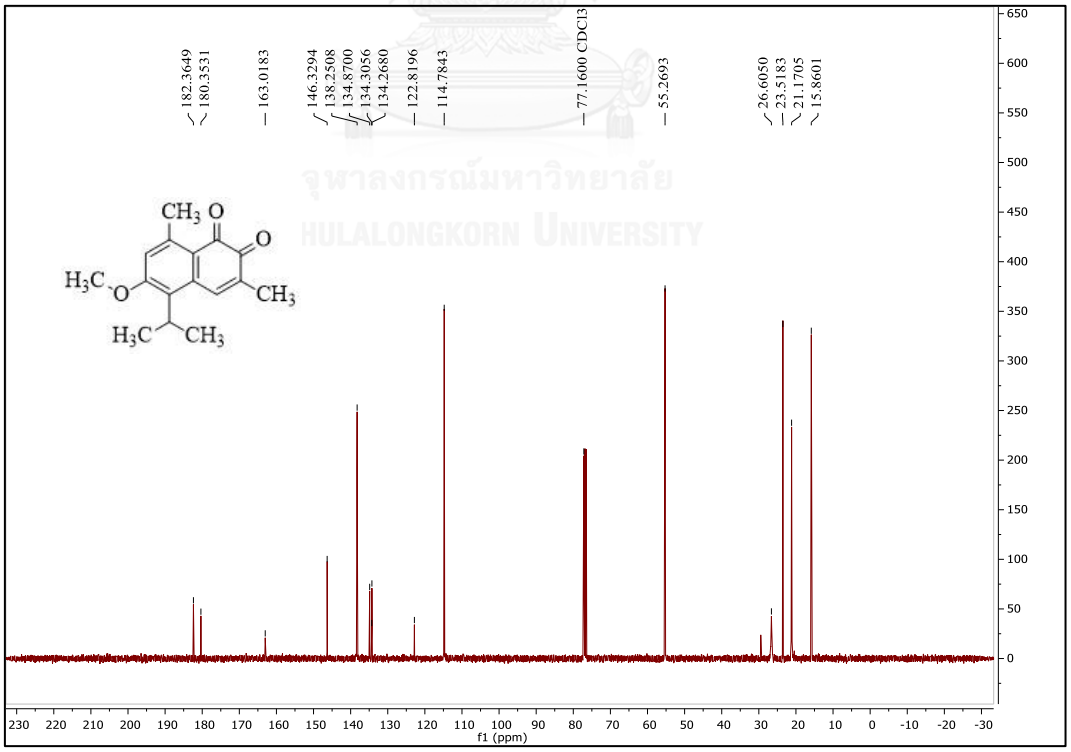

Figure 3.3 The ^{13}C NMR spectrum of **G01**

G02–**G05**, four aliphatic ether analogues of mansonone G were attained from the alkylation of mansonone G (**6**) with EtBr, *n*-butyl bromide, octyl bromide and dodecyl bromide in the presence of K_2CO_3, respectively. The yield and appearance were recorded as presented in Table 3.5. Their ^{1}H and ^{13}C NMR spectra of these new semisynthetic compounds are collected in Figures 3.4-3.11 and their tentative chemical shift assignments are presented in Tables 3.7-3.8.

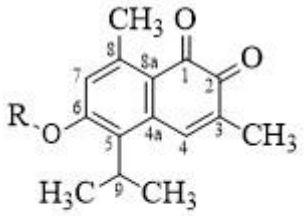

G01 R = CH_3

G02 R = C_2H_5

G03 R = C_4H_9

G04 R = C_8H_9

G05 R = $C_{12}H_{25}$

Table 3.7 Tentative ^{1}H NMR chemical shift assignments of **G02**–**G05**

Position	δ_H (ppm)			
	G02	**G03**	**G04**	**G05**
4	7.64 (s, 1H)	7.64 (s, 1H),	7.71 (s, 1H)	7.64 (s, 1H)
7	6.51 (s, 1H)	6.59 (s, 1H)	6.59 (s, 1H)	6.52 (s, 1H)
9	3.57 (m, 1H)	3.56 (m, 1H)	3.59 (m, 1H)	3.53 (m, 1H)
3-CH_3	1.98 (s, 3H)	1.98 (s, 3H)	2.10 (s, 3H)	1.97 (s, 3H)
8-CH_3	2.55 (s, 3H)	2.55 (s, 3H)	2.62 (s, 3H)	2.54 (s, 3H)
9-$(CH_3)_2$	1.32 (d, *J* = 6.20	1.31 (d, *J* = 6.20	1.41 (d, *J* = 6.20	1.31 (d, *J* = 6.92
	Hz, 6H).	Hz, 6H),	Hz, 6H)	Hz, 6H)
6-OR	-CH_2CH_3	-$(CH_2)_3CH_3$	-$(CH_2)_7CH_3$	-$(CH_2)_{11}CH_3$
	4.08 (q, *J* = 6.96	3.99 (t, *J* = 6.48	4.04 (t, *J* = 6.44	3.97 (t, *J* = 6.40
	Hz, 2H)	Hz, 2H)	Hz, 2H)	Hz, 2H)
	1.43 (t, *J* = 6.96	1.01 (t, *J* = 7.36	1.86 (m, 2H)	1.78 (m, 2H),
	Hz, 3H)	Hz, 3H), and	1.50 (m, 2H)	1.43 (m, 2H),
		0.95 (m, 4H)	1.32 (m, 8H)	1.22 (m, 16H)
			0.89 (t, *J* = 6.12	0.80 (t, *J* = 6.04
			Hz, 3H)	Hz, 3H).

Table 3.8 Tentative ^{13}C NMR chemical shift assignments of **G02–G05**

Position	δ_C (ppm)			
	G02	**G03**	**G04**	**G05**
1	182.6	182.6	182.6	182.6
2	180.5	180.5	180.5	180.4
3	162.6	162.8	162.8	162.8
4	146.5	146.5	146.5	146.5
4a	138.3	138.4	138.4	138.4
5	135.1	135.0	135.0	135.0
6	134.5	134.4	134.5	134.4
7	134.3	134.4	134.3	134.3
8	122.9	122.7	122.8	122.8
8a	115.5	115.5	115.5	115.5
6-OR	14.6, 16.1, 21.3, 23.7, 26.9, 64.1	13.7, 16.0, 19.4, 21.4, 23.7, 26.9, 31.1, 68.3	14.1, 16.1, 21.4, 22.6, 23.7, 26.2, 27.0, 29.0, 29.2, 31.8, 68.6	14.1, 16.0, 21.4, 22.6, 23.7,26.2, 29.0, 29.2, 29.3, 29.5, 29.5, 29.6 31.9, 68.6

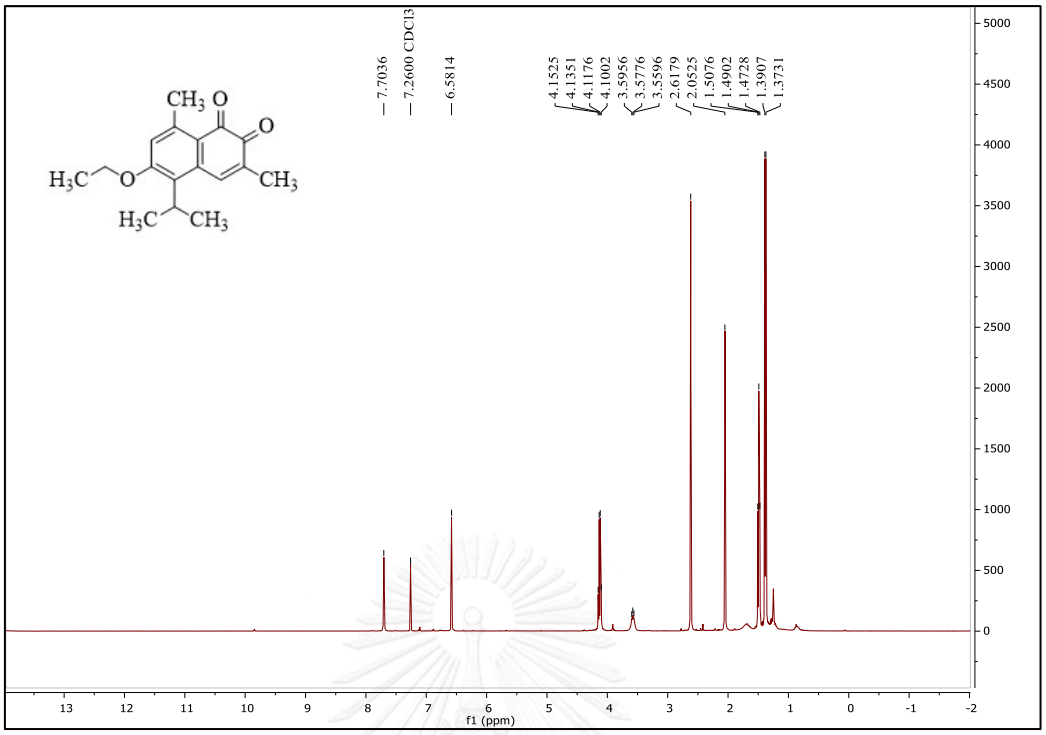

Figure 3.4 The ^{1}H NMR spectrum of **G02**

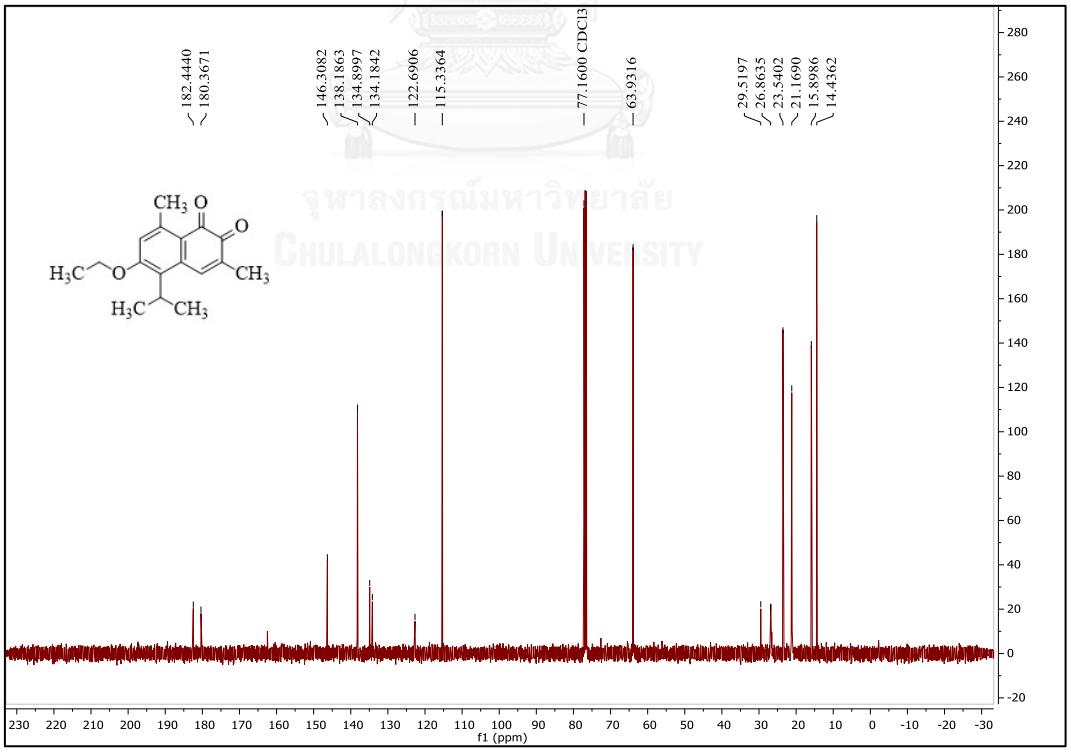

Figure 3.5 The ^{13}C NMR spectrum of **G02**

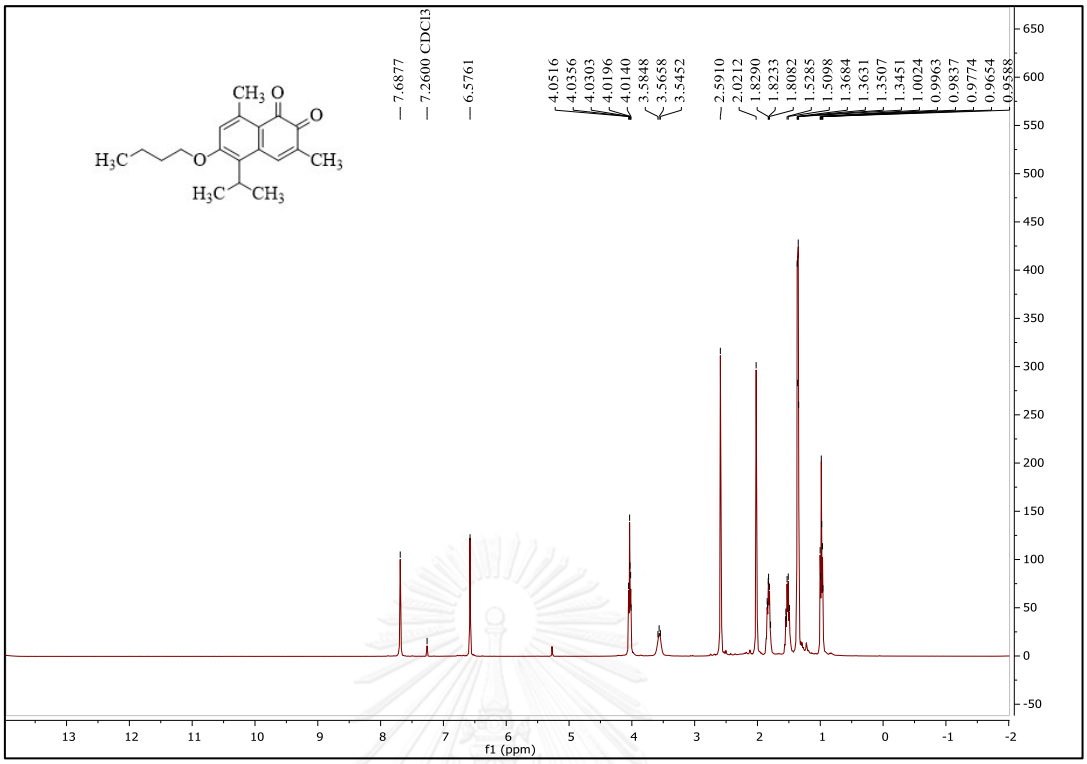

Figure 3.6 The ^{1}H NMR spectrum of **G03**

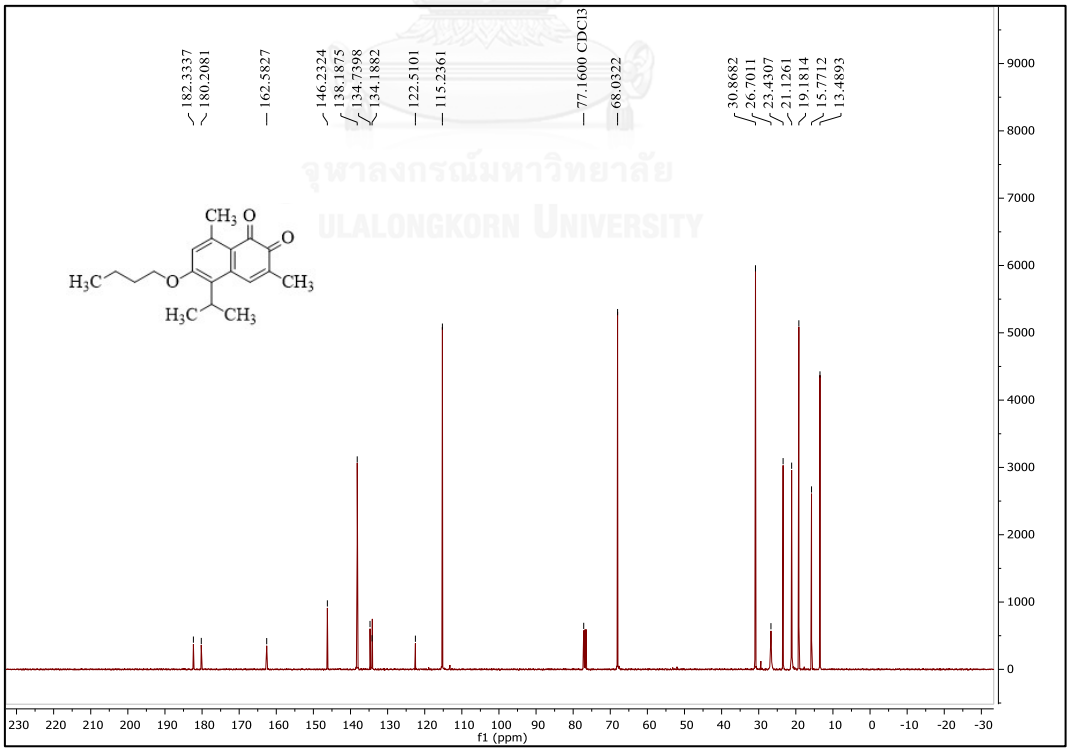

Figure 3.7 The ^{13}C NMR spectrum **of G03**

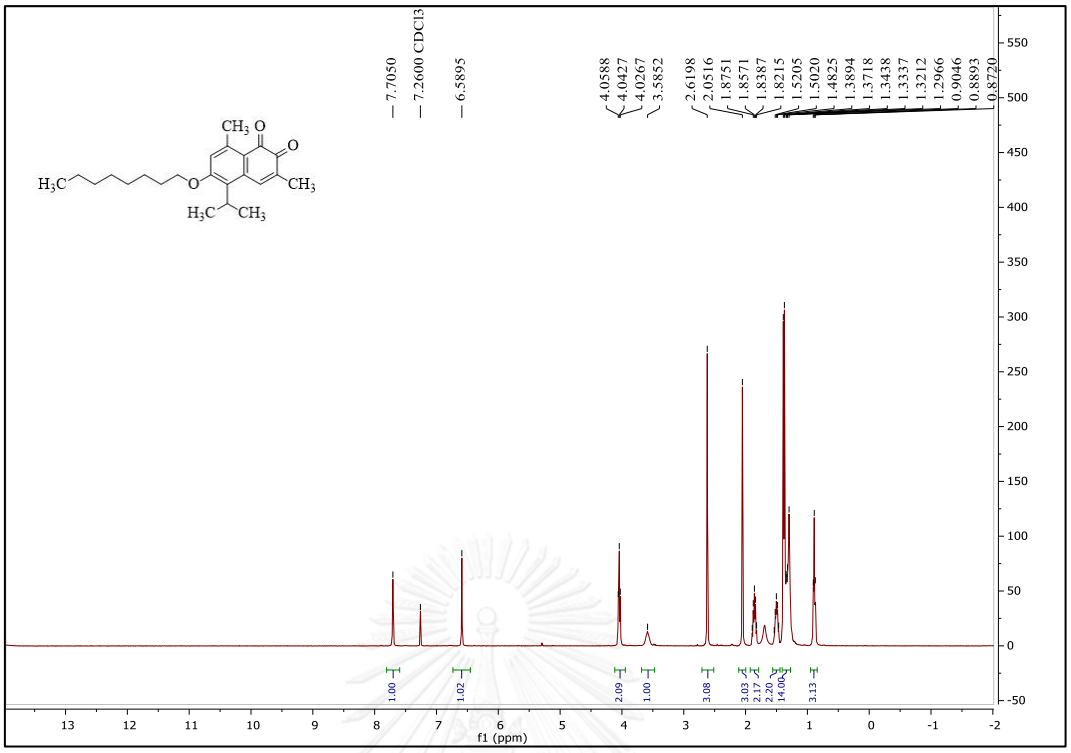

Figure 3.8 The ^{1}H NMR spectrum of **G04**

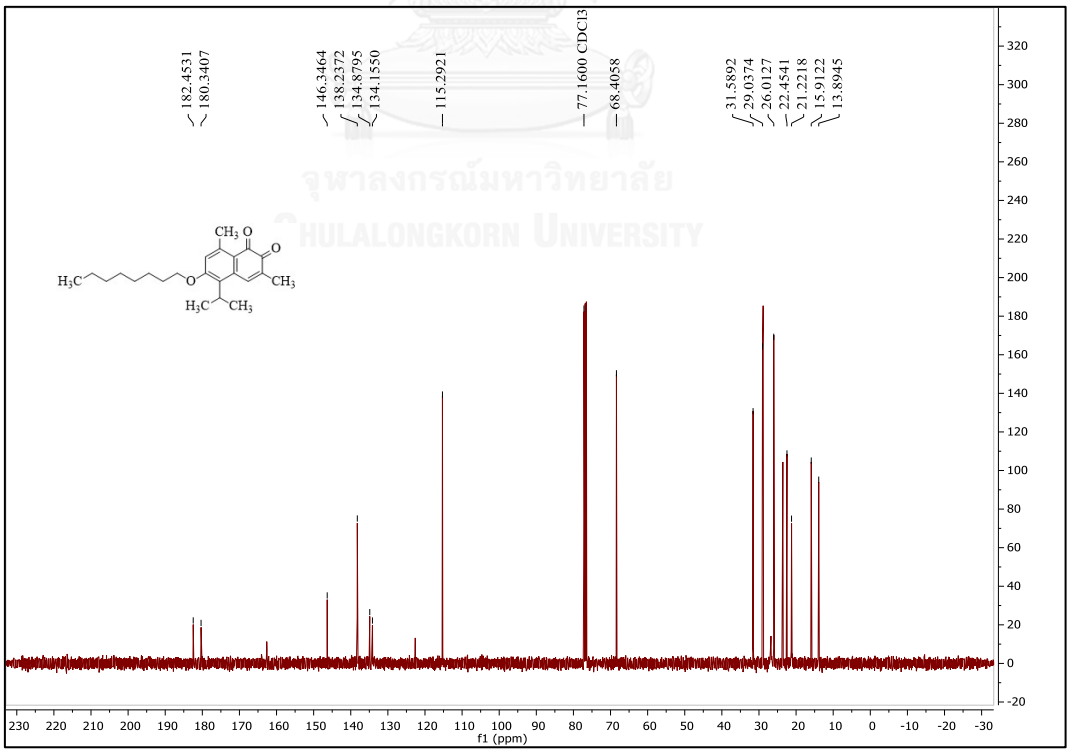

Figure 3.9 The ^{13}C NMR spectrum of **G04**

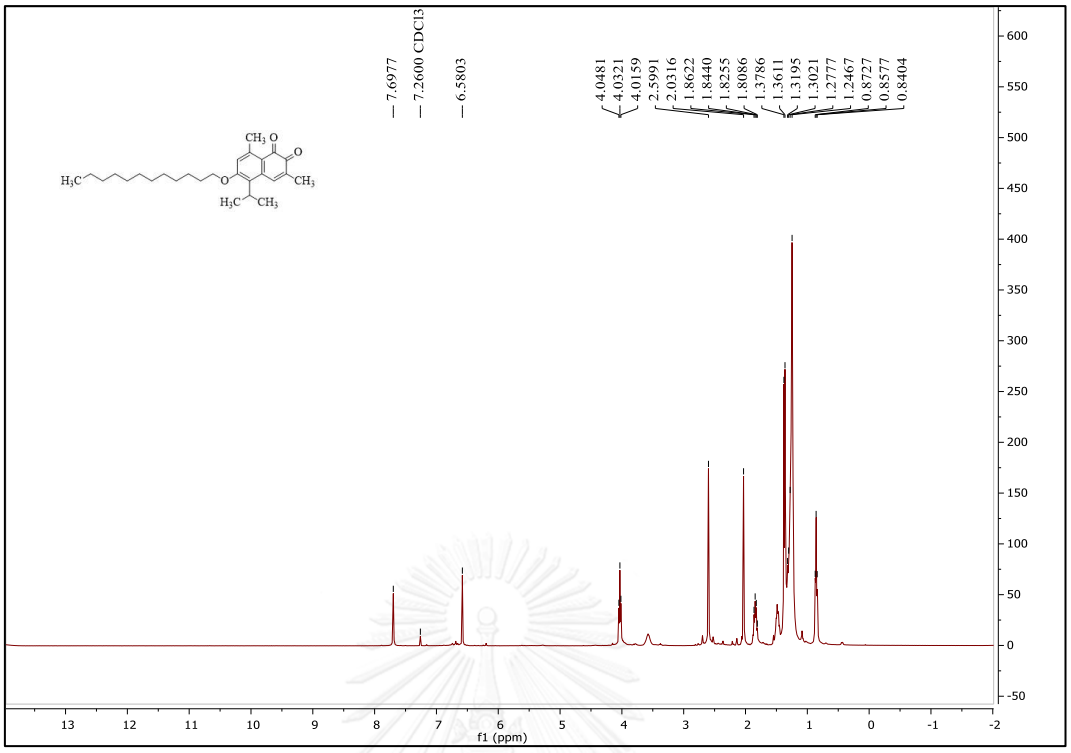

Figure 3.10 The ^{1}H NMR spectrum of **G05**

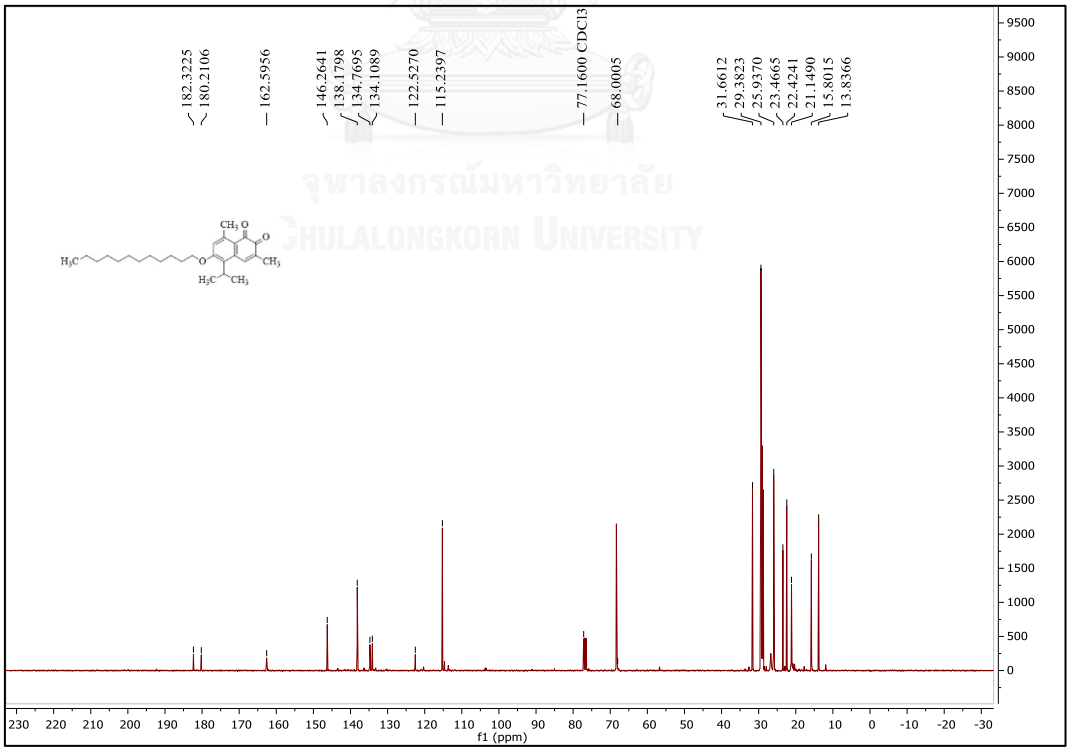

Figure 3.11 The ^{13}C NMR spectrum of **G05**

For **G06**–**G10**, the synthesis for these five new semisynthetic compounds was carried out by the same fashion as those for **G02**–**G05**, except for using benzyl bromide, allyl bromide, 3,3-dimethylallyl bromide, geranyl bromide, and cinnamyl bromide, respectively. Their yield and characteristics were collected as in Table 3.5. The ^{1}H and ^{13}C NMR spectra of all new semisynthetic compounds are displayed in Figures 3.12-3.21. and their chemical shift assignments are shown in Tables 3.9 and 3.10, respectively.

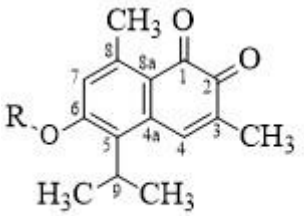

G06 R = benzyl
G07 R = allyl
G08 R = 3,3-dimethylallyl
G09 R = geranyl
G10 R = cinnamyl

Table 3.9 Tentative ^{1}H NMR chemical shift assignments of **G06–G10**

Position	δ_H (ppm)				
	G06	**G07**	**G08**	**G09**	**G10**
4	7.72 (s, 1H)	7.71 (s, 1H),	7.71 (s, 1H)	7.71 (s, 1H)	7.72 (s, 1H)
7	6.70 (s, 1H)	6.59 (s, 1H)	6.59 (s, 1H)	6.60 (s, 1H)	6.66 (s, 1H)
9	3.63 (m, 1H)	3.60 (m, 1H)	3.58 (m, 1H)	3.57 (m, 1H)	3.63 (m, 1H)
3-CH_3	2.06 (s, 3H)	2.05 (s, 3H)	2.05 (s, 3H)	2.05 (s, 3H)	2.06 (s, 3H)
8-CH_3	2.62 (s, 3H)	2.61 (s, 3H)	2.62 (s, 3H)	2.63 (s, 3H)	2.64 (s, 3H)
9-$(CH_3)_2$	1.38 (d, *J* =	1.39 (d, *J* =	1.36 (d, *J* =	1.37 (d, *J* =	1.42 (d, *J* =
	7.08 Hz, 6H).	7.08 Hz, 6H),	7.04 Hz, 6H)	6.96 Hz, 6H).	7.04 Hz, 6H)
6-OR	benzyl	allyl	3,3-	geranyl	cinnamyl
	5.16 (s, 2H)	4.63 (d, *J* =	dimethylallyl	1.25 (m, 2H)	4.80 (m, 2H),
	7.42 (m, 5H)	5.20 Hz, 2H),	1.76 (s, 3H)	1.61 (s, 3H)	6.76 (m, 1H),
		5.34 (m, 1H)	1.82 (s, 3H)	1.67 (s, 3H)	6.42 (m, 1H),
		5.44 (m, 1H)	4.60 (d, *J* =	1.75 (s, 3H)	7.37 (m, 5H)
		6.07 (m, 1H)	6.64 Hz, 2H),	2.12 (m, 2H),	
			5.48 (t, *J* =	4.62 (d, *J* =	
			5.44 Hz, 1H)	6.60 Hz, 2H),	
				5.09 (t, *J* =	
				5.80 Hz, 1H),	
				5.49 (t, *J* =	
				6.32 Hz, 1H)	

Table 3.10 Tentative ^{13}C NMR chemical shift assignments of **G06–G10**

Position	δ_C (ppm)				
	G06	**G07**	**G08**	**G09**	**G10**
1	182.6	182.6	182.8	182.5	182.7
2	180.7	180.7	180.7	180.4	180.7
3	135.9	135.2	134.8	134.9	135.3
4	146.5	146.5	146.6	146.3	146.5
4a	134.8	132.3	134.7	131.8	134.7
5	127.7	123.2	123.0	123.4	126.8
6	162.4	162.3	162.8	162.4	162.2
7	116.2	116.1	116.0	115.7	116.1
8	138.5	138.5	138.6	141.9	138.5
8a	123.4	122.4	120.5	122.2	123.3
9	27.0	27.0	27.1	29.5	27.2
3-CH3	16.2	16.2	16.2	15.9	16.2
8-CH3	21.6	21.4	21.5	21.2	21.6
9-(CH3)2	23.8	23.8	23.8	23.6	23.9
6-OR	benzyl 70.8, 128.5, 128.9, 134.7, 135.3	allyl 69.3, 118.4, 134.6	3,3-dimethylallyl 18.5, 23.9, 25.9, 65.5, 135.1, 138.9	geranyl 16.5, 17.6, 25.5, 26.1, 39.3, 65.2, 118.5, 119.6, 128.3, 138.3	cinnamyl 69.3, 128.4, 128.8, 134.1, 134.8, 135.3

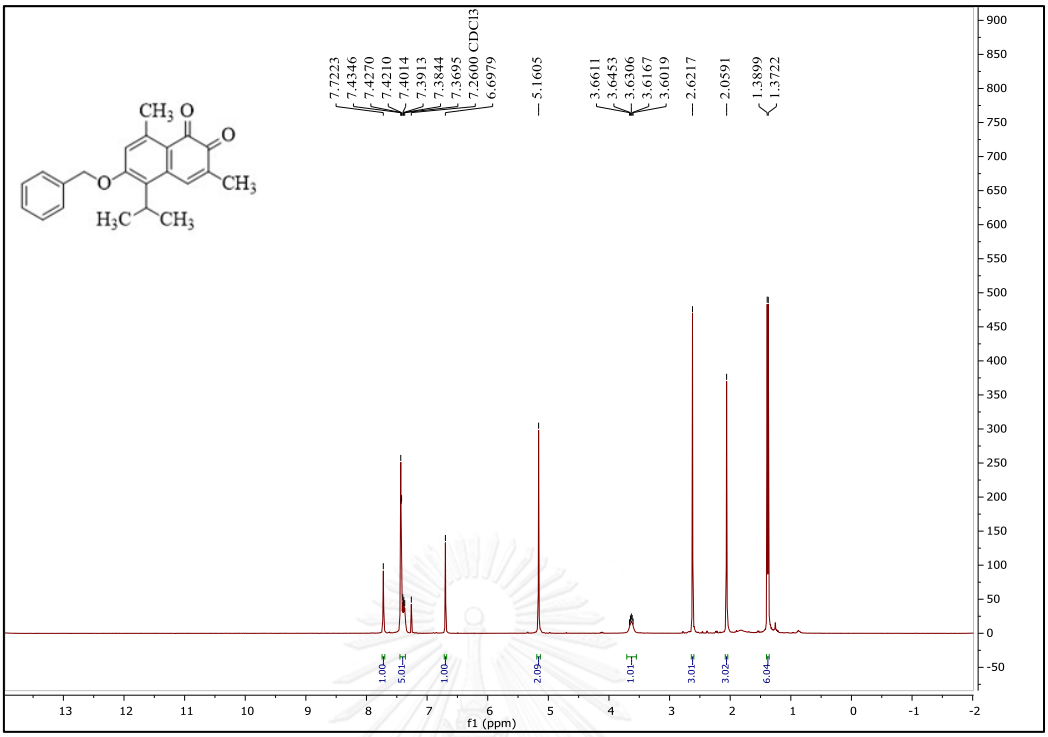

Figure 3.12 The ^{1}H NMR spectrum of **G06**

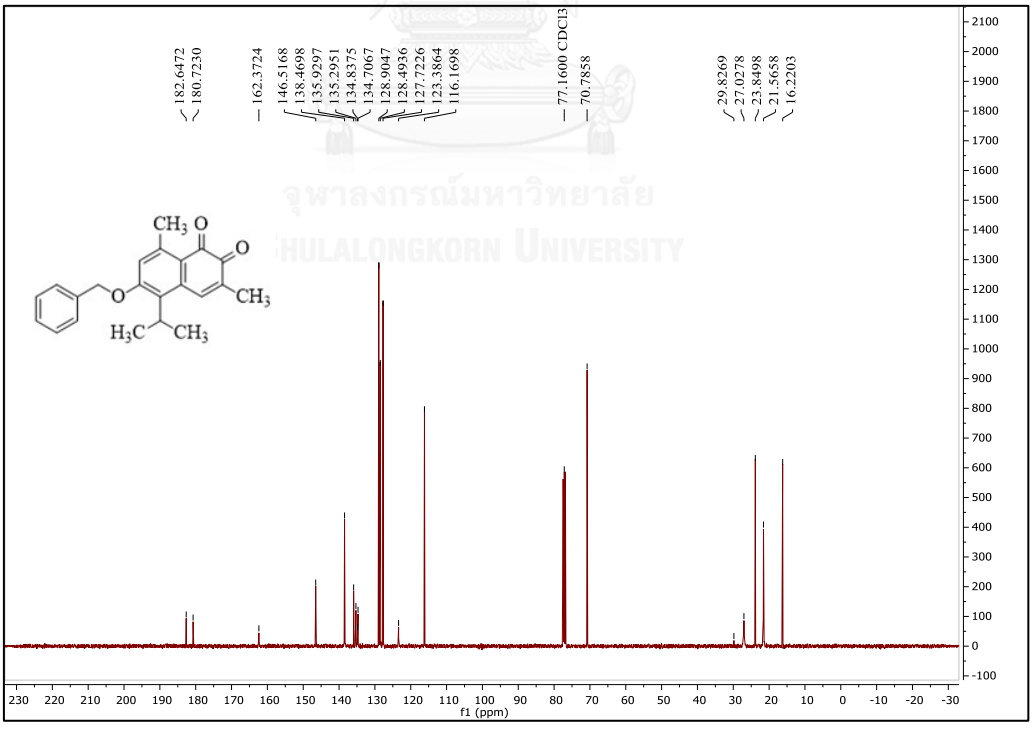

Figure 3.13 The ^{13}C NMR spectrum of **G06**

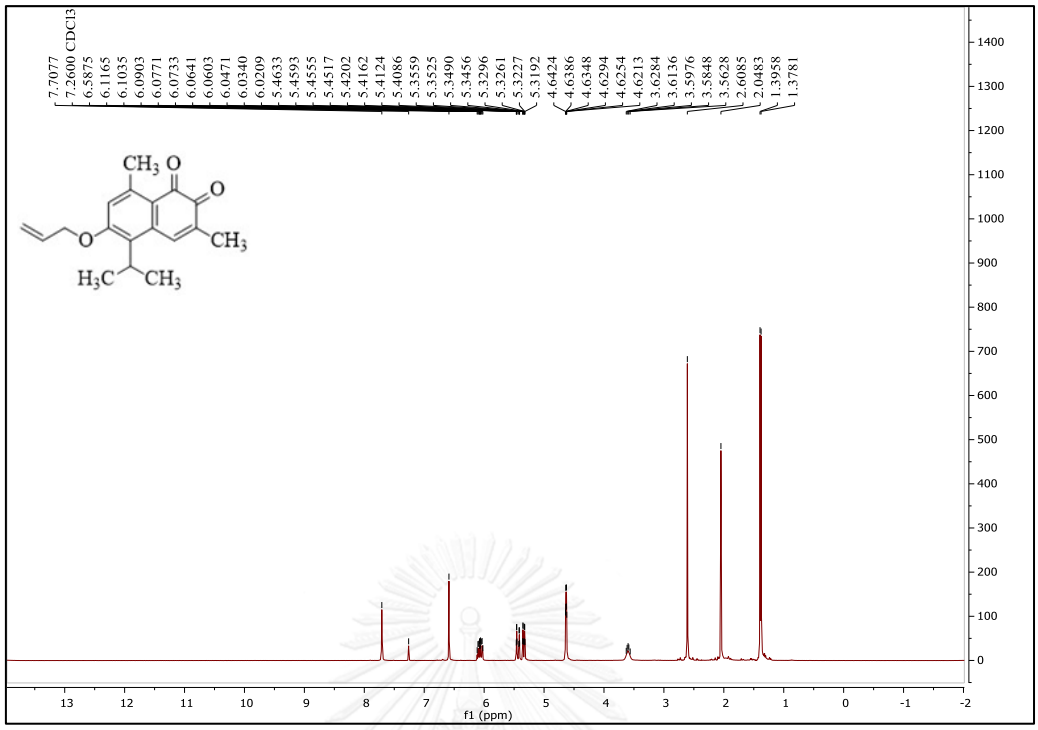

Figure 3.14 The ^{1}H NMR spectrum of **G07**

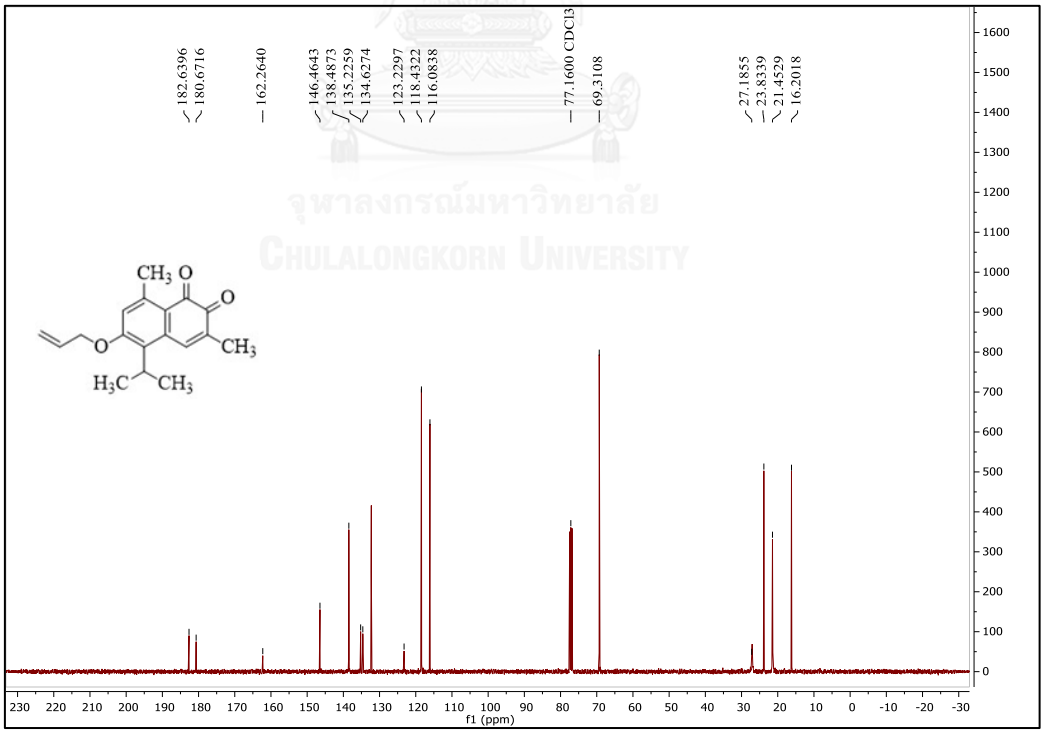

Figure 3.15 The ^{13}C NMR spectrum of **G07**

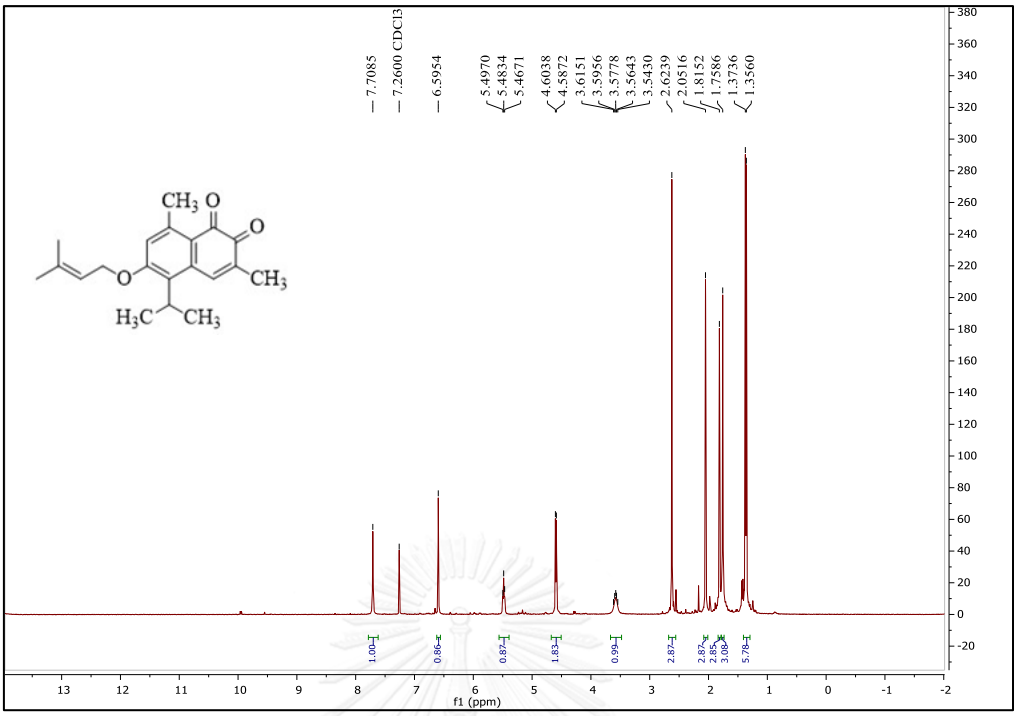

Figure 3.16 The ^{1}H NMR spectrum of **G08**

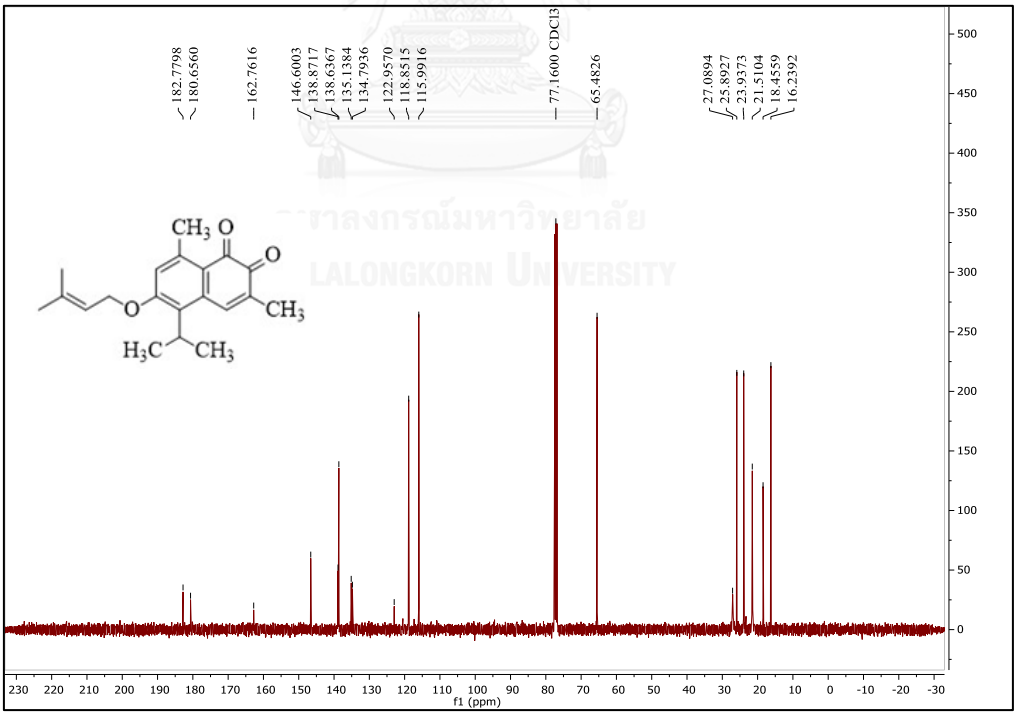

Figure 3.17 The ^{13}C NMR spectrum of **G08**

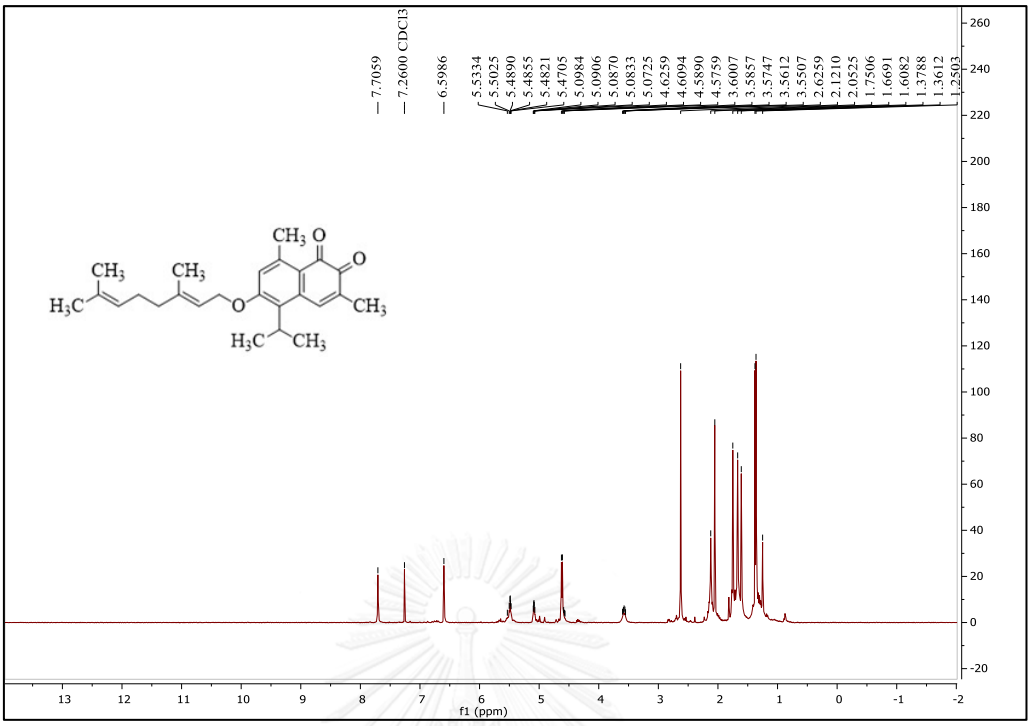

Figure 3.18 The ^{1}H NMR spectrum of **G09**

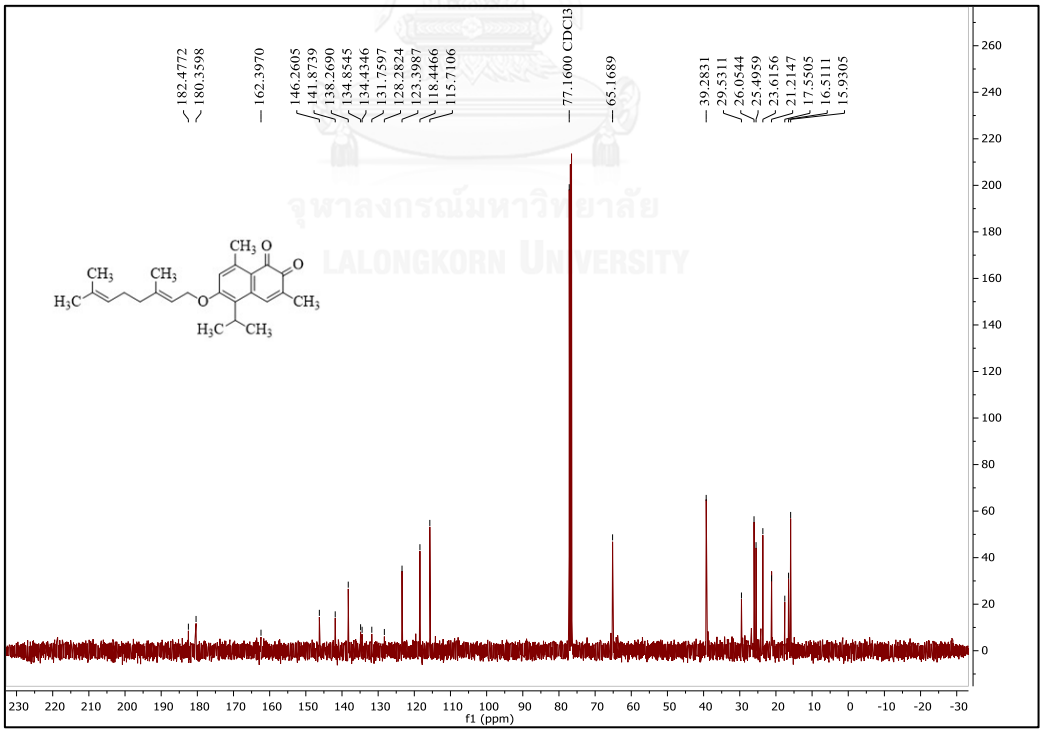

Figure 3.19 **The ^{13}C NMR spectrum of G09**

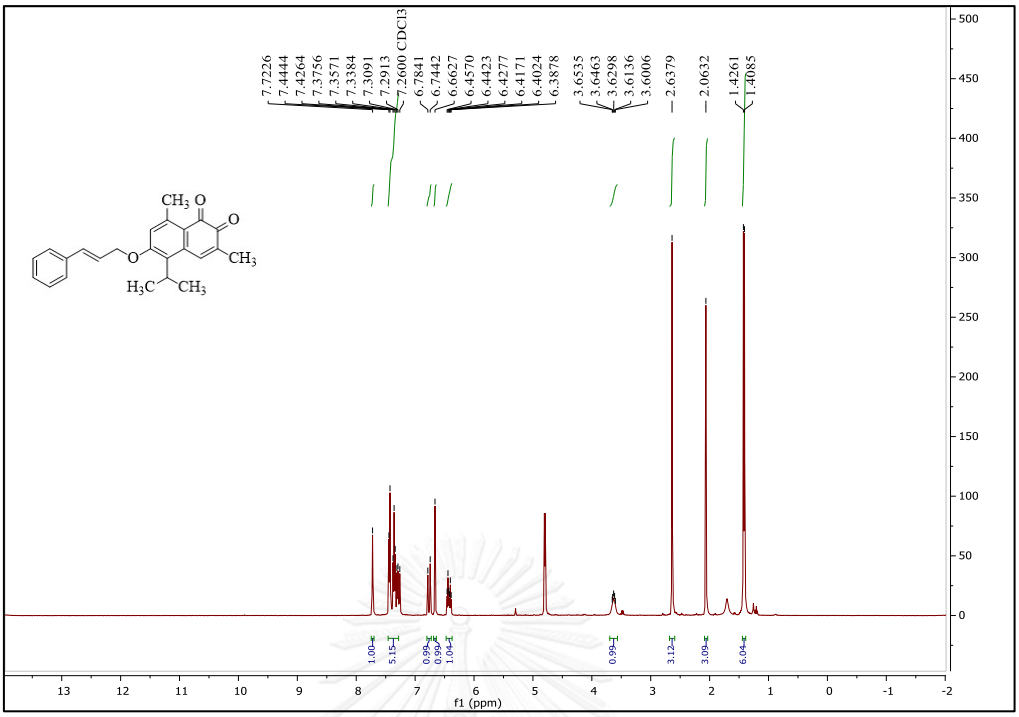

Figure 3.20 The ^{1}H NMR spectrum of **G10**

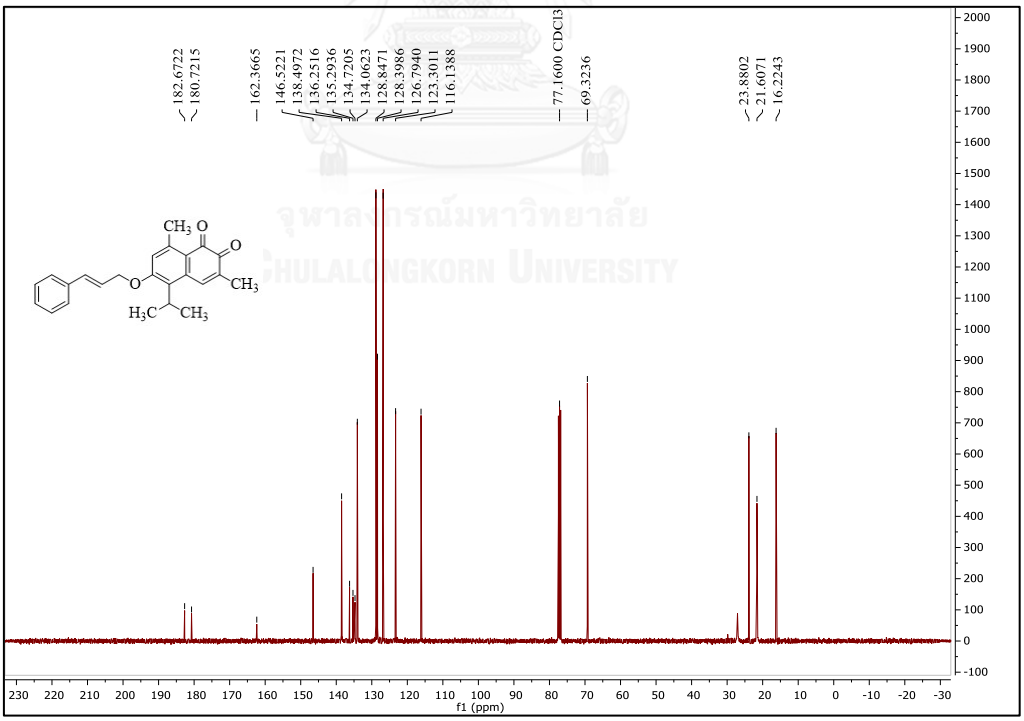

Figure 3.21 The ^{13}C NMR spectrum of **G10**

3.5.3 Ester Analogues of Mansonone G

The synthesis of ester analogues of mansonone G (**G11–G18**), was performed *via* two steps. In this reaction, PPh_3, trichloroacetonitrile, carboxylic acid, 4-picoline in CH_2Cl_2 were used to furnish the ester analogues of mansonone G (Scheme 3.2). Eight diverse carboxylic acids were used including *n*-butyric acid, caproic acid, caprylic acid, capric acid, benzoic acid, 2-chlorobenzoic acid, 2-methoxybenzoic acid and 4-methoxybenzoic acid. After refluxed, further extraction and purification by silica gel column, eight desired products were obtained as ester analogue of mansonone G (**6**). All of these ester analogues were recognized as new semisynthetic compounds (**G11**–**G18**). The yields and characteristics of the ester analogues of mansonone G are presented in Table 3.11.

Table 3.11 The yields and characteristics of ether analogues of mansonone **G** (**G11–G18**)

Ether analogues	Remarks	Weight (mg)	Yield (%)	Remarks
G11	Orange brown oil	84	69	New
G12	Orange brown oil	15	12	New
G13	Orange brown oil	14	79	New
G14	Orange brown oil	34	76	New
G15	Orange powder	84.4	98	New
G16	Orange powder	77.9	50	New
G17	Orange powder	34.1	39	New
G18	Orange powder	42.6	50	New

The reaction of mansonone G with *n*-butyric acid gave product in moderate yield (**G11**, 69%), while for the others (**G12**–**G14**) were in poor yield (12–28%).

3.5.4 Structural Elucidation of Ester Analogues of Mansonone G

All eight ester analogues were identified as new semisynthetic compounds and their structures were confirmed by NMR and MS analysis. The ^{1}H and ^{13}C NMR spectra of aliphatic ester analogues of mansonone G are presented in Tables 3.12 and 3.13, respectively, while those for aromatic ester analogues are presented in Tables 3.14 and 3.15, respectively.

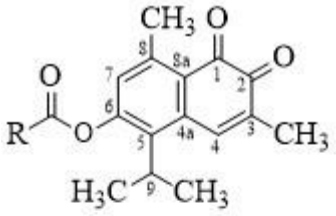

G11 R = C_3H_8

G12 R = C_6H_{12}

G13 R = C_7H_{16}

G14 R = C_9H_{20}

G15 R = 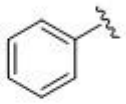

G16 R = 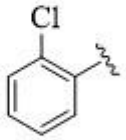

G17 R = 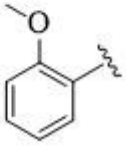

G18 R = 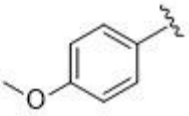

Table 3.12 Tentative ^{1}H NMR chemical assignments of **G11–G14**

Position	Chemical shift (ppm)			
	G11	G**12**	G**13**	**G14**
4	7.72 (1H, s)	7.63 (1H, s)	7.64 (1H, s)	7.70 (1H, s)
7	6.86 (1H, s)	6.78 (1H, s)	6.78 (1H, s)	6.85 (1H, s)
9	3.47 (1H, m)	3.39 (1H, m)	3.39 (1H, m)	3.46 (1H, m)
3-CH_3	2.07 (3H, s)	2.00 (3H, s)	2.00 (3H, s)	2.07 (3H, s)
8-CH_3	2.61 (3H, s)	2.54 (3H, s)	2.53 (3H, s)	2.60 (3H, s)
9-$(CH_3)_2$	1.36 (6H, d, *J*=6.72 Hz)	1.29 (6H, d, *J*=7.16 Hz)	1.29 (6H, d, *J*=7.08 Hz)	1.35 (6H, d, *J*=7.16 Hz)
6-COOR	-$(CH_2)_2$-CH_3 2.61 (2H, t, *J*=7.28 Hz), 1.82 (2H, m), 1.07 (3H, t, *J*=7.40 Hz)	-$(CH_2)_4$-CH_3 1.14 (2H, m), 1.72 (2H, m), 1.35 (2H, m), 2.54 (2H, t, *J*=7.28 Hz) 0.87 (3H, t, *J*=6.84 Hz)	-$(CH_2)_6$-CH_3 2.54 (2H, t, *J*=7.24 Hz) 1.35 (2H, m), 1.71 (2H, m), 1,22 (6H, m) 0.83 (3H, t, *J*=5.60 Hz)	-$(CH_2)_8$-CH_3 2.62 (2H, t, *J*=7.60 Hz) 1.75 (2H, m), 1.40 (2H, m), 1,29 (10H, m) 0.87 (3H, t, *J*=6.08 Hz)

Table 3.13 Tentative ^{13}C NMR chemical shift assignments of **G11–G14**

Position	Chemical shift (ppm)			
	G11	**G12**	**G13**	**G14**
1	181.3	181.33	181.32	181.33
2	181.7	181.74	181.73	181.75
3	137.0	136.94	136.96	136.94
4	138.0	137.97	137.99	137.96
4a	135.5	135.54	135.54	135.54
5	135.2	135.25	135.23	135.25
6	154.0	153.97	153.98	153.98
7	127.7	127.76	127.75	127.77
8	144.5	144.57	144.55	144.57
8a	128.2	128.22	128.22	128.22
9	26.8	26.78	26.77	26.78
3-CH_3	16.0	16.04	16.02	16.03
8-CH_3	22.8	22.85	22.84	22.84
9-$(CH_3)_2$	21.9	21.95	21.95	21.96
6-COOR	-$(CH_2)_2$-CH_3	-$(CH_2)_4$-CH_3	-$(CH_2)_6$-CH_3	-$(CH_2)_8$-CH_3
	13.6, 18.2, 36.4, 171.4	13.9, 22.3, 24.3, 31.3, 34.5, 171.6	14.0, 22.6, 24.7, 28.9, 29.1, 31.7, 34.6, 171.6	14.1, 22.6, 24.7, 29.1, 29.2, 29.4, 29.7, 31.8, 34.6, 171.6

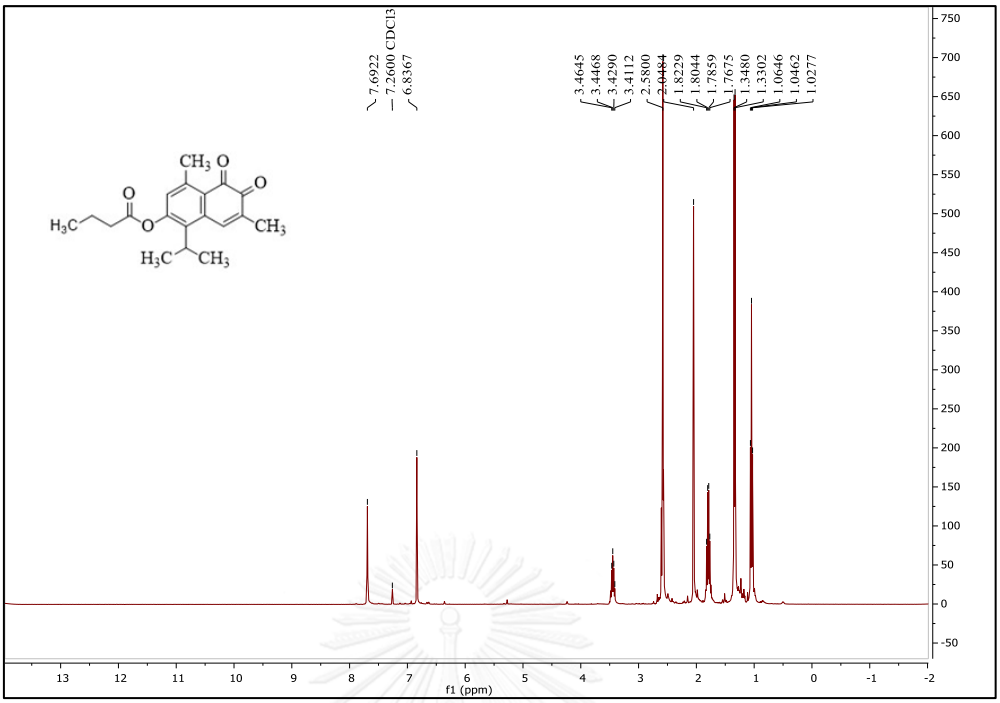

Figure 3.22 The ^{1}H NMR spectrum **of G11**

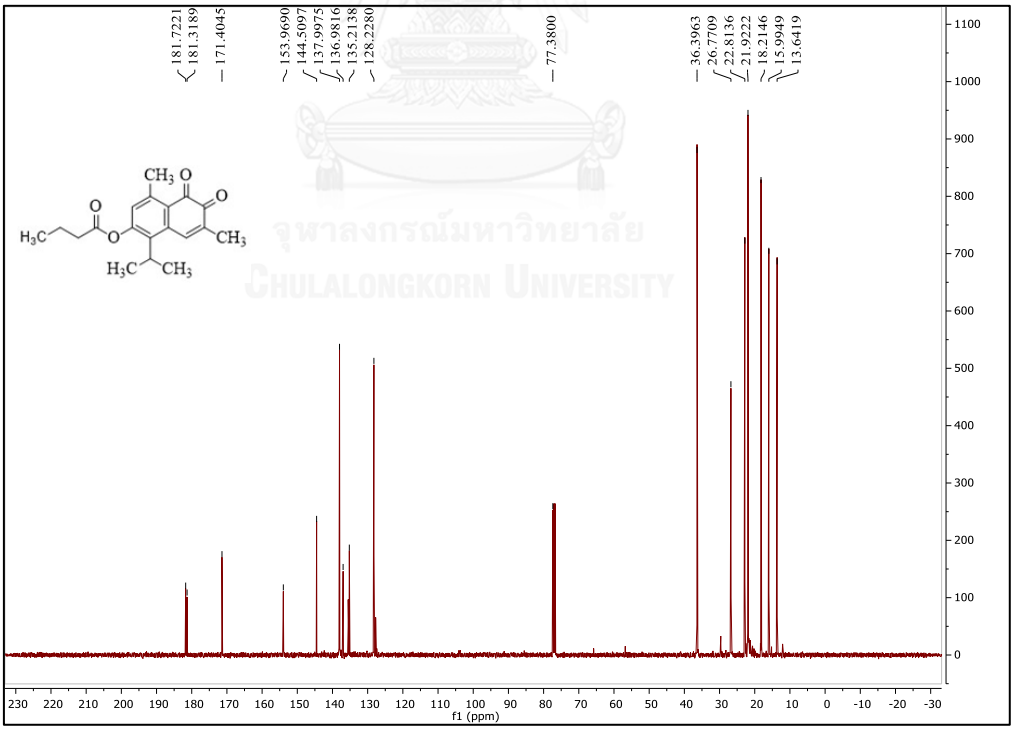

Figure 3.23 The ^{13}C NMR spectrum **of G11**

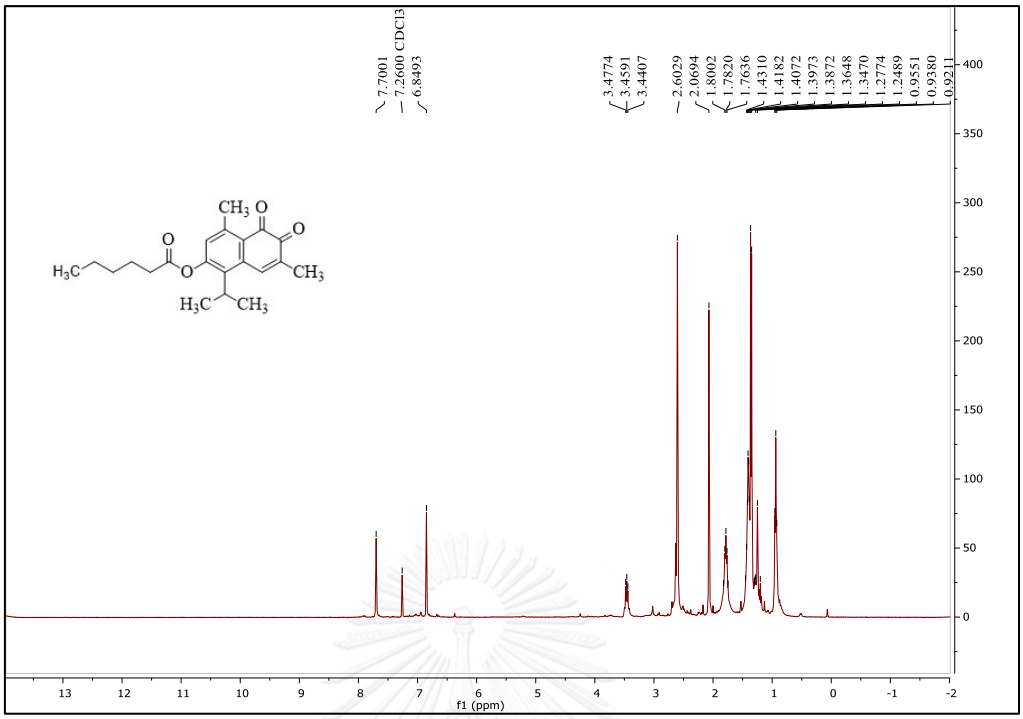

Figure 3.24 The ^{1}H NMR spectrum of **G12**

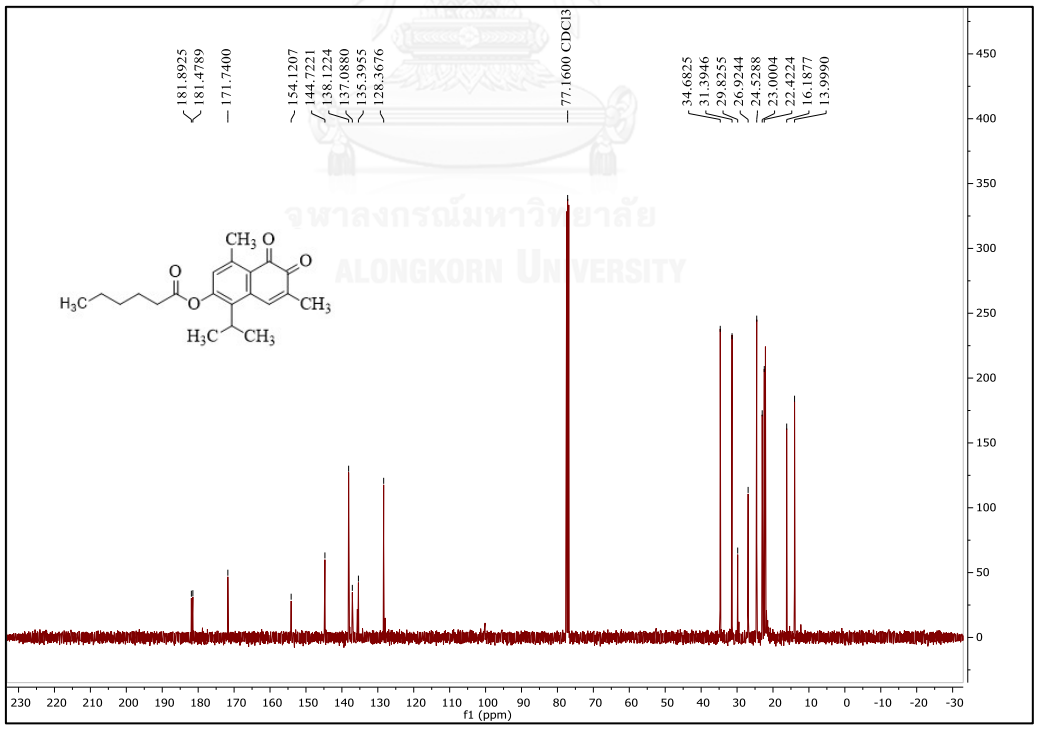

Figure 3.25 The ^{13}C NMR spectrum of **G12**

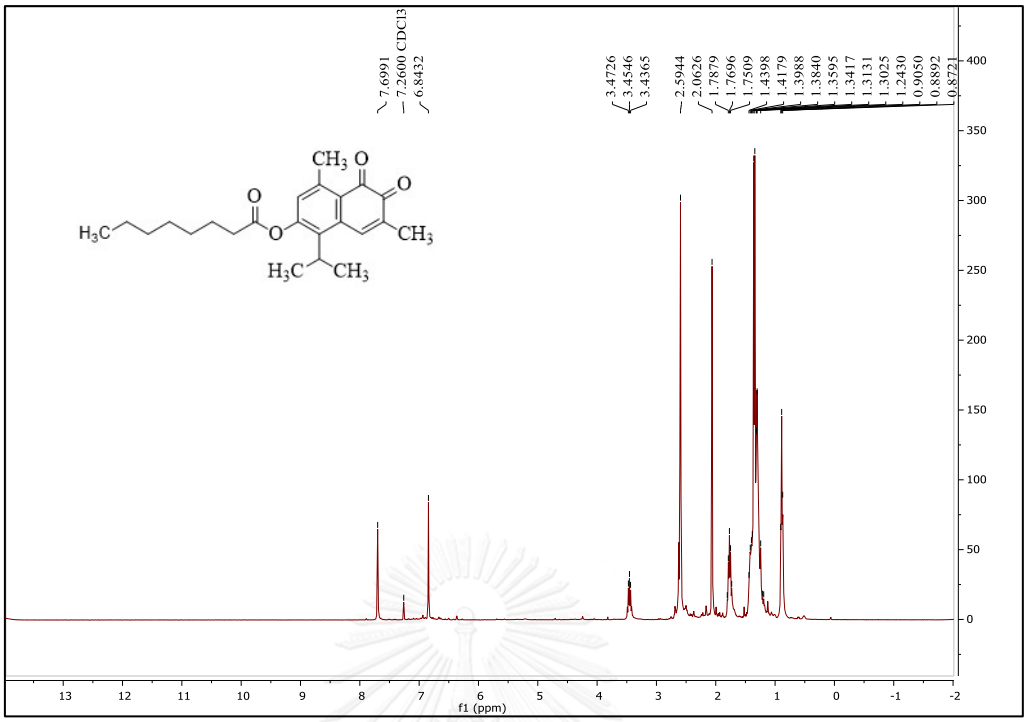

Figure 3.26 The ^{1}H NMR spectrum of G13

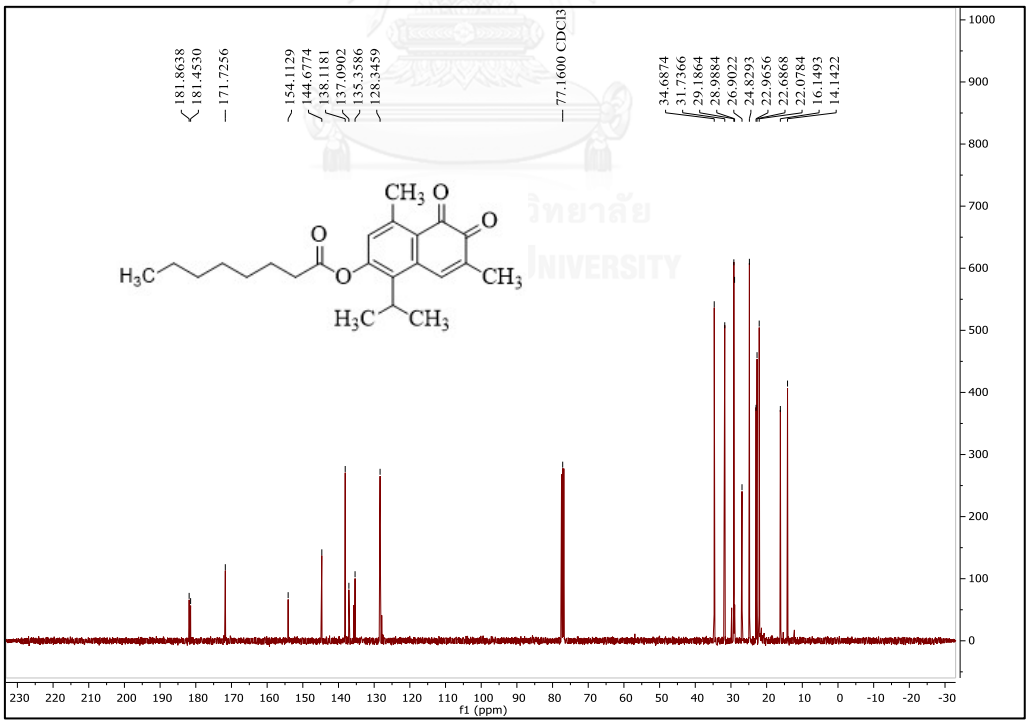

Figure 3.27 The ^{13}C NMR spectrum of **G13**

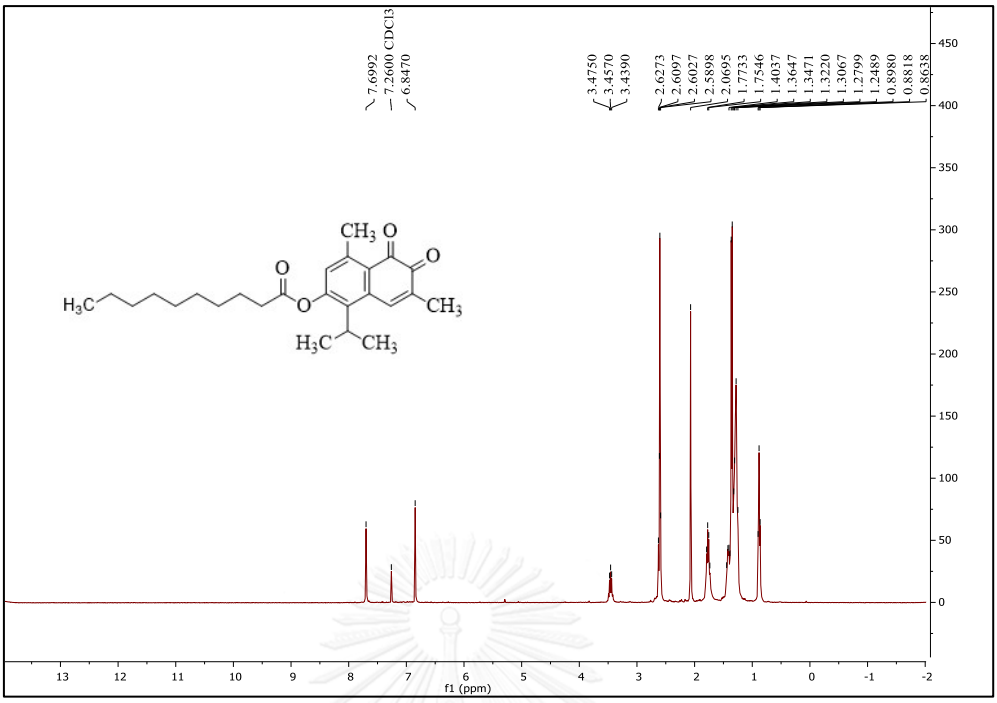

Figure 3.28 The ^{1}H NMR spectrum of **G14**

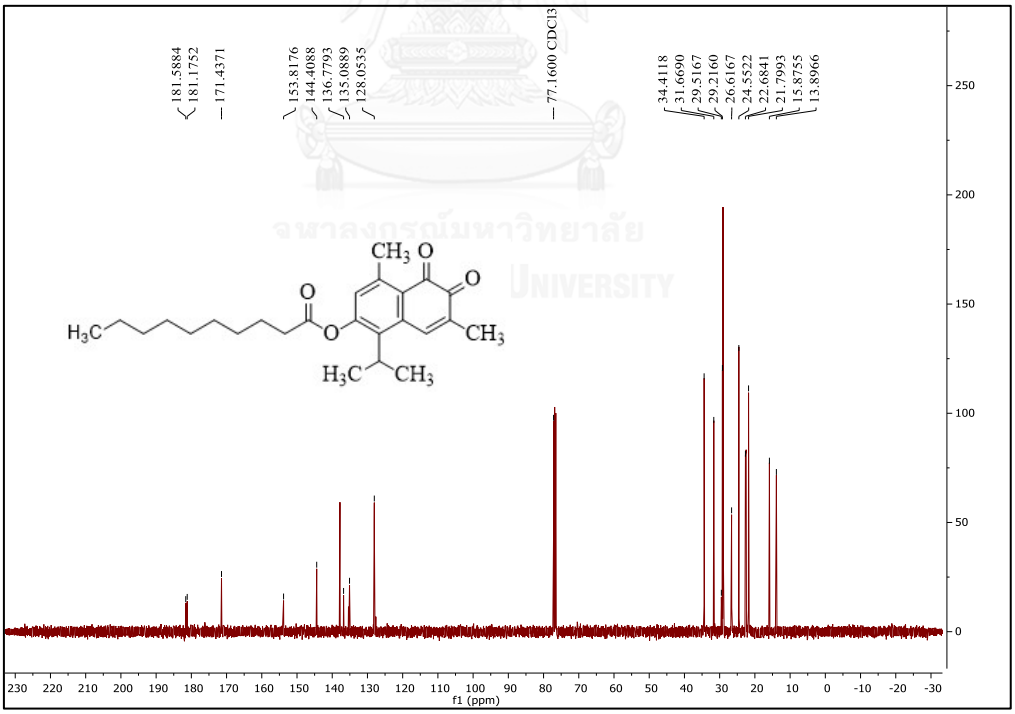

Figure 3.29 The ^{13}C NMR spectrum of **G14**

Table 3.14 Tentative ^{1}H NMR chemical shift assignments of G15–G18

Position	Chemical shift (ppm)			
	G15	G**16**	G**17**	**G18**
4	7.74 (s, 1H)	7.74 (s, 1H	7.74 (s, 1H)	7.70 (s, 1H)
7	6.98 (s, 1H)	7.01 (s, 1H)	6.98 (s, 1H)	6.96 (s, 1H)
9	3.53 (m, 1H)	3.53 (m, 1H)	3.56 (m, 1H)	3.52 (m, 1H)
3-CH_3	2.09 (s, 3H)	2.08 (s, 3H)	2.07 (s, 3H)	2.08 (s, 3H)
8-CH_3	2.63 (s, 3H)	2.64 (s, 3H)	2.61 (s, 3H)	2.63 (s, 3H)
9-$(CH_3)_2$	1.39 (d, *J* = 7.12 Hz, 6H)	1.37 (d, *J* = 7.16 Hz, 6H)	1.38 (d, *J* = 7.16 Hz, 6H)	1.38 (d, *J* = 7.08 Hz, 6H)
6-COOR	7.59 (m, 2H), 7.69 (t, *J* = 7.48 Hz, 2H), 8.21 (d, *J* = 7.12 Hz, 2H)	7.44 (m, 1H), 7.55 (m, 2H), 8.06 (d, *J* = 8.48 Hz, 1H)	3.94 (s, 3H), 7.07 (m, 1H), 7.58 (m, 1H), 8.03 (d, *J* = 7.92 Hz, 1H)	3.91 (s, 3H), 7.02 (d, *J* = 8.80 Hz, 2H), 8.15 (d, *J* = 8.76 Hz, 2H)

Table 3.15 Tentative ^{13}C NMR chemical shift assignments of **G15, G16, and G18**

Position	Chemical shift (ppm)		
	G**15**	G**16**	G**18**
1	181.9	181.8	181.9
2	181.5	181.5	181.6
3	137.4	137.4	137.5
4	144.8	144.8	144.7
4a	135.5	135.5	135.4
5	135.7	135.9	135.7
6	154.4	153.9	154.6
7	128.6	127.1	127.9
8	138.1	138.1	138.1
8a	129.0	128.2	128.8
9	27.1	27.0	27.1
3-CH_3	16.2	16.2	16.2
8-CH_3	23.0	23.0	23.0
9-$(CH_3)_2$	22.1	22.2	22.1
6-COOR	129.0, 130.5, 134.3, 137.4, 138.0, 164.8	131.8, 128.6, 134.0, 163.6	55.7, 127.9, 129.6, 129.8, 132.7, 133.7, 133.8, 134.7, 164.5, 164.5

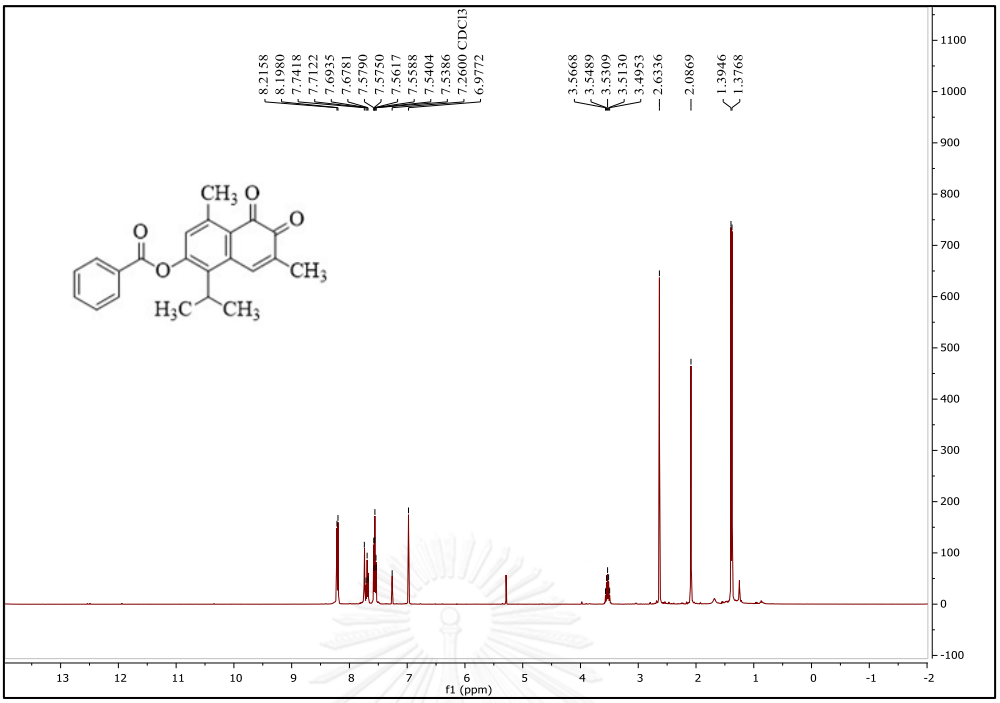

Figure 3.30 The ^{1}H NMR spectrum **of G15**

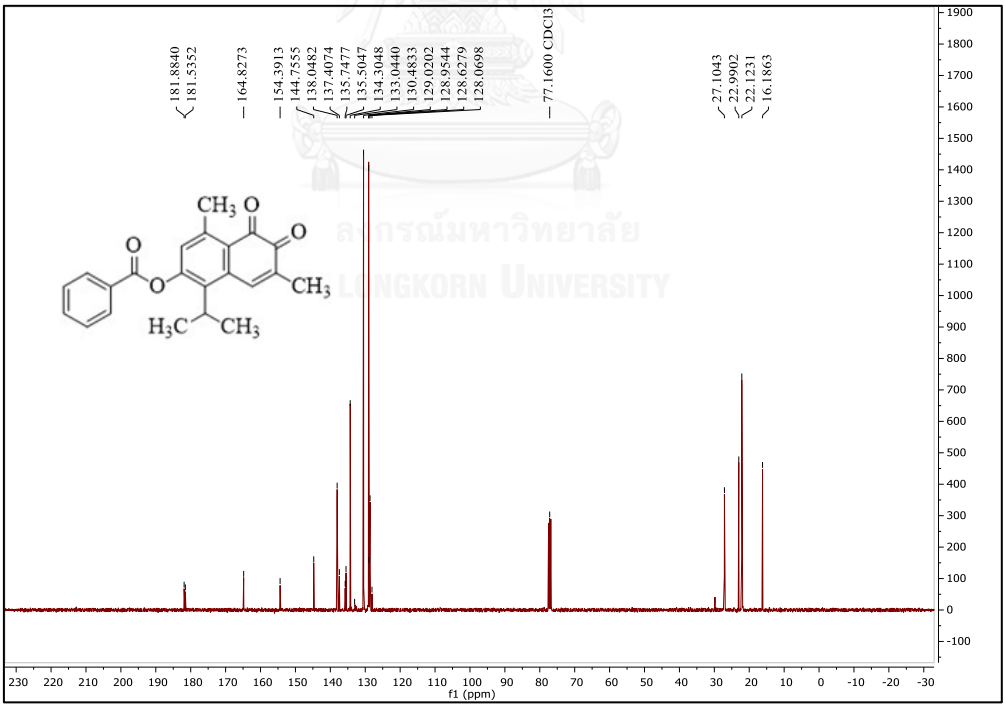

Figure 3.31 The ^{13}C NMR spectrum of **G15**

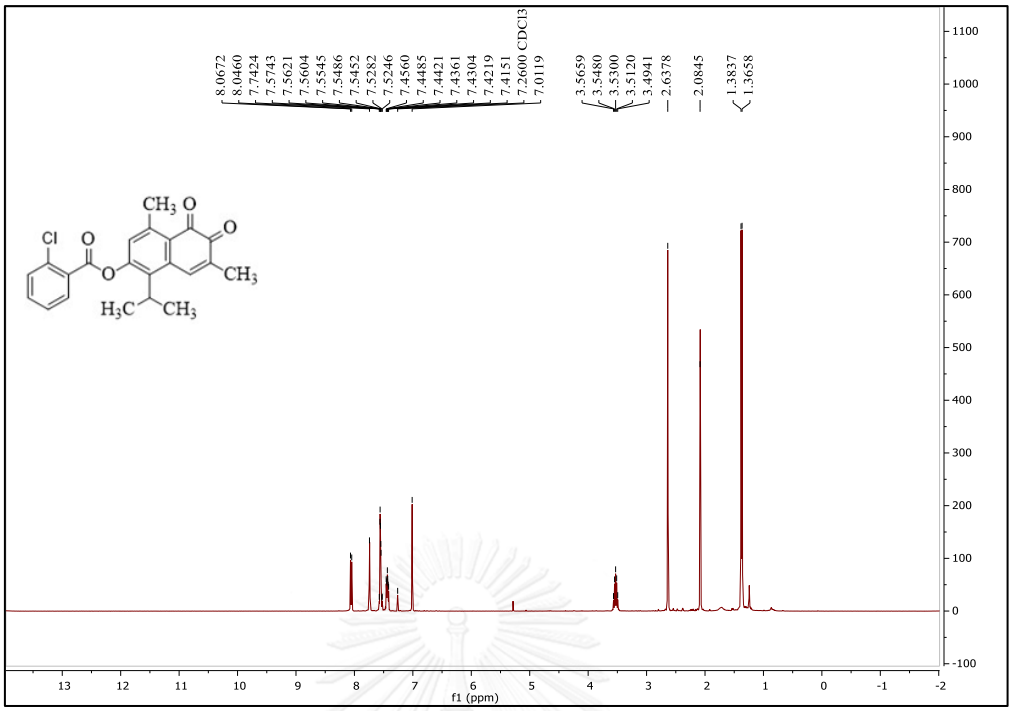

Figure 3.32 The ^{1}H NMR spectrum of **G16**

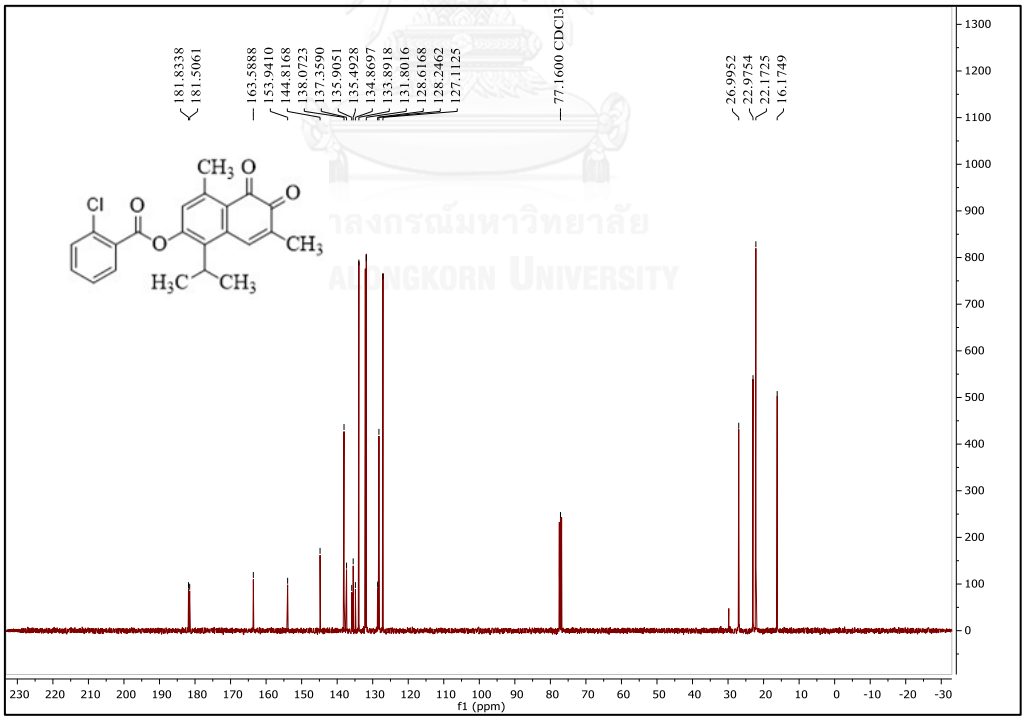

Figure 3.33 The ^{13}C NMR spectrum of **G16**

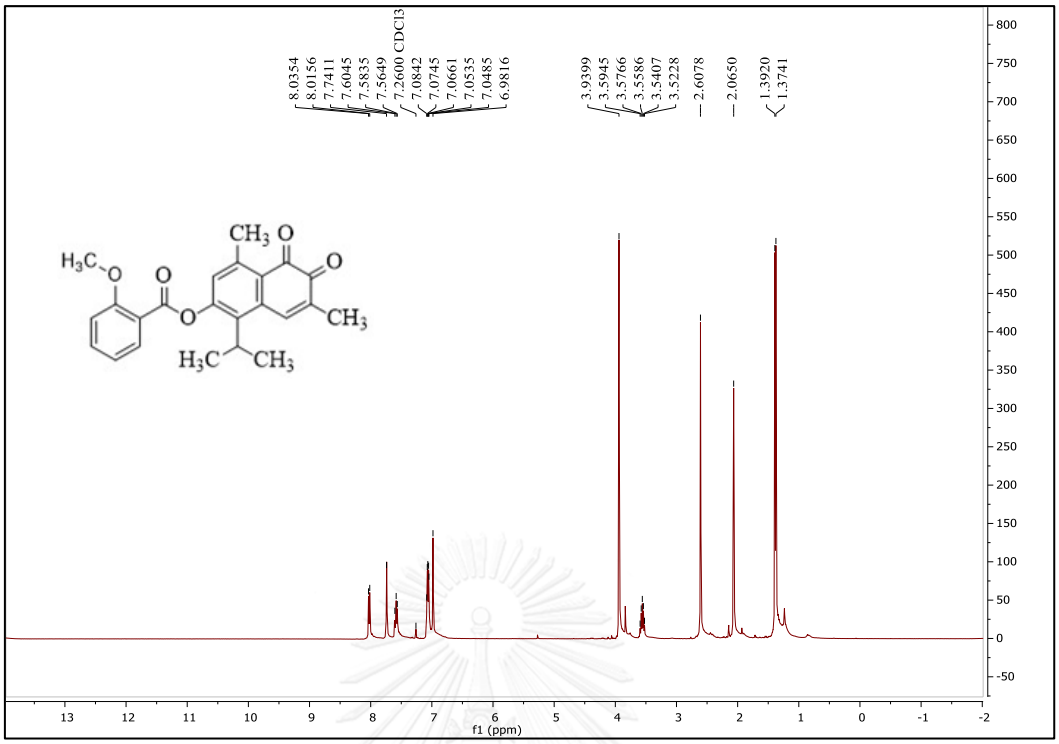

Figure 3.34 The ^{1}H NMR spectrum of **G17**

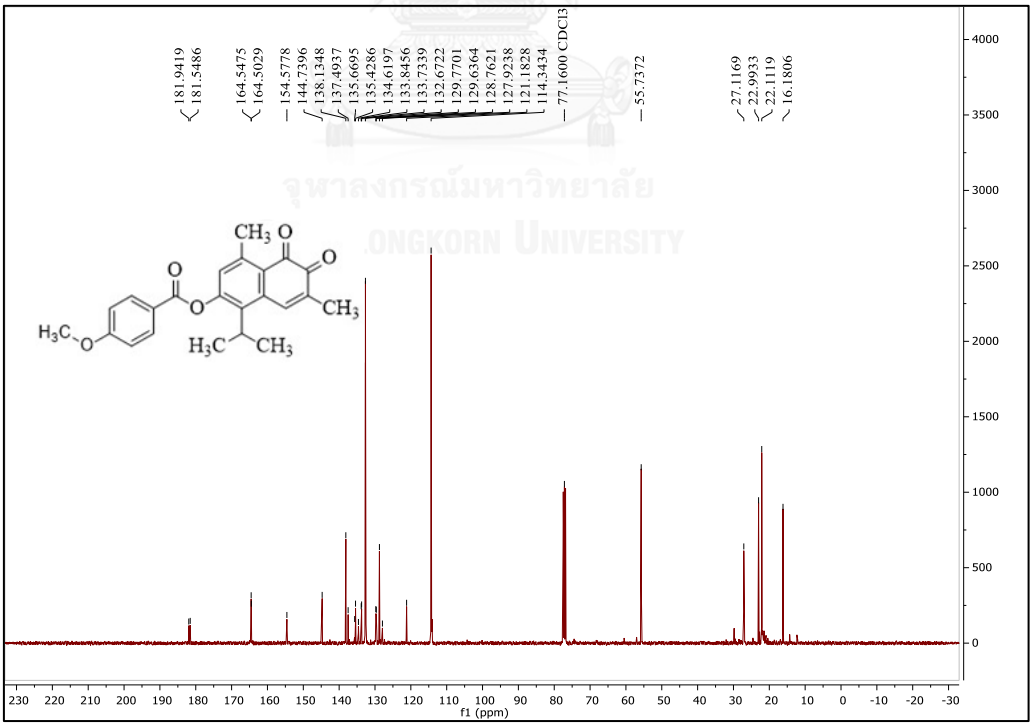

Figure 3.35 The ^{1}H NMR spectrum of **G18**

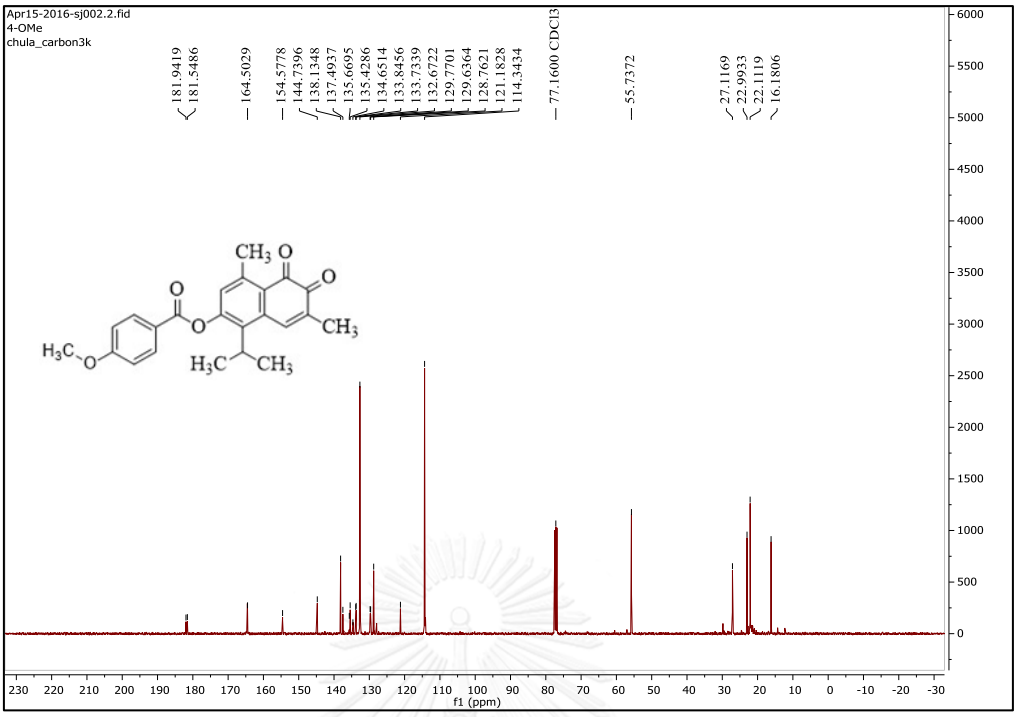

Figure 3.36 The ^{1}H NMR spectrum of **G18**

3.5.5 Mansonone G Derivatives from Epichlorohydrin

Another typical mansonone G derivatives were carried out using epichlorohydrin in the presence of NaOH. In this reaction, mansonone G (**6**) was reacted with excess of epichlorohydrin and an ethanolic solution of NaOH. After purification using silica gel column, the desired products (**G19** and **G20**) were obtained.

NaOH acted as a strong base resulted in the conversion of epichlorohydrin into epoxypropanol intermediate, which was further reacted with mansonone G (**6**) to form mansonone G oxirane. **G19**, could be occurred by following two-step mechanisms: a) the formation of chlorohydrin intermediate and b) dehydrohalogenation of chlorohyrin to glycidyl ether. The yield and appearance of **G19**–**G20** are presented in Table 3.16

Table 3.16 The yields and characteristics of **G19 and G20**

Compound	Appearance	Weight (mg)	Yield (%)	Remarks
G19	Orange powder	63	52	New
G20	Orange powder	30	25	New

3.5.6 Structural Elucidation of G19 and G20

G19 was obtained as orange powder. Its ^{1}H NMR spectrum (Figure 3.37) displayed the signal of 7.71 (s, 1H), 6.59 (s, 1H), 4.37 (dd, *J* = 2.8, 2.8 Hz, 1H), 3.99 (dd, *J* = 6.08, 6.08 Hz, 1H), 3.60 (m, 1H), 3.42 (m, 1H), 2.96 (t, *J* = 4.52 Hz, 1H), 2.78 (dd, *J* = 2.6, 2.6 Hz, 1H), 2.62 (s, 3H), 2.06 (s, 3H), and 1.40 (dd, *J* = 3.2, 3.2 Hz, 6H). The ^{13}C NMR spectrum (Figure 3.38) showed several signals at δ_C 182.6, 180.7, 162.1, 146.5, 138.4, 135.4, 134.6, 123.6, 115.9, 69.5, 49.9, 44.7, 29.8, 27.2, 23.8, 21.5, and 16.2 ppm. Its HRMS (ESI): calculated for $C_{18}H_{20}O_4$ [M+Na]$^+$: 323.1259, found 323.1257.

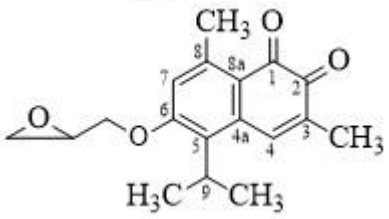

G19

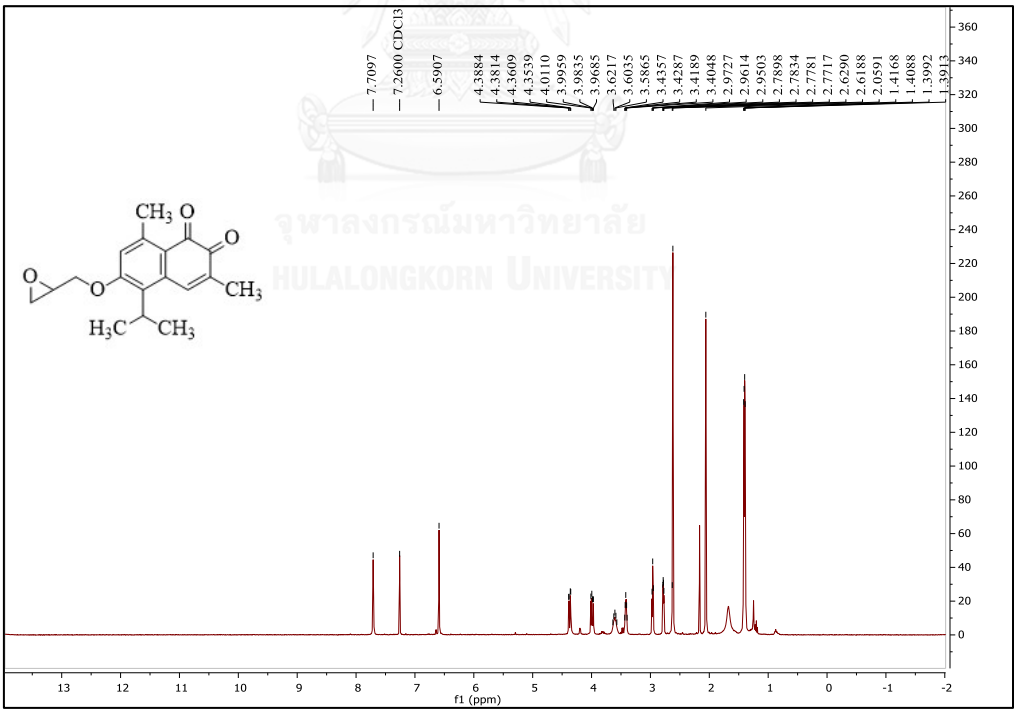

Figure 3.37 The ^{1}H NMR spectrum of **G19**

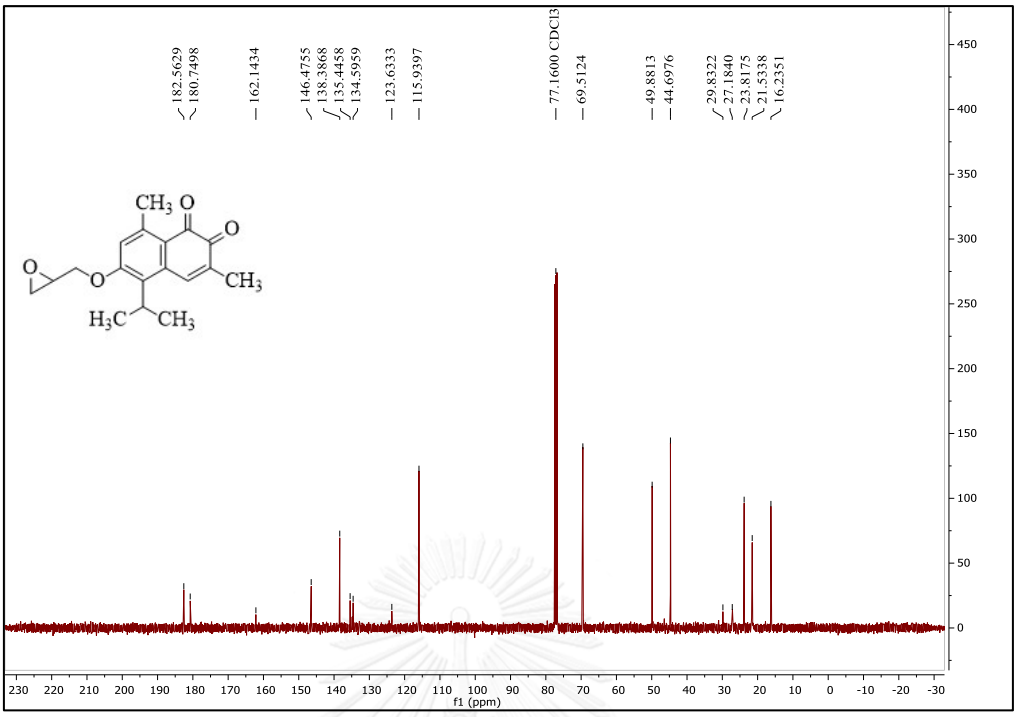

Figure 3.38 The ^{13}C NMR spectrum of **G19**

G20 was also obtained as yellow powder and its ^{1}H NMR spectrum displayed chemical shift at 7.76 (s, 1H), 6.76 (s, 1H), 5.58 (s, 1H), 3.99 (t, *J* = 9.16 Hz, 3H), 3.64 (m, 2H), 3.53 (m, 1H), 2.39 (s, 3H), 1.81 (s, 3H), and 1.19 (d, *J* = 6.88 Hz, 6H). ^{13}C NMR: δ_c (ppm) 181.7, 180.1, 162.1, 145.3, 138.0, 135.0, 134.2, 133.8 122.7, 116.0, 69.7, 68.6, 46.6, 26.3, 23.1, 21.2, 18.2, and 15.5. HRMS (ESI): calculated for $C_{18}H_{21}O_4Cl$ $[M+H]^+$: 325.1416, found 337.1237.

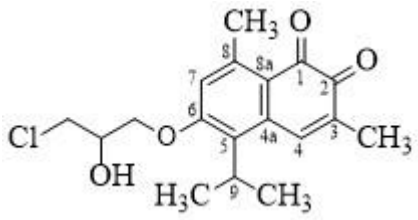

G20

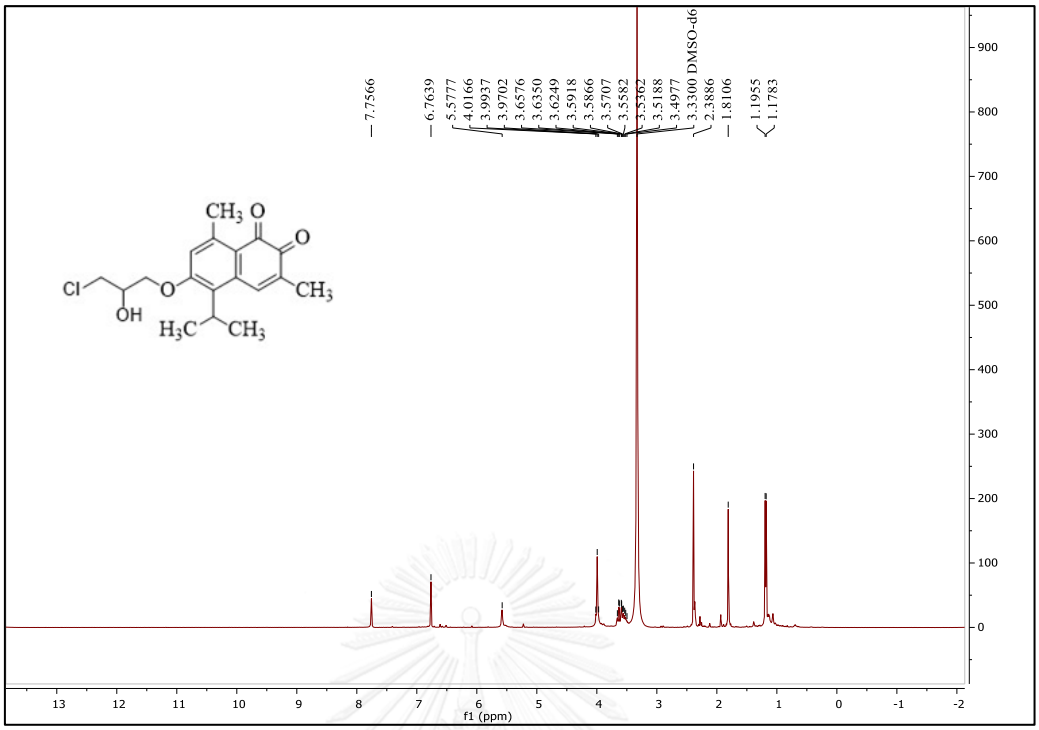

Figure 3.39 The ^{1}H NMR spectrum of **G20**

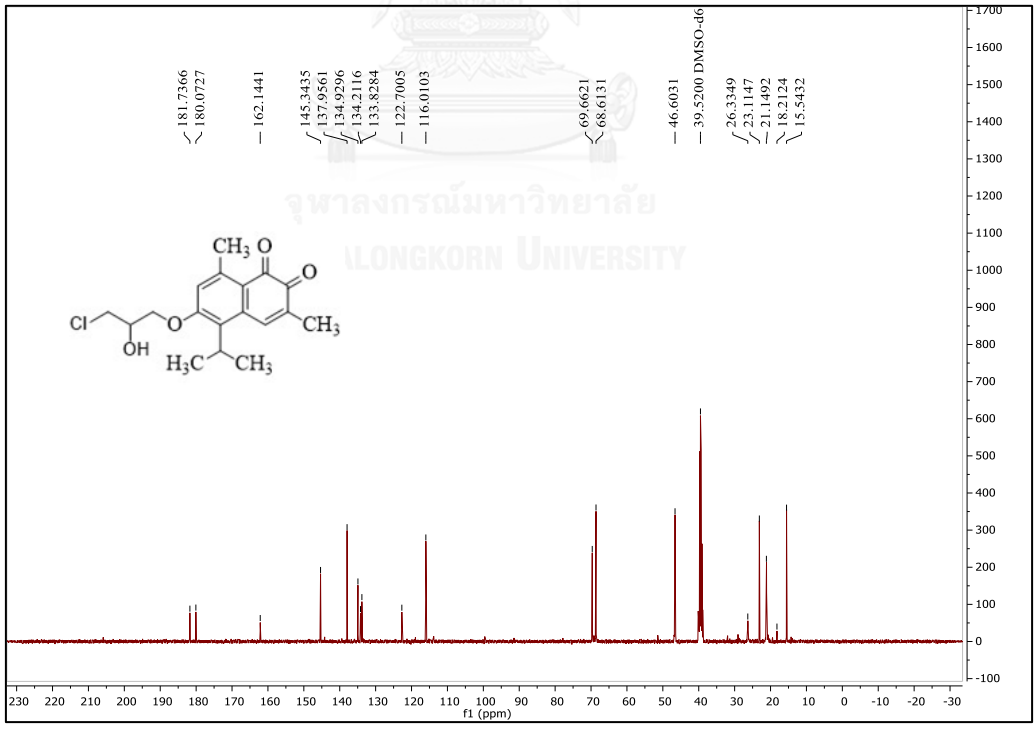

Figure 3.40 The ^{13}C NMR spectrum of **G20**

3.6 Antibacterial Activity of Mansonone Derivatives

All mansonone G analogues were then evaluated for their antibacterial activity as presented in Table 3.17. Most of mansonone G derivatives possessed better activity than their natural compound, mansonone G (**6**). These results signified that the changing of –OH group at position C6 of mansonone G (**6**) become other functional groups would give the influence on the antibacterial activity. Other previous study in typical 1,2-naphthoquinones reported that the derivatives of these groups displayed potential activity in antibacterial assay. Suh and coworkers in 2006, synthesized mansonone F analogues by varying substituent at C6 and C9 for investigation of the anti-MRSA activity, resulted that most of the analogues displayed good or excellent anti-MRSA activity especially 6-*n*-butyl mansonone F.[81] In 2016, Souza and coworkers reported that biflorin derivatives (typical 1,2-naphthoquinones) including its methyloxime and ethyloxime exhibited similar or even better activity than that of biflorin against *Enterococcus faecalis* (ATCC 4083), *Escherichia coli* (27), and *Staphylococcus aureus* (ATCC 25923 and 358).

Table 3.17 Diameter of inhibition zone of mansonone G and its derivatives

Compound (1mM)	Diameter of inhibition zone (mm)				
	S. aureus ATCC 25923	*S. mutans* ATCC 25175	*S. sobrinus* KCCM 11898	*P. acnes* KCCM 41747	*S. typhi* ATCC 422
Mansonone G (**6**)	13.7±1.15	14.7±0.58	10.0±0.00	15.6±1.23	11.9±1.18
G01	15.3±0.58	11.3±1.15	10.7±1.15	13.2±0.76	10.7±1.18
G02	16.0±1.00	18.0±1.00	14.3±0.58	13.3±0.00	10.8±0.43
G03	18.0±0.00	18.3±0.58	15.7±0.58	13.6±1.01	12.0±1.80
G04	20.0±0.00	20.0±1.73	16.7±1.15	14.6±1.13	16.3±1.26
G05	9.0±0.00	9.0±1.00	8.0±0.00	11.9±1.13	11.5±0.25
G06	21.7±0.58	18.3±0.58	17.0±0.53	17.0±0.93	13.9±0.88
G07	23.0±0.00	17.3±0.58	15.7±0.58	13.8±1.66	14.5±0.43
G08	21.7±1.53	17.7±0.58	16.0±0.00	13.6±0.29	16.3±0.76
G09	14.0±0.45	16.2±0.14	11.5±0.00	11.1±1.01	14.0±0.42
G10	11.0±0.75	13.1±1.28	12.7±0.14	12.8±0.95	13.9±0.14
G11	18.0±1.00	12.7±1.53	13.7±0.58	13.0±0.66	10.7±1.04
G12	14.7±0.58	12.0±0.00	12.7±0.58	11.3±1.09	8.7±0.52
G13	8.7±0.58	10.3±1.15	11.3±0.58	11.6±0.76	9.6±1.26
G14	7.0±0.00	9.7±0.58	10.7±0.58	11.4±0.52	9.2±0.80
G15	19.7±0.58	14.7±0.58	15.3±1.15	13.1±1.01	11.6±0.30
G16	11.7±1.15	14.3±0.58	14.3±1.53	13.2±0.72	14.8±1.51
G17	17.3±1.15	15.3±0.58	17.3±1.53	12.1±1.28	13.2±1.15
G18	10.0±1.00	15.0±0.00	14.0±0.00	10.8±1.09	12.8±1.04
G19	18.3±0.58	13.7±1.15	13.0±0.00	13.2±0.85	12.7±0.88
G20	14.5±1.31	11.5±1.17	11.1±0.76	12.9±1.44	13.1±0.95
Chloramphenicol (0.5 mM)	20.7±0.58	25.7± 0.58	25.3±1.52	30.0±0.90	24.8±0.75

Values are presented as mean ±SD of triplicate experiments

Diameter of inhibition zone including diameter of well (6 mm)

Note: 6.0 = no activity, 6.1 – 8.0 = weak, 8.1 – 10.0 = moderate, 10.1 – 13.0 = good, 13.1 – 15.0 = very good, >15 = excellent

The diameter inhibition zone (mm) of mansonone G derivatives were ranging from 7.0 – 23.7 against *S. aureus*, 9.0 – 20.0 against *S. mutans*, 8.0 – 16.7 against *S. sobrinus*, 11.1 – 17.1 against *P. acnes*, and 8.2 – 16.3 against *S. typhi*. These results indicated that mansonone G derivatives displayed broad spectrum in antibacterial activity because of their abilities to inhibit the growth of both Gram-positive and negative bacteria.

Moreover, their potential activities would contribute to the development of infectious drug discovery which dramatic increase due to of antibiotic resistance. In this study, two strains bacteria belong to Gram-positive bacteria can cause skin disease, *i.e. S. aureus* and *P. acnes*. Several mansonone G derivatives (**G01**, **G02**, **G03**, **G04**, **G06**, **G07**, **G08**, **G11**, **G15**, **G17**, and **G19**) showed excellent activities towards *S. aureus*, in contrast to *P.* acnes, only **G06** displayed excellent activity. It seemed that *P. acnes* which known can cause acnes, was rather difficult to inhibit than *S. aureus*. The results indicated that these derivatives possibly preferred to cure staphylococcal skin infection such as wound infection, dermatitis, scabies, cellulitis, and impetigo. On the other hand, the abilities of some mansonone G derivatives against *S. aureus* would give a way in discovery of anti-methicillin-resistant *S. aureus* (anti-MRSA) drug.

In addition several mansonone G derivatives (**G02, G03, G04, G06**, **G07**, **G08**, **G09**, and **G17)** also showed excellent activities towards *S. mutans*, and these compounds except for **G02** and **G09** towards *S. sobrinus*. The results showed that these derivatives were easier to inhibit *S. mutans* than *S. sobrinus*, which both bacteria are known to have major role in oral disease.

Furthermore, only **G04** and **G08** exhibited excellent activities towards *S. typhi* which is known to contribute a typhoid fever. The difficulty to inhibit this kind of bacteria caused by the characteristic of its membrane cell wall which have discussed in previous chapter.

Based on the antibacterial activity results, the ether analogues of mansonone G showed a correlation between the numbers of alkyl chain length with the antibacterial activity. Mansonone G derivatives with aliphatic substituents including one, two, four, eight, and twelve carbon atoms exhibited the increasing of the radius of inhibition zone with the number of carbon atoms in the chain from one to eight (**G01** – **G04**), in which **G04** revealed the highest inhibition among aliphatic ether analogues with its diameter of inhibition 20.0 against *S. aureus* and *S. mutans*, 15.7 against *S. sobrinus*, 14.6 against *P. acnes*, and 16.3 against *S. typhi* (Table 3.13). While the ether analogue of mansonone G containing twelve carbon atoms (**G05**) displayed a descending order in antibacterial activity. The relationship between these numbers of carbon atoms and antibacterial activity are described in Figure 3.41

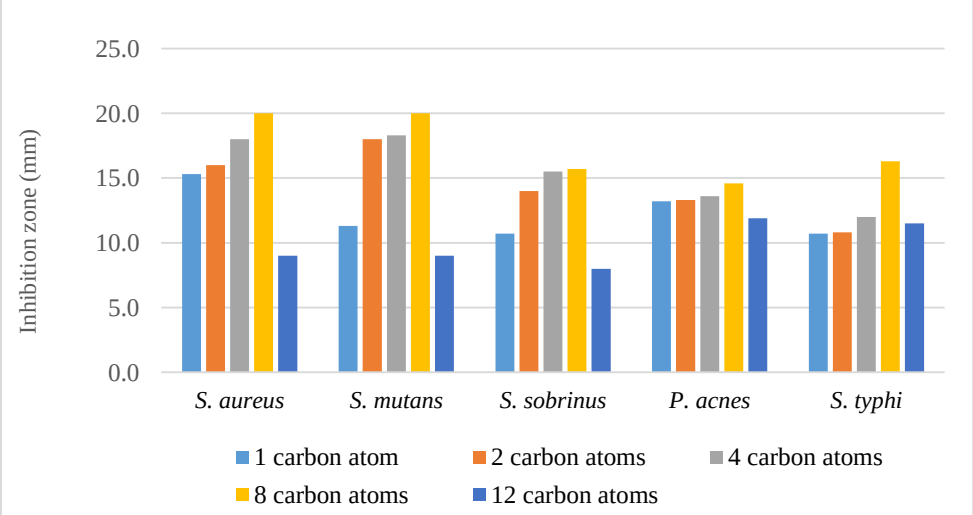

Figure 3.41 The relationship of the number of carbon atoms with antibacterial activity of **G01–G05**

These results showed that by increasing alkyl chain length of ether analogues of mansonone G from one carbon atom (methyl, **G01**) to eight carbon atoms (octyl, **G04**), could increase their antibacterial activities. The increasing of alkyl chain length was assumed to have a contribution to the extent of membrane interference. The increasing of alkyl chain length on ether analogues made the compounds more hydrophobic in which could facilitate the access to the lipophilic cell wall microbial.

Some studies reported that the increasing the hydrophobicity of compound resulted in increasing the activity. In 1994, Kanazawa and coworkers revealed that the phosphonium salts with long alkyl chains upto 18 carbon atoms were found to display high levels of antibacterial activity.[125] Birnie and coworkers in 2000 found the relationship between antimicrobial activity with increasing chain length of *N*-alkyl betaines and *N*-alkyl-*N*,*N*-dimethylamine oxides homologs.[126] Sahariah and coworkers in 2015 reported that there was the relationship between antibacterial activity and the length of the alkyl chain, as it increased from methyl to hexyl of *N*-alkyl chitosan derivatives.[127] In another investigation by Altay and coworkers at the same year reported that cationic pyridinium polymer with hexyl unit presented the highest bactericidal activity towards *E. coli*.[128]

However, after increased the carbon atoms numbers to twelve (**G05**), the activity was reduced. This result indicated that the ether analogues exponentially increased the activity until eight carbon atoms (**G04**) as the optimum of the activity. This phenomenon is known as a "cut of effect" which often displays a non-linear dependence on chain length that is quasi parabolic due to the decreasing of activity for the more lipophilic substances.[129] This effect can occur *via* some previous proposed hypothesis which have been summarized by Devinsky, *et. al.*[129] as follows:

1. Limited solubility by Janoff, *et. al*. and Pringle, *et. al*., in 1981.[130, 131]
   In this case, the higher alkyl chain lengths will reduce the activity due to the limitation of membrane partition coefficient (lipid/aqueous). The coefficient partition between membrane as the site of action and aqueous phase, increases less rapidly with the chain length than the aqueous solubility decreases, until a point is reached at which the optimum attainable concentration at the site of action is significantly lower than that required to affect the maximum of biological activity.
2. Limited volume by Franks and Lieb in 1986.[132]
   After binding at site of action of membrane which has a limited volume, the compound could act in which the volume becomes full by increasing the chain length and a decrease in binding occurs.

3. Compartment theory by Hansch and Fujita (1964), Lien, *et. al.* (1968), Balaz, *et. al.* (1988).[133-135]

   The phenomenon of "cut off effect" caused by the partition in time through several compartments, *e.g.* a series of lipid bilayers separated by aqueous layers, as the compound get through to the site of action.

4. Pertubartion theory by Lee (1976).[136]

   The phenomenon of "cut off effect" happens due to the interaction between long chain amphiphilic substances with the site of action.

5. Physical theory by Devinsky, *et. al* (1978).[137]

   This phenomenon relates to the physical properties of compound (*e.g.* stereochemistry).

This similar phenomenon also occurred for ether analogues containing allyl, prenyl or geranyl substituents (three, five, and ten carbon atoms with unsaturation portion), the activity increased from three to five carbon atoms (**G07** – **G08**), then decreased at ten carbon atoms (**G09**). **G07** and **G08** exhibited better activity than **G09** for some bacterial strain with their inhibition zone respectively 23.0 and 23.7 against *S. aureus*, 16.0 and 16.7 against *S. sobrinus*, 14.8 and 15.0 against *P. acnes*. The results also pointed out that the presence of double bonds in **G07** and **G08** also played an important role in antibacterial activity. The relationship of the number of carbon atoms of allyl and/or prenyl ether analogues of mansonone G are presented in Figure 3.42.

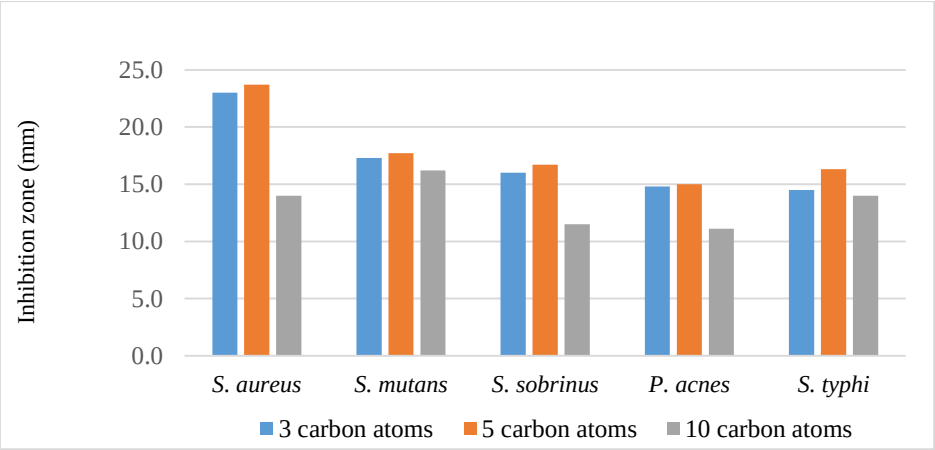

Figure 3.42 The relationship of carbon atom numbers with antibacterial activity of compounds **G07–G09** (3–10 carbon atoms)

Previous study reported that chalcones bearing prenyl or geranyl groups as well as their derivatives were found to inhibit Gram-positive bacteria.[138] The other study revealed that by replacing the *iso*prenyl group with a geranyl group of thiourea derivative was found to reduce antibacterial activity.[139] These previous studies supported the finding result in this research in which ether analogues of mansonone G containing geranyl substituent (**G09**) would decrease the activity.

Furthermore, for **G06** and **G10** which contained benzyl and cinnamyl substituents gave the different results. **G06** displayed better activity than **G10**. It could be described that even though **G10** had a double bond but its antibacterial activity was slightly lower than **G06**. Previous study reported that all of the synthesized compounds substituted benzyl ether derivatives exhibited good to moderate activity against Gram positive bacteria.[140]

Aliphatic ester analogues of mansonone G (**G11–G14**) showed slightly lower inhibition compared to aliphatic ether analogues. In contrast with ether analogues, the increasing of alkyl chain length from four to ten carbon atoms (**G11–G14**) caused the decreasing of the activity, in which the alkyl chain containing four carbon atoms (**G11**) displayed the highest activity, then followed by the decreasing activity with six, eight, and ten carbon atoms (**G12**, **G13**, and **G14**). **G11** exhibited good to excellent activities. The higher alkyl chain lengths more than four carbon atoms in aliphatic ester analogues

of mansonone G made the compounds more hydrophobic which may cause the limitation of partition coefficient in membrane cell, and further this compounds rather difficult to penetrate into membrane cell wall. The relationship of carbon atoms number and antibacterial activities of compounds **G11**–**G14** are shown in Figure 3.43.

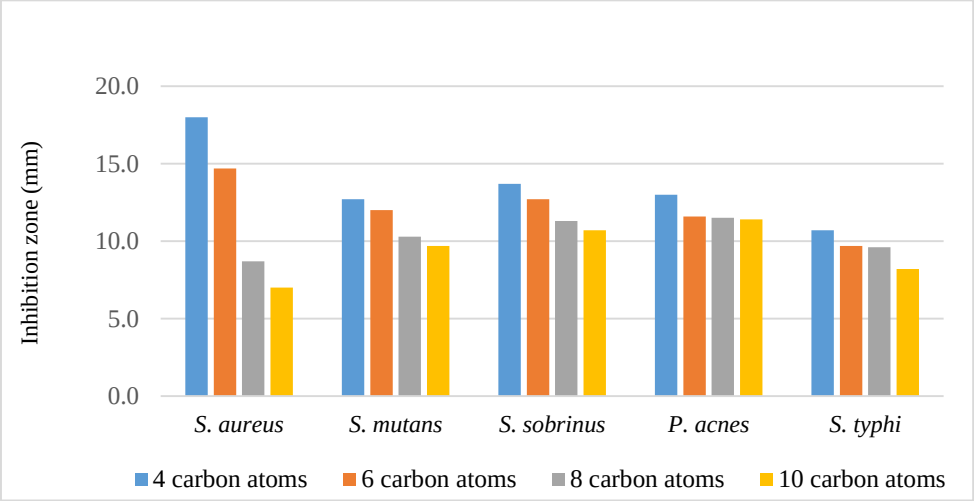

Figure 3.43 The relationship of carbon atoms number and antibacterial activities of **G11–G14**

In addition, aromatic ester analogues of mansonone G (**G15**–**G18**) were presented antibacterial activities towards both Gram positive and negative bacteria. In this group, the presence of aromatic substituents influenced the activity. Based on Table 3.14, **G15** and **G17** exhibited excellent activities against *S. aureus* and *S. sobrinus*. Moreover **G17** also displayed excellent activity towards *S. mutans*. In this case, the presence of electron donating group such as a methoxy group at *ortho* position in aromatic induced antibacterial activity. This result slightly different from that bearing a methoxy group at *para* position (**G18**) with lessen activity. While the presence of electron withdrawing substituent such as chloro group at *ortho* position (**G16**) gave moderate to very good activities.

In comparison between aliphatic and aromatic ester analogues of mansonone G, in general the results showed that aromatic ester analogues were better than aliphatic esters. Investigation by Al-Abdullah, *et. al.* in 2014 revealed that the increasing

the lipophilicity of compounds by replacing the aliphatic substituents with aromatics improved antibacterial activity.[141]

Mansonone G derivatives which derived from epichlorohydrin (**G19** and **G20**) exhibited from good to excellent activities. **G19** displayed better activities towards *S. aureus*, *S. mutans, S. sobrinus*, and *P. acnes*, than **G20**. The results suggested that the epoxide substituent in **G19** have the influence to enhance antibacterial activity.

In this antibacterial activity test, chloramphenicol as a control positive was used towards all bacteria tested due to the broad spectrum of this antibiotic. The diameter of inhibition zone of this control positive was ranging from 20.7 to 30.0 mm.

3.7 Minimum Inhibitory Concentration (MIC) of Mansonones and Their Derivatives

Four natural mansonones (**4**–**7**) along with several analogues which exhibited high activity for each bacterial strains were picked up to determined their MIC. MIC is considered as a standard to determine the susceptibility of bacteria to antibacterial agents.[142] In order to determine the MIC of these analogues, a broth microdilution was performed in 96-well plate. In addition, resazurin was employed as an indicator of bacteria growth. Resazurin is a blue-purple non-fluorescent and non-toxic dye that then changes the color become pink and fluorescent when reduced to resorufin which is further reduced to hydroresorufin (uncolored and non-fluorescent).[143, 144]

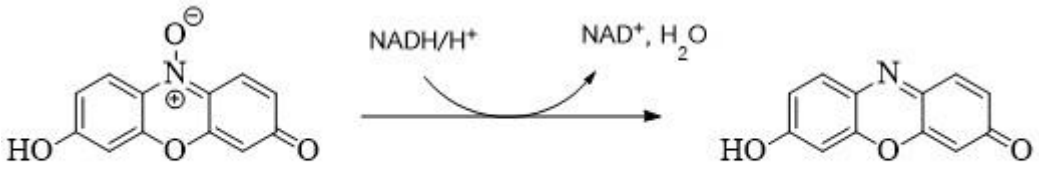

resazurin resorufin

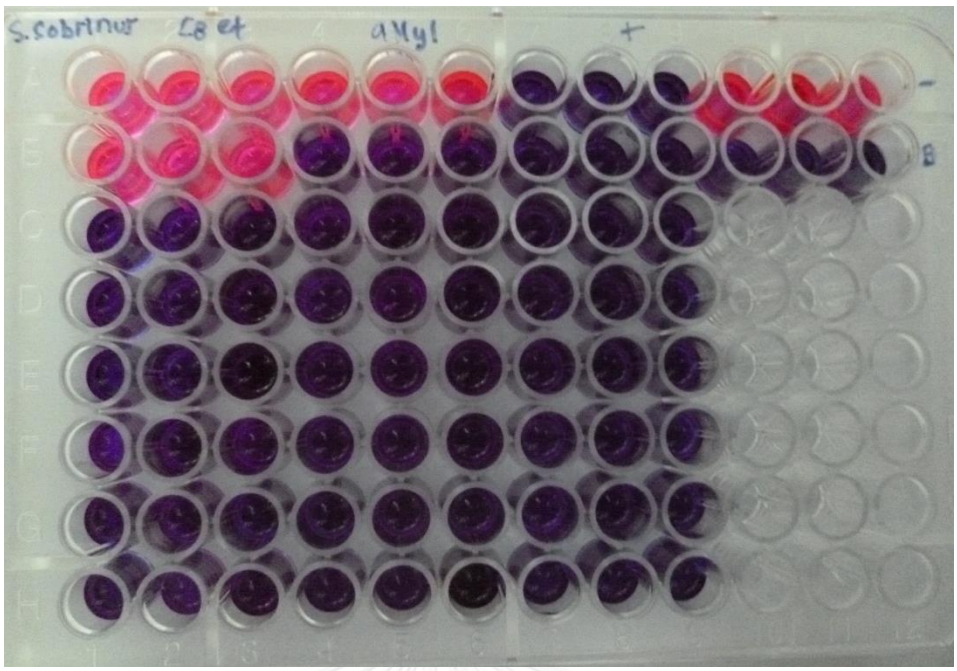

Figure 3.44 Performance of MIC determination in 96-well plate by resazurin assay

The MIC of four natural mansonones (**4**–**7**) and several mansonone G derivatives are presented in Table 3.18. Amongst mansonones, the data indicated that mansonone E (**5**) showed the lowest MIC against *S. aureus*, *S. sobrinus*, and *S. mutans*. **G07** and **G08** exhibited the lowest MIC (0.975 μM) among other analogues and natural mansonones against *S. aureus*. This compound also showed sixty-four times lower in MIC than its natural mansonone G (**6**, 31.25 μM). Moreover, **G04** exhibited lower MIC (15.6 μM) than **3** against *S. sobrinus*. Other analogues such as **G02** showed potential antibacterial agent against *S. mutans*, *P. acnes*, and *S. typhi* with MICs of 7.8, 15.6, and 3.9 μM, respectively.

Table 3.18 MIC of natural mansonones and mansonone G derivatives

Compound	Minimum Inhibitory Concentration (MIC, μM)				
	S. aureus ATCC 25923	*P. acnes* KCCM 41747	*S. sobrinus* KCCM 11898	*S. mutans* ATCC 25175	*S. typhi* ATCC 422
Mansonone C (**4**)	62.5	62.5	31.25	15.6	31.25
Mansonone E (**5**)	31.25	31.25	15.6	3.9	15.6
Mansonone G (**6**)	62.5	31.25	31.25	31.25	15.6
Mansonone H (**7**)	250	125	62.5	62.5	31.25
G02	-	62.5	31.25	62.5	-
G03	15.6	15.6	125	7.8	3.9
G04	15.6	31.25	31.25	31.25	31.25
G06	15.6	62.5	125	31.25	62.5
G07	0.975	31.25	15.6	31.25	62.5
G08	0.975	31.25	31.25	31.25	62.5
G09	-	-	-	-	125
G11	62.5	-	-	-	-
G15	62.5	-	-	-	-

3.8 Anti-Adipogenic Activity

3.8.1 Preliminary Screening Anti-Adipogenic Activity

In order to screen for promising candidates possessing anti-adipogenic activity, all compounds including natural and semisynthetic were evaluated, except for mansorin C (**3**) due to its limited amount. To date, there have been no previous studies on the anti-adipogenic activity of mansorins and mansonones and their derivatives.

To investigate the effects of these compounds on anti-adipogenic activity, confluent 3T3-L1 pre-adipocytes cell lines were treated with the absence (vehicle) and presence of 10 μM compound during differentiation (day 0 – 6). Every 2 day, cells were

observed under light microscope to notice the viability of cells. The compounds that made cells die were categorized as toxic compounds. According to the observation, mansonone E (**5**) and some mansonone derivatives: **G01**, **G04**, **G06**, **G08**, **G10**, **G18**, and **G19**, were found to be very toxic to the cells because all cells were died after treatment. Moreover, certain compounds: **G02**, **G03**, **G05**, and **G07** could also be categorized as toxic compounds. While some other compounds such as mansorin A (**1**), mansorin B (**2**), mansonone H (**7**), **G09**, **G11**, **G12**, **G13**, **G14**, and **G20**, did not show any significant suppression or toxic effect to the cells.

On day 7, the cells were fixed with 10% formalin and incubated for 2 days. Fixation has purpose to preserve cellular architecture and composition of cells in the tissue to let them to withstand further step.[145] On day 9, the differentiated adipocytes were stained with Oil Red O solution, and the cells images (Figure 3.45) were scanned by scanner. Subsequently, the lipid contents were quantified spectrophotometrically at 500 nm. The results were expressed as % optical density (Table 3.19). All experiments were done in duplicate.

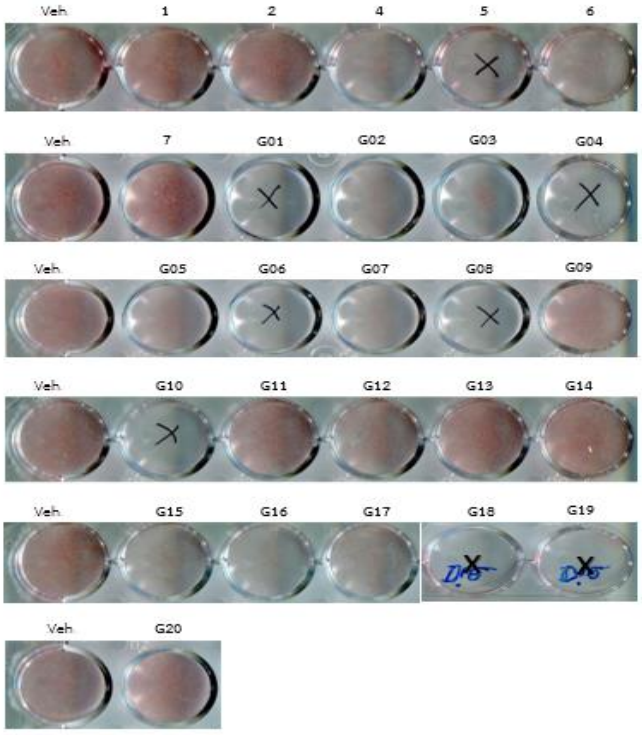

Figure 3.45 Cells images using scanner after ORO stain

Table 3.19 Percentage optical density of cells treated with isolated compounds and mansonone derivatives on anti-adipogenic activity

Compound	% optical density	Remarks
Mansorin A (**1**)	100	Not suppressed, not toxic
Mansorin B (**2**)	100	Not suppressed, not toxic
Mansonone C (**4**)	53.0	Suppressed, not toxic
Mansonone E (**5**)	-	Very toxic
Mansonone G (**6**)	46.0	Suppressed, not toxic
Mansonone H (**7**)	100	Not suppressed, not toxic
G01	-	Very toxic
G02	58.1	Suppressed, toxic
G03	48.8	Suppressed, toxic
G04	-	Very toxic
G05	80	Suppressed, toxic
G06	-	Very toxic
G07	60	Suppressed, toxic
G08	-	Very toxic
G09	100	Not suppressed, not toxic
G10	-	Very toxic
G11	100	Not suppressed, not toxic
G12	100	Not suppressed, not toxic
G13	100	Not suppressed, not toxic
G14	100	Not suppressed, not toxic
G15	37.6	Suppressed, not toxic
G16	34.7	Suppressed, not toxic
G17	46.7	Suppressed, not toxic
G18	-	Very toxic
G19	-	Very toxic
G20	100	Not suppressed, not toxic
Vehicle	100.0	Not suppressed, not toxic

The percentage of optical density (%OD) described for the amount of lipid accumulation. The higher % OD, the higher adipogenesis to form lipid. Vehicle with no treated compound exhibited 100 % OD. According this result, it showed that mansonones presented better activity than mansorins due to no suppression exhibited by neither mansorins A (**1**) nor B (**2**). In addition, mansonones C (**4**) and G (**6**) showed lower % OD indicating significantly reduce lipid accumulation in 3T3T-L1 during differentiation day. While for other mansonones such as mansonone E (**5**), due to the structure of this compound containing ether linkage, hence very toxic to the cells at the first day of differentiation day. In contrast with mansonone H (**7**), even though its structure had ether linkage, but the presence of –OH group at other position made this compound not toxic to the cells and did not suppress the adipogenesis.

Most of ether derivatives of mansonone G were toxic to the cells even some compounds showed the suppression, except **G09** due to this compound containing more than one of double bond of allyl. While for aliphatic ester derivatives of mansonone G (**G11** – **G14**), no compound displayed any suppression in adipogenesis. In contrast to aromatic ester derivatives of mansonone G, some of these compounds (**G15** – **G17**) exhibited suppression in adipogenesis.

3.8.2 Anti-Adipogenic Activity of Candidate Compounds by Dose-Dependent Manner

According preliminary screening of twenty-five compounds including natural and semisynthetic, five compounds (**4**, **6**, **G15**, **G16**, and **G17**) were picked up as candidates for further investigation in anti-adipogenic activity by dose-dependent manner (varying the concentrations as 0, 1, 5, 10, and 20 μM). In general, this assay was the same as preliminary screening in anti-adipogenic activity. The results are presented in Figure 3.46.

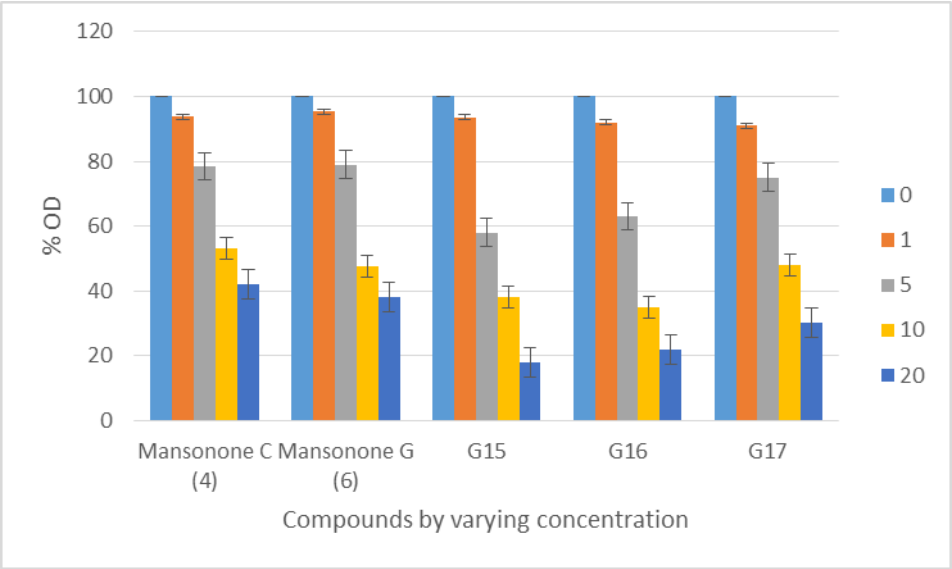

Figure 3.46 % OD of compounds in anti-adipogenic activity by dose-dependent manner

Based on Figure 3.16, it showed that by increasing the concentration, the anti-adipogenic was also increased. By calculating the linear equation of each compound, the IC_{50} (μM) of each compound in anti-adipogenic activity could be obtained as shown in Table 3.20.

Table 3.20 The IC_{50} (μM) of tested compounds in anti-adipogenic activity

Compound	IC_{50} (μM)
Mansonone C (**4**)	15.4
Mansonone G (**6**)	14.0
G15	10.0
G16	10.4
G17	12.6

The data in Table 3.20 presented that mansonone G (**6**) had lower IC_{50} than mansonone C (**4**). In addition the data also indicated that **G15**, **G16**, and **G17** exhibited lower IC_{50} as 10.0, 10.4, and 12.6 μM, respectively than that of natural compound

(mansonone G, **6**). This data suggested for further investigation for preliminary mechanism study of compounds mansonone G (**6**), **G15**, **G16**, and **G17**, in anti-adipogenic activity.

3.8.3 Expression of Adiponectin in Anti-Adipogenic Activity

Adiponectin is known as one of adipogenesis-related factor which is secreted from adipocytes during adipogenesis. In order to determine the mechanism action of compounds **6**, **G15**, **G16**, and **G17**, in anti-adipogenic activity, adiponectin was introduced after 6 days differentiation by western blot analysis. The result is presented in Figure 3.47.

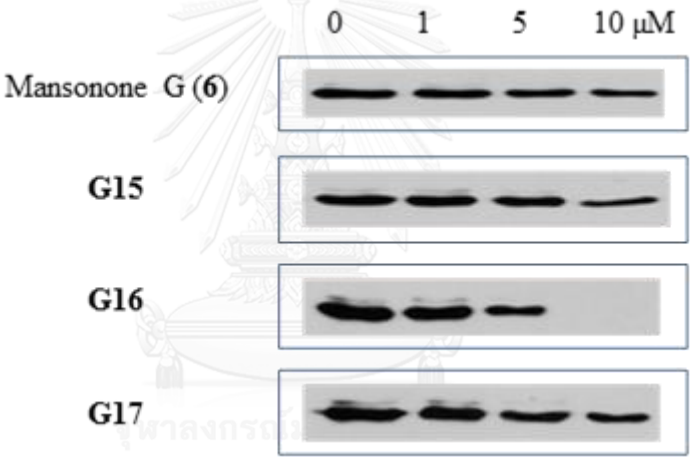

Figure 3.47 Adiponectin expression in anti-adipogenic activity of compounds **6, G15, G16, and G17**

Based on Figure 3.47, even though mansonone G (6) did not show significant decreasing of adiponectin level, but its derivatives such as compound **G16** displayed the best suppression of adiponectin. Other compounds such as **G15** and **G17** exhibited little suppression of adiponectin. This result suggesting that compounds **G15–G17** have potential inhibition in adipogenesis by suppressing the production of adiponectin.

CHAPTER IV
CONCLUSION

During the course of this study, the CH_2Cl_2 extract of *Mansonia gagei* Drumm. heartwoods was chosen as plant material due to the interesting compounds isolated from this extract (1,2-naphthoquinone and coumarin-based compounds) as well as their great biological activities reported previously. Three naturally occurring coumarins named mansorin A (**1**), mansorin B (**2**), and mansorin C (**3**), together with four naturally occurring 1,2-naphthoquinones named mansonone C (**4**), mansonone E (**5**), mansonone G (**6**), and mansonone H (**7**), have been isolated from this extract and investigated for their antibacterial and anti-adipogenic activities.

In antibacterial activity test, agar well diffusion method was performed against both Gram positive and negative bacteria including *Staphylococcus aureus* ATCC 25923, *Streptococcus mutans* ATCC 25175, *Streptococcus sobrinus* KCCM 11898, *Propionibacterium acnes* KCCM 41747, and *Salmonella typhi* ATCC 422.

According to the antibacterial activity of these isolated compounds, it can be seen that in general mansonones exhibited better activity than mansorins. In addition, it also gave the information that mansonones E (**5**) and G (**6**) presented higher activity than others. Attributable to mansonone G (**6**) displayed good activity and was obtained in large amount among other mansonones, therefore some derivatives of mansonone G were carried out and examined for their antibacterial activity.

Derivatization of mansonone G (**6**) was performed into three domain analogues which known as ether, and ester analogues of mansonone G, and mansonone G analogues derived from epichlorohydrin. For ether analogues, ten derivatives known as methyl ether mansonone G (**G01**), ethyl ether mansonone G (**G02**), butyl ether mansonone G (**G03**), octyl ether mansonone G (**G04**), dodecyl ether mansonone G (**G05**), benzyl ether mansonone G (**G06**), allyl ether mansonone G (**G07**), 3,3-dimethylallyl ether mansonone G (**G08**), geranyl ether mansonone G (**G09**), and cinnamyl ether mansonone G (**G10**) were manipulated. For ester analogues, eight

analogues of mansonone G have been synthesized, which identified as mansonone G butyrate (**G11**), mansonone G hexanoate (**G12**), mansonone G octanoate (**G13**), mansonone G decanoate (**G14**), mansonone G benzoate (**G15**), mansonone G 2-chloro benzoate (**G16**), mansonone G 2-methoxy benzoate (**G17**), and mansonone G 4-methoxy benzoate (**G18**). The reaction between mansonone G with epichlorohydrin yielded two compounds G**19** and **G20**. Amongst these derivatives, **G02** – **G20** are reported for the first time as new semisynthetic compounds.

The antibacterial activity of these compounds indicated that several mansonone G derivatives exhibited better activity than that of natural compound (mansonone G, **6**). **G07** and **G08** showed the lowest MIC (0.975 μM) among other mansonone G derivatives and natural mansonones towards *S. aureus*. These derivatives also displayed sixty-four times lower in MIC than its natural mansonone G (**6**, 31.25 μM).

For the anti-adipogenic activity, mansonone C (**4**) and mansonone G (**6**) possessed the suppression in 3T3-L1 pre-adipocytes differentiation with IC_{50} 15.4 and 14.0 μM, respectively. In addition, some mansonone G derivatives including **G15**, **G16**, and **G17** exhibited the suppression with IC_{50} 10.0, 10.4, and 12.6 μM, respectively. In order to investigate their mechanism action in anti-adipogenic, western blot analysis was performed for evaluating the expression of adiponectin. The results showed that **G16** displayed the highest suppression of adiponectin production. This result also suggesting that **G15 – G17** have good activity in adipogenesis by suppressing the production of adiponectin.

REFERENCES

[1] Farnsworth, N.R., and Morris, R. W. Higher plants-the sleeping giant of drug development. American Journal of Pharmacy 147 (1976): 46-52.

[2] Sarker, S.D., Latif, Z., and Gray, A.I. Natural products isolation. Second ed. Vol. Methods in Biotechnology. Totowa: Humana Press, 2005.

[3] Dewick, P.M. Medicinal natural products: A biosynthetic approach. USA: John Wiley & Sons, Ltd, 2011.

[4] Bernhoft, A. A brief review on bioactive compounds in plants. in Bernhoft, A. (ed.)Bioactive compounds in plants – benefits and risks for man and animals, pp. 11-17. Novus forlag, Oslo: The Norwegian Academy of Science and Letters, 2008.

[5] Bourgaud, F., Gravot, A., Milesi, S., and Gontier, E. Production of plant secondary metabolites: a historical perspective. Plant Science 161(5) (2001): 839-851.

[6] Newman, D.J.a.C., G. M. . Natural products as drugs and lead to drugs: the historical perspective. Natural product chemistry for drug discovery. Cambridge: RSC Publishing, 2010.

[7] Phillipson, J.D. Phytochemistry and medicinal plants. Phytochemistry 56(3) (2001): 237-243.

[8] Gurib-Fakim, A. Medicinal plants: traditions of yesterday and drugs of tomorrow. Mol Aspects Med 27(1) (2006): 1-93.

[9] Mahidol, C., Prawat, H., Prachyawarakorn, H., and Ruchirawat, S. Investigation of some bioactive Thai medicinal plants. Phytochemistry Reviews 1 (2002): 11.

[10] Seigler, D.S. Plant Secondary Metabolism. Massachusetts: Kluwer Academic, 1998.

[11] Thomson, R.H. Naturally occurring quinones. Second ed. New York: Academic Press, 1971.

[12] Didry, N., Pinkas, M., and Dubreuil, L. Antimicrobial activity of some naphtoquinones found in plants. Annales Pharmaceutiques Francaises 44(1) (1986): 73-78.

[13] Wellington, K.W. Understanding cancer and the anticancer activities of naphthoquinones - a review. RSC Advances 5(26) (2015): 20309-20338.

[14] Sendl, A., Chen, J.L., Jolad, S. D., Stoddart, C., Rozhon, E., Kernan, , Nanakorn, W., and Balick, M. Two new naphthoquinones with antiviral activity from *Rhinacanthus nasutus.* Journal of Natural Products 59 (1996): 808 - 811.

[15] Likhitwitayawuid, K., Kaewamatawong, R., Ruangrungsi, N., and Krungkrai, J. Antimalarial naphthoquinones from *Nepenthes thorelii.* Planta Medica 64 (1998): 237 - 241.

[16] Gafner, S., Wolfender, J.-L., Nianga, M., Stoeckli-Evans, H., and Hostettmann, K. Antifungal and antibacterial naphthoquinones from Newbouldia laevis roots. Phytochemistry 42(5) (1996): 1315-1320.

[17] Souza, L.G.d.S., et al. Synthesis, antibacterial and cytotoxic activities of new biflorin-based hydrazones and oximes. Bioorganic & Medicinal Chemistry Letters 26(2) (2016): 435-439.

[18] Hook, I., Mills, C., and Sheridan, H. Bioactive naphthoquinones from higher plants. in Atta-ur-Rahman (ed.)Studies in natural products chemistry, pp. 119-160. Oxford: Elsevier Science & Technology, 2014.

[19] Eyong, K.O., Kuete, V., and Efferth, T. Quinones and benzophenones from the medicinal plants of Africa. in Kuete, V. (ed.)Medicinal plant research in Africa, pp. 351-391. Oxford: Elsevier, 2013.

[20] Babula, P., Adam, V., Havel, L., and Kizek, R. Noteworthy secondary metabolites naphthoquinones – their occurrence, pharmacological properties and analysis Current Pharmaceutical Analysis 5(1) (2009): 47-68.

[21] Uc-Cachón, A.H., et al. Naphthoquinones isolated from *Diospyros anisandra* exhibit potent activity against pan-resistant first-line drugs *Mycobacterium tuberculosis* strains. Pulmonary Pharmacology & Therapeutics 27(1) (2014): 114-120.

[22] Crosby, I.T., et al. Antiviral agents 2. Synthesis of trimeric naphthoquinone analogues of conocurvone and their antiviral evaluation against HIV. Bioorganic & Medicinal Chemistry 18(17) (2010): 6442-6450.

[23] Yoshihira, K., Tezuka, M., and Natori, S. Naphthoquinone derivatives from *Diospyros* spp.: bisisodiospyrin, a tetrameric naphthoquinone. Tetrahedron Letters 11(1) (1970): 7-10.

[24] Luo, P., et al. Anti-inflammatory and analgesic effect of plumbagin through inhibition of nuclear factor-$_{K}$B activation. Journal of Pharmacology and Experimental Therapeutics 335(3) (2010): 735-742.

[25] de Paiva, S.R., Figueiredo, M.R., Aragão, T.V., and Kaplan, M.A.C. Antimicrobial activity in vitro of plumbagin isolated from *Plumbago* species. Memórias do Instituto Oswaldo Cruz 98(7) (2003): 959 - 961.

[26] Jeyachandran, R., Mahesh, A., Cindrella, L., Sudhakar, S., and Pazhanichamy, K. Antibacterial activity of plumbagin and root extracts of *Plumbago zeylanica* L. Acta Biologica Cracoviensia 51(1) (2009): 17-22.

[27] Gomathinayagam, R., Sowmyalakshmi, S., Mardhatillah, F., Kumar, R., Akbarsha, M.A., and Damodaran, C. Anticancer mechanism of plumbagin, a natural compound, on non-small cell lung cancer cells. Anticancer Research 28 (2008): 785 - 792.

[28] Dhingra, D. and Bansal, S. Antidepressant-like activity of plumbagin in unstressed and stressed mice. Pharmacological Reports 67(5) (2015): 1024-1032.

[29] Checker, R., Sharma, D., Sandur, S.K., Khanam, S., and Poduval, T.B. Anti-inflammatory effects of plumbagin are mediated by inhibition of NF-kappaB activation in lymphocytes. International Immunopharmacology 9 (2009): 949-958.

[30] Wei, Y., et al. Anti-fibrotic effect of plumbagin on CCl_4. Cellular Physiology and Biochemistry 35 (2015): 1599-1608.

[31] Jeon, J.-H., Lee, C.-H., Kim, M.K., and Lee, H.-S. Antibacterial effects of juglone and its derivatives against oral pathogens. Journal of the Korean Society for Applied Biological Chemistry 52(6) (2009): 720-725.

[32] Xu, H.-L., et al. Anti-proliferative effect of Juglone from *Juglans mandshurica* Maxim on human leukemia cell HL-60 by inducing apoptosis through the mitochondria-dependent pathway. European Journal of Pharmacology 645 (2010): 14-22.

[33] Fang, F., et al. Juglone exerts antitumor effect in ovarian cancer cells. Iranian Journal of Basic Medical Sciences 18(6) (2015): 544-548.

[34] Ashnagar, A.S., A. Isolation and characterization of 2-hydroxy-1,4-naphthoquinone (lawsone) from the powdered leaves of henna plant marketed in Ahwaz city of Iran. International Journal of ChemTech Research 3(4) (2011): 1941-1944.

[35] Rahmoun, N.M., Boucherit-Otmani, Z., Boucherit, K., Benabdallah, M., Villemin, D., and Choukchou-Braham, N. Antibacterial and antifungal activity of lawsone and novel naphthoquinone derivatives. Médecine et maladies infectieuses 42 (2012): 270 - 275.

[36] Saeed, S.M.G., et al. A new method for the isolation and purification of lawsone from *Lawsonia inermis* and its ROS inhibitory activity. Pakistan Journal of Botany 45(4) (2013): 1431-1436.

[37] Souza, M.A., et al. The antimicrobial activity of lapachol and its thiosemicarbazone and semicarbazone derivatives. Memórias do Instituto Oswaldo Cruz 108(3) (2013): 342 - 351.

[38] Guiraud, P., Steiman, R., Campos-Takaki, G.M., Seigle-Murand, F., and Simeon de Buochberg, M. Comparison of antibacterial and antifungal activities of lapachol and β-lapachone. Planta Medica 60(373 - 374) (1994).

[39] Fonseca, S.G.d.C., Braga, R.M.C., and Pereira de Santana, D. Lapachol: chemistry, pharmacology and assay methods. Revista Brasileira de Farmácia 84(1) (2003): 9-16.

[40] Mata-Santos, T., et al. Anthelmintic activity of lapachol, β-lapachone and its derivatives against *Toxocara canis* larvae. Rev Inst Med Trop Sao Paulo 57(3) (2015): 197-204.

[41] De Almeida, E.R., Da Silva, F.A.A., Dos Santos, E.R., and Lopes, C.A. Antiinflammatory action of lapachol. Journal of Ethnopharmacology 29(2) (1990): 239 - 241.

[42] Epifano, F., Genovese, S., Fiorito, S., Mathieu, V., and Kiss, R. Lapachol and its congeners as anticancer agents: a review. Phytochemistry Reviews 13(1) (2014): 37-49.

[43] Chen, X., et al. Shikonin, a component of chinese herbal medicine, inhibits chemokine receptor function and suppresses human immunodeficiency virus type 1. Antimicrobial Agents and Chemotheraphy 47(9) (2003): 2810 - 2816.

[44] Lee, H., Kang, R., and Yoon, Y. Shikonin inhibits fat accumulation in 3T3-L1 adipocytes. Phytotheraphy Research 24(3) (2010): 344-51.

[45] Lee, H., et al. Shikonin inhibits adipogenesis by modulation of the WNT/β-catenin pathway. Life Sciences 88(7–8) (2011): 294-301.

[46] Jang, Y.J., Jung, C.H., Ahn, J., Gwon, S.Y., and Ha, T.Y. Shikonin inhibits adipogenic differentiation via regulation of mir-34a-FKBP1B. Biochemical and Biophysical Research Communications 467(941 - 947) (2015).

[47] Gwon, S.Y., Ahn, J.Y., Jung, C.H., Moon, B.K., and Ha, T.Y. Shikonin suppresses ERK 1/2 phosphorylation during the early stages of adipocyte differentiation in 3T3-L1 cells. BMC Complementary and Alternative Medicine 13(1) (2013): 1-8.

[48] Gwon, S.Y., et al. Shikonin protects against obesity through the modulation of adipogenesis, lipogenesis, and β-oxidation in vivo. Journal of Functional Foods 16 (2015): 484-493.

[49] De Moura, K.C.G., et al. Studies on the trypanocidal activity of semi-synthetic pyran[b-4,3]naphtho[1,2-d]imidazoles from β-lapachone. European Journal of Medicinal Chemistry 39(7) (2004): 639-645.

[50] Macedo, L., Fernandes, T., Silveira, L., Mesquita, A., Franchitti, A.A., and Ximenes, E.A. β-Lapachone activity in synergy with conventional antimicrobials against methicillin resistant Staphylococcus aureus strains. Phytomedicine 21(1) (2013): 25-29.

[51] Pardee, A.B., Li Yz Fau - Li, C.J., and Li, C.J. Cancer therapy with beta-lapachone. Current Cancer Drug Targets 2(3) (2002): 227 - 242.

[52] Moon, D.-O., Choi, Y.H., Kim, N.-D., Park, Y.-M., and Kim, G.-Y. Anti-inflammatory effects of β-lapachone in lipopolysaccharide-stimulated BV2 microglia. International Immunopharmacology 7(4) (2007): 506-514.

[53] Ferreira, S.B., et al. Synthesis and anti-Trypanosoma cruzi activity of β-lapachone analogues. European Journal of Medicinal Chemistry 46(7) (2011): 3071-3077.

[54] Gupta, D., et al. β-lapachone, a novel plant product, overcomes drug resistance in human multiple myeloma cells. Experimental Hematology 30(7) (2002): 711-720.

[55] Perez-Sacau, E., Estevez-Braun, A., Ravelo, A.G., Yapu, D.G., and Turba, A.G. Antiplasmodial activity of naphthoquinones related to lapachol and beta-lapachone. Chemistry & Biodiversity 2 (2005): 264 - 274.

[56] Montenegro, R.C., Burbano, R.R., Da Silva, M.N., Lemos, T.G., and Vasconcellos, M.C. Biflorin, a naphthoquinone, inhibitsegfr in breast cancer cells. Medicinal Chemistry 3(1) (2013): 179-182.

[57] Wisintainer, G.G.N.D.S., et al. *O*-naphthoquinone isolated from *Capraria biflora* L. induces selective cytotoxicity in tumor cell lines. Genetics and Molecular Research 14(4) (2015): 17472 - 17481.

[58] Wisintainer, G.G.N.S., et al. Biflorin: an *o*-naphthoquinone of clinical significance. Anais da Academia Brasileira de Ciências 86 (2014): 1907-1914.

[59] Fonseca, A.M., Pessoa, O.D.L., Silveira, E.R., Monte, F.J.Q., Braz-Filho, R., and Lemos, T.L.G. Total assignments of 1H and 13C NMR spectra of biflorin and bis-biflorin from *Capraria biflora.* Magnetic Resonance in Chemistry 41(12) (2003): 1038-1040.

[60] Vasconcellos, M.C., et al. Antitumor activity of biflorin, an *o*-naphthoquinone isolated from *Capraria biflora.* Biological & Pharmaceutical Bulletin 30(8) (2007): 1416 - 1421.

[61] Vasconcellos, M.C., et al. Evaluation of the cytotoxic and antimutagenic effects of biflorin, an antitumor 1,4 o-naphthoquinone isolated from *Capraria biflora* L. Archives of Toxicology 84 (2010): 799 - 810.

[62] Inoue, K., Ueda, S., Nayeshiro, H., and Inouyet, H. Quinones of streptocarpus dunnii. Phytochemistry 22(3) (1983): 737-741.

[63] Bian, J., et al. Synthesis and evaluation of (±)-dunnione and its ortho-quinone analogues as substrates for NAD(P)H:quinone oxidoreductase 1 (NQO1). Bioorganic & Medicinal Chemistry Letters 25(6) (2015): 1244-1248.

[64] Khambay, B.P., Batty, D., Jewess, P.J., Bateman, G.L., and Hollomon, D.W. Mode of action and pesticidal activity of the natural product dunnione and of some analogues. Pest Management Science 59 (2003): 174 -182.

[65] Sutton, D.C., Gillan, F.T., and Susic, M. Naphthofuranone phytoalexins from the grey mangrove, *Avicennia marina.* Phytochemistry 24(12) (1985): 2877-2879.

[66] Cheeptham, N. and Towers, G.H.N. Light-mediated activities of some Thai medicinal plant teas. Fitoterapia 73(7–8) (2002): 651-662.

[67] Siriwatanametanon, N., Fiebich, B.L., Efferth, T., Prieto, J.M., and Heinrich, M. Traditionally used Thai medicinal plants: In vitro anti-inflammatory, anticancer and antioxidant activities. Journal of Ethnopharmacology 130(2) (2010): 196-207.

[68] Tiew, P., Ioset, J.R., Kokpol, U., Chavasiri, W., and Hostettmann, K. Antifungal, antioxidant and larvicidal activities of compounds isolated from the heartwood of *Mansonia gagei.* Phytotherapy Research 17(2) (2003): 190-193.

[69] Tiew, P., Puntumchai, A., Kokpol, U., and Chavasiri, W. Coumarins from the heartwoods of *Mansonia gagei* Drumm. Phytochemistry 60(8) (2002): 773-776.

[70] Tiengtham, P. Chemical constituents and their biological activities of the roots and the leaves of *Mansonia gagei* Drumm. Degree of Master of Science in Chemistry, Department of Chemistry Chulalongkorn University, 2004.

[71] Tiew, P. Bioactive compounds from *Mansonia gagei* Drumm. Doctoral of Philosophy in Chemistry Department of Chemistry Chulalongkorn University, 2002.

[72] El-Halawany, A.M., Chung, M.H., Ma, C.-M., Komatsu, K., Nishihara, T., and Hattori, M. Anti-estrogenic activity of mansorins and mansonones from the heartwood of *Mansonia gagei* Drumm. Chemical and Pharmaceutical Bulletin 55(9) (2007): 1332-1337.

[73] Bettòlo, G.B.M., Casinovi, C.G., and Galeffi, C. A new class of quinones: sesquiterpenoid quinones of *Mansonia altissima* chev. Tetrahedron Letters 6(52) (1965): 4857-4864.

[74] Tanaka, N., Yasue, M., and Imamura, H. The quinonoid pigments of *Mansonia altissima* wood. Tetrahedron Letters 7(24) (1966): 2767-2773.

[75] Galeffi, C., Delle Monache, E.M., Casinovi, C.G., and Bettòlo, G.B.M. A new quinone from the heartwood of *Mansonia altissima* Chev: mansonone L. Tetrahedron Letters 10(40) (1969): 3583-3584.

[76] Puckhaber, L.S. and Stipanovic, R.D. Thespesenone and dehydrooxoperezinone-6-methyl ether, new sesquiterpene quinones from *Thespesia populnea.* Journal of Natural Products 67 (2004): 1571-1573.

[77] Krishnamoorthy, V. and Thomson, R.H. Mansonone C in Elm wood. Phytochemistry 10(7) (1971): 1669-1670.

[78] Wang, D., Xia, M.Y., Cui, Z., Tashiro, S., S., O., and Ikejima, T. Cytotoxic effects of mansonone E and F isolated from *Ulmus pumila.* Biological and Pharmaceutical Bulletin 27(7) (2004): 1025 - 1030.

[79] El-Halawany, A.M., Salah El Dine, R., and Hattori, M. Anti-estrogenic activity of mansonone G and mansorin A derivatives. Pharm Biol 51(8) (2013): 948-954.

[80] Shin, D.Y., et al. Syntheses and anti-MRSA activities of the C3 analogs of mansonone F, a potent anti-bacterial sesquiterpenoid: insights into its structural requirements for anti-MRSA activity. Bioorganic & Medicinal Chemistry Letters 14 (2004): 4519-4523.

[81] Suh, Y.G., et al. The structure-activity relationships of mansonone F, a potent anti-MRSA sesquiterpenoid quinone: SAR studies on the C6 and C9 analogs. Bioorganic & Medicinal Chemistry Letters 16 (2006): 142-145.

[82] Wu, W.B., et al. Synthesis and evaluation of mansonone F derivatives as topoisomerase inhibitors. European Journal of Medicinal Chemistry 46 (2011): 3339-3347.

[83] Huang, Z.-H., et al. Design, synthesis and biological evaluation of novel mansonone E derivatives prepared via CuAAC click chemistry as topoisomerase II inhibitors. European Journal of Medicinal Chemistry 68 (2013): 58-71.

[84] Gupte, S. The short textbook of medical microbiology (including parasitology). 10th ed. New Delhi: Jaypee Brothers Medical Publisher (P) LTD, 2010.

[85] Hollar, S. Introduction to biology : A closer look at bacteria, algae, and protozoa. First ed. New York: Britannica Educational Publishing in association with Rosen Educational Services, 2012.

[86] Koch, A.L. The bacteria: their origin, structure, function, and antibiosis. Netherland: Springer, 2007.

[87] Andersoon, R.J., Groundwater, P.W., Todd, A., and Worsley, A.J. Antibacterial agents : chemistry, mode of action, mechanisms of resistance and clinical applications. United Kingdom: John Wiley & Sons, 2012.

[88] Wiwanitkit, V. *Escherichia coli* infections. First ed.: Internet Medical Publishing, 2011.

[89] Hauser, A.R. Antibiotic basics for clinicians : the ABCs of choosing the right antibacterial agent. Second ed. Philadelphia: Lippincott William & Wilkins, 2013.

[90] Berlutti, F., Catizone, A., Ricci, G., Frioni, A., Natalizi, T., Valenti, P., Polimeni, A. *Streptococcus mutans* and *Streptococcus sobrinus* are able to adhere and invade human gingival fibroblast cell line. International Journal of Immunopathology and Pharmacology 23(4) (2010): 1253-1260.

[91] Nascimento, M.M., Lemos, J.A., Abranches, J., Goncalves, R.B., and Burne, R.A. Adaptive acid tolerance response of *Streptococcus sobrinus.* J Bacteriol 186(19) (2004): 6383-6390.

[92] Clarke, J.K. On the Bacterial Factor in the Etiology of Dental Caries. British journal of experimental pathology 5(3) (1924): 141-147.

[93] Loesche, W.J. Role of Streptococcus mutans in human dental decay. Microbiological Reviews 50(4) (1986): 353-380.

[94] Belli, W.A., Marquis, R.E. Adaptation of *Streptococcus mutans* and *Enterococcus hirae* to acid stress in continuous culture. APPLIED AND ENVIRONMENTAL MICROBIOLOGY 57(4) (1991): 1134 - 1138.

[95] Perry, A.L. and Lambert, P.A. Propionibacterium acnes. Lett Appl Microbiol 42(3) (2006): 185-8.

[96] Park, H.J., et al. Clinical significance of *Propionibacterium acnes* recovered from blood cultures: analysis of 524 episodes. J Clin Microbiol 49(4) (2011): 1598-601.

[97] Kirschbaum, J.O. and Kligman, A.M. THe pathogenic role of corynebacterium acnes in acne vulgaris. Archives of Dermatology 88(6) (1963): 832-833.

[98] Ajay Bhatia, J.-F.M., and David H. Persing. Propionibacterium acnes and chronic diseases. in Knobler S.L., O.C.S., Lemon S.M., Najafi, M. (ed.)The Infectious Etiology of Chronic Diseases: Defining the Relationship, Enhancing the Research, and Mitigating the Effects. Washington (DC): National Academies Press, 2004.

[99] Zhang, X.L., Jeza Vt Fau - Pan, Q., and Pan, Q. *Salmonella typhi*: from a human pathogen to a vaccine vector. Cellular & Molecular Immunology 5(2) (2008): 91-97.

[100] Organization, W.H. Background document: The diagnosis, treatment and prevention of typhoid fever. Biologicals, D.o.V.a., Editor. 2003, World Health Organization: Switzerland.

[101] Kidgell, C., et al. *Salmonella typhi*, the causative agent of typhoid fever, is approximately 50,000 years old. Infection, Genetics and Evolution 2 (2002): 39-45.

[102] Kohanski, M.A., Dwyer, D.J., and Collins, J.J. How antibiotics kill bacteria: from targets to networks. Nature Reviews Microbiology 8(6) (2010): 423-35.

[103] Jardetzky, O. Studies on the mechanism of action of chloramphenicol. I. The conformation of chloramphenicol in solution. The Journal of Biological Chemistry 238(2498-2508) (1963).

[104] Corbett, M.D. and Chipko, B.R. Synthesis and antibiotic properties of chloramphenicol reduction products. Antimicrobial Agents and Chemotheraphy 13(2) (1978): 193-198.

[105] Bartz, Q.R. Isolation and characterization of chloromycetin. Journal of Biological Chemistry 172(2) (1948): 445-450.

[106] Fair, R.J. and Tor, Y. Antibiotics and bacterial resistance in the 21st century. Perspective in Medicinal Chemistry 6 (2014): 25-64.

[107] Lefterova, M.I. and Lazar, M.A. New developments in adipogenesis. Trends in Endocrinolgy and Metabolism 20(3) (2009): 107-114.

[108] Ford, N.A., DiGiovanni, J., and Hursting, S.D. Metabolic perturbations associated with adipose tissue dysfunction and the obesity–cancer link. Adipose tissue and cancer. New York: Springer, 2013.

[109] Stephens, J.M. The fat controller: adipocyte development. PLoS Biology 10(11) (2012): 1-3.

[110] Dani, C. and Billon, N. Adipose tissue biology. New York: Springer, 2012.

[111] Fantuzzi, G. and Mazzone, T. Adipose tissue and adipokines in health and disease, ed. Bendich, A. New Jersey: Humana Press, 2007.

[112] Enerback, S. Brown adipose tissue in humans. International Journal of Obesity 34(S1) (2010): S43-S46.

[113] Saely, C.H., Geiger, K., and Drexel, H. Brown versus white adipose tissue : a mini-review. Gerontology 58(1) (2012): 15-23.

[114] Ali, A.T., Hochfeld, W.E., Myburgh, R., and Pepper, M.S. Adipocyte and adipogenesis. European Journal of Cell Biology 92(6–7) (2013): 229-236.

[115] Camp, H.S., Ren, D., and Leff, T. Adipogenesis and fat-cell function in obesity and diabetes. TRENDS in Molecular Medicine 8(9) (2002).

[116] Bluher, M. Adipose tissue dysfunction contributes to obesity related metabolic diseases. Best Practice & Research Clinical Endocrinology & Metabolism 27 (2013): 163-177.

[117] Bjorndal, B., Burri, L., Staalesen, V., Skorve, J., and Berge, R.K. Different adipose depots: their role in the development of metabolic syndrome and mitochondrial response to hypolipidemic agents. Journal of Obesity (2011): 1-15.

[118] Chaysripongkul, S. Reagent development for the preparation of acid chloride for synthesis of bioactive compound. Master of Science, Department of Chemistry Chulalongkorn University, 2003.

[119] Nouailhas, H., Aouf, C., Le Guerneve, C., Caillol, S., Boutevin, B., and Fulcrand, H. Synthesis and properties of biobased epoxy resins. part 1. Glycidylation of

flavonoids by epichlorohydrin. Journal of Polymer Science Part A: Polymer Chemistry 49(10) (2011): 2261-2270.

[120] Karuppiah, P. and Mustaffa, M. Antibacterial and antioxidant activities of Musa sp. leaf extracts against multidrug resistant clinical pathogens causing nosocomial infection. Asian Pacific Journal of Tropical Biomedicine 3(9) (2013): 737-742.

[121] Sawasdee, S. Screening for Antimicrobial Substance Producing Actinomycetes from Soil Master, Microbiology Prince of Songkla, 2012.

[122] Bio-Rad. Mini-PROTEAN®Tetra Cell, Instruction Manual. Bio-Rad Laboratories, Inc.: USA.

[123] Shahwar, D., Raza, M.A. In vitro antibacterial activity of extracts of *Mimusops elengi* against gram positive and gram negative bacteria. African Journal of Microbiology Research 3(8) (2009): 458-462.

[124] Ahmad Barudin, N.H., Sreekantan, S., Ong, M.T., and Lai, C.W. Synthesis, characterization and comparative study of nano-Ag–TiO2 against Gram-positive and Gram-negative bacteria under fluorescent light. Food Control 46 (2014): 480-487.

[125] Kanazawa, A., Ikeda, T., and Endo, T. Synthesis and antimicrobial activity of dimethyl- and trimethyl-substituted phosphonium salts with alkyl chains of various lengths. Antimicrobial Agents and Chemotherapy 38(5) (1994): 945-952.

[126] Birnie, C.R., Malamud, D., and Schnaare, R.L. Antimicrobial Evaluation of N-Alkyl Betaines and N-Alkyl-N,N-Dimethylamine Oxides with Variations in Chain Length. Antimicrobial Agents and Chemotherapy 44(9) (2000): 2514-2517.

[127] Sahariah, P., et al. Impact of Chain Length on Antibacterial Activity and Hemocompatibility of Quaternary N-Alkyl and N,N-Dialkyl Chitosan Derivatives. Biomacromolecules 16(5) (2015): 1449-1460.

[128] Altay, E., Yapaöz, M.A., Keskin, B., Yucesan, G., and Eren, T. Influence of alkyl chain length on the surface activity of antibacterial polymers derived from ROMP. Colloids and Surfaces B: Biointerfaces 127 (2015): 73-78.

[129] Devinsky, F., Kopecka-Leitmanova, A., Sersen, F., and Balgavy, P. Cut-off effect in antimicrobial activity and in membrane perturbation efficiency of the

homologous series of N,N-dimethylalkylamine oxides. Journal of Pharmacy and Pharmacology 42 (1990): 790-794.

[130] Janoff, A.S., Pringle, M.J., and Miller, K.W. Correlation of general anesthetic potency with solubility in membranes. Biochimica et Biophysica Acta (BBA) - Biomembranes 649(1) (1981): 125-128.

[131] Pringle M. J., B., K. B., Miller, K. W. Can the lipid theories of anesthesia account for the cutoff in anesthetic potency in homologous series of alcohols? Molecular Pharmacology 19 (1981): 49-55.

[132] Franks N. P., L., W. R. Partitioning of long-chain alcohols into lipid bilayers: implications for mechanisms of general anesthesia. Biophysics 83 (1986): 5.

[133] Hansch, C. and Fujita, T. p-**σ**-**π** Analysis. A method for the correlation of biological activity and chemical structure. Journal of the American Chemical Society 86(8) (1964): 1616-1626.

[134] Lien, E.J.C., Hansch, C., and Anderson, S.M. Structure-activity correlations for antibacterial agents on gram-positive and gram-negative cells. Journal of Medicinal Chemistry 11(3) (1968): 430-441.

[135] Baláž, Š., Šturdík, E., Rosenberg, M., Augustín, J., and Škára, B. Kinetics of drug activities as influenced by their physico-chemical properties: Antibacterial effects of alkylating 2-furylethylenes. Journal of Theoretical Biology 131(1) (1988): 115-134.

[136] Lee, A.G. Interactions between anesthetics and lipid mixtures. Normal alcohols. Biochemistry 15(11) (1976): 2448-2454.

[137] Devinsky, F., Lacko, I., and Krasnec, L. Amine oxides. I. Synthesis, ^{1}H-n.m.r., and infrared spectra of 4-alkylmorpholine-N-oxides. Chemical Papers 32(1) (1978): 10.

[138] Sugamoto, K., Matsusita, Y.-i., Matsui, K., Kurogi, C., and Matsui, T. Synthesis and antibacterial activity of chalcones bearing prenyl or geranyl groups from *Angelica keiskei*. Tetrahedron 67(29) (2011): 5346-5359.

[139] Vega-Perez, J.M., et al. Isoprenyl-thiourea and urea derivatives as new farnesyl diphosphate analogues: synthesis and in vitro antimicrobial and cytotoxic activities. European Journal of Medicinal Chemistry 58 (2012): 591-612.

[140] Güven, Ö.Ö., Erdoğan, T., Göker, H., and Yıldız, S. Synthesis and antimicrobial activity of some novel phenyl and benzimidazole substituted benzyl ethers. Bioorganic & Medicinal Chemistry Letters 17(8) (2007): 2233-2236.

[141] Al-Abdullah, E.S., Asiri, H.H., Lahsasni, S., Habib, E.E., Ibrahim, T.M., and El-Emam, A.A. Synthesis, antimicrobial, and anti-inflammatory activity, of novel S-substituted and N-substituted 5-(1-adamantyl)-1,2,4-triazole-3-thiols. Drug Design, Development and Therapy 8 (2014): 505-518.

[142] Andrews, J.M. Determination of minimum inhibitory concentrations. Journal of Antimicrobial Chemotheraphy 48 (2001): 5-16.

[143] Sarker, S.D., Nahar, L., and Kumarasamy, Y. Microtitre plate-based antibacterial assay incorporating resazurin as an indicator of cell growth, and its application in the in vitro antibacterial screening of phytochemicals. Methods 42 (2007): 321-324.

[144] Guerin, T.F., Mondido, M., McClenn, B., and Peasley, B. Application of resazurin for estimating abundance of contaminant-degrading micro-organisms. Lett Appl Microbiol 32(5) (2001): 340-345.

[145] Thavarajah, R., Mudimbaimannar, V.K., Elizabeth, J., Rao, U.K., and Ranganathan, K. Chemical and physical basics of routine formaldehyde fixation. Journal of Oral and Maxillofacial Pathology : JOMFP 16(3) (2012): 400-405.

APPENDIX

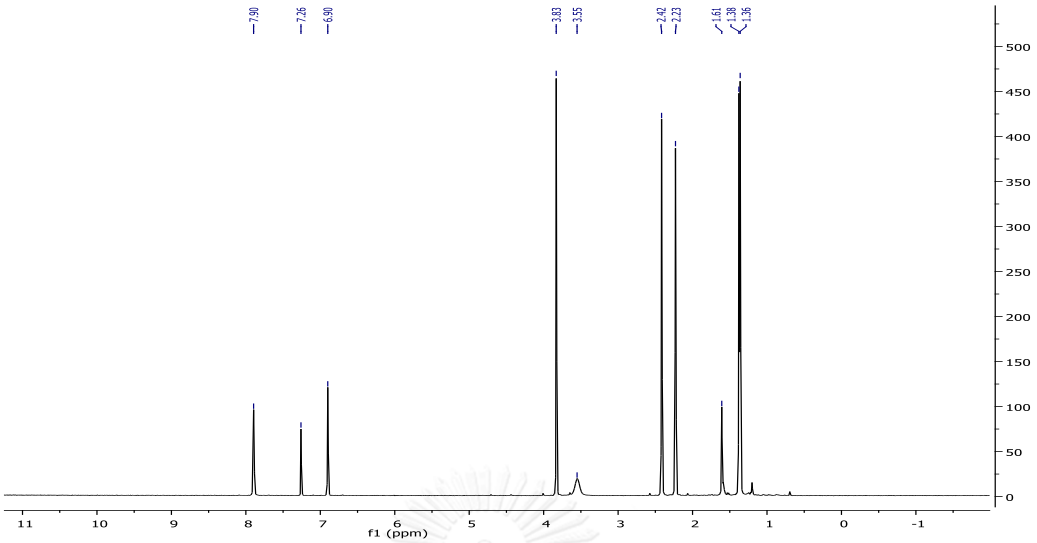

Appendix 1. The ^{1}H NMR spectrum ($CDCl_3$) of mansorin A (**1**)

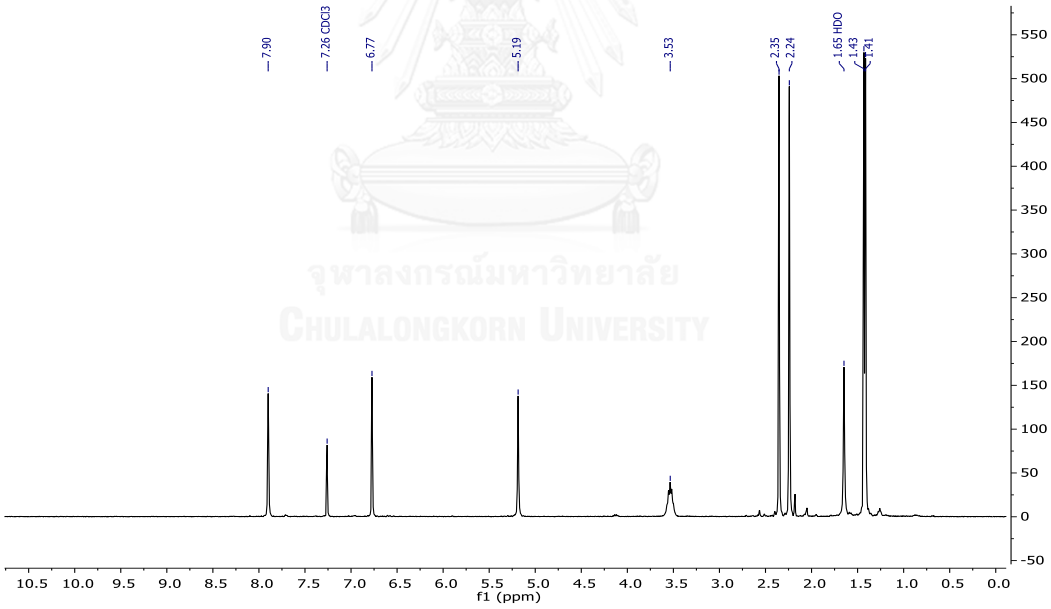

Appendix 2. The ^{1}H NMR spectrum ($CDCl_3$) of mansorin B (**2**)

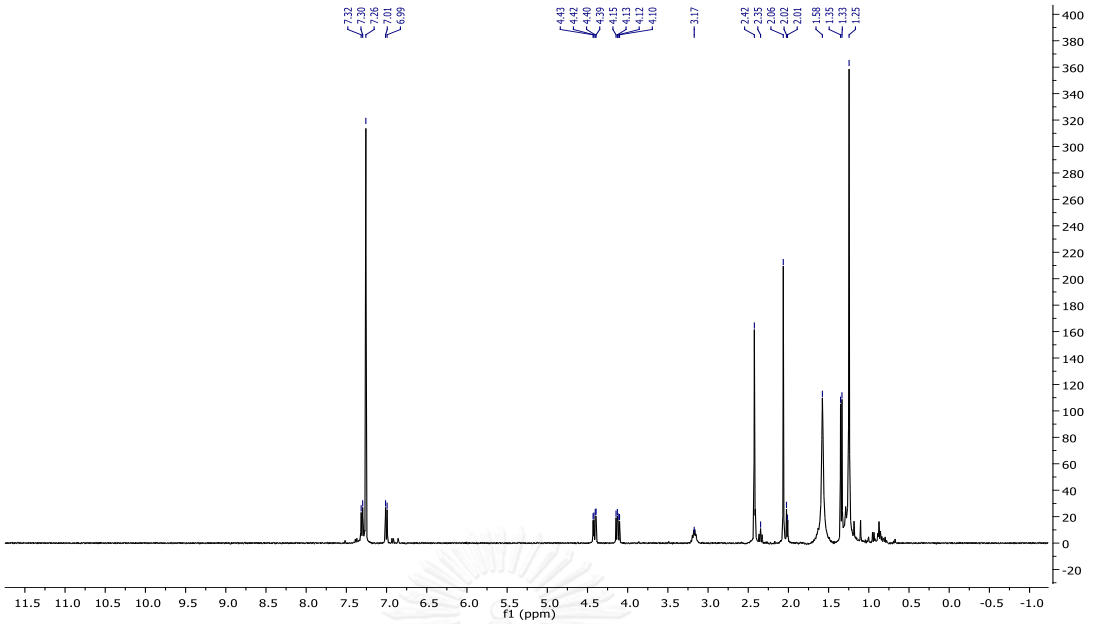

Appendix 3. The ^{1}H NMR spectrum ($CDCl_3$) of mansorin C (**3**)

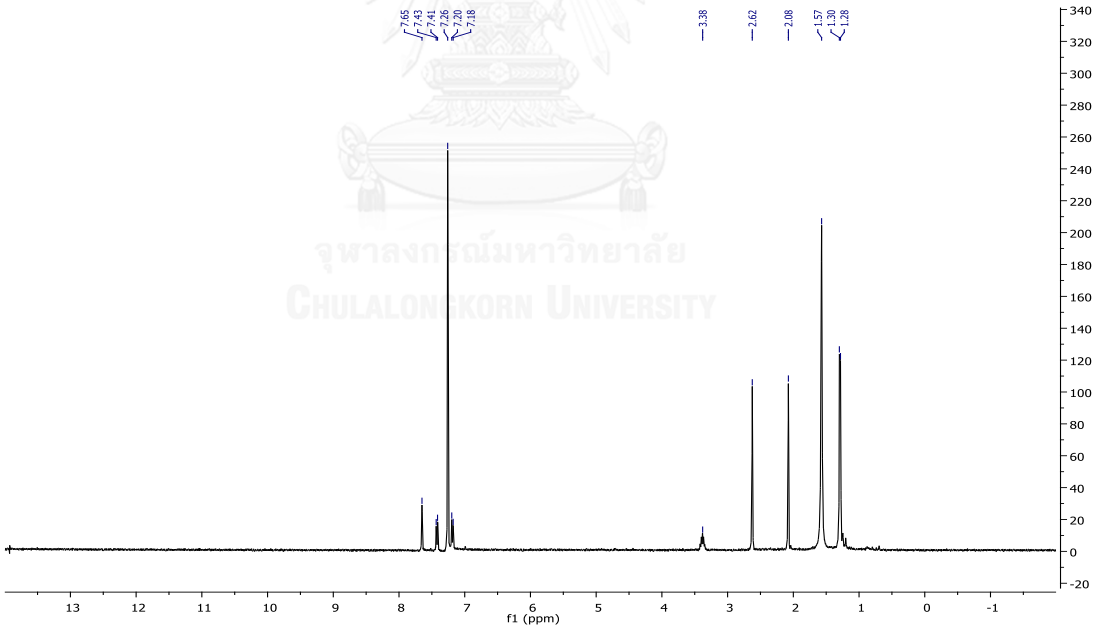

Appendix 4. The ^{1}H NMR spectrum ($CDCl_3$) of mansonone C (**4**)

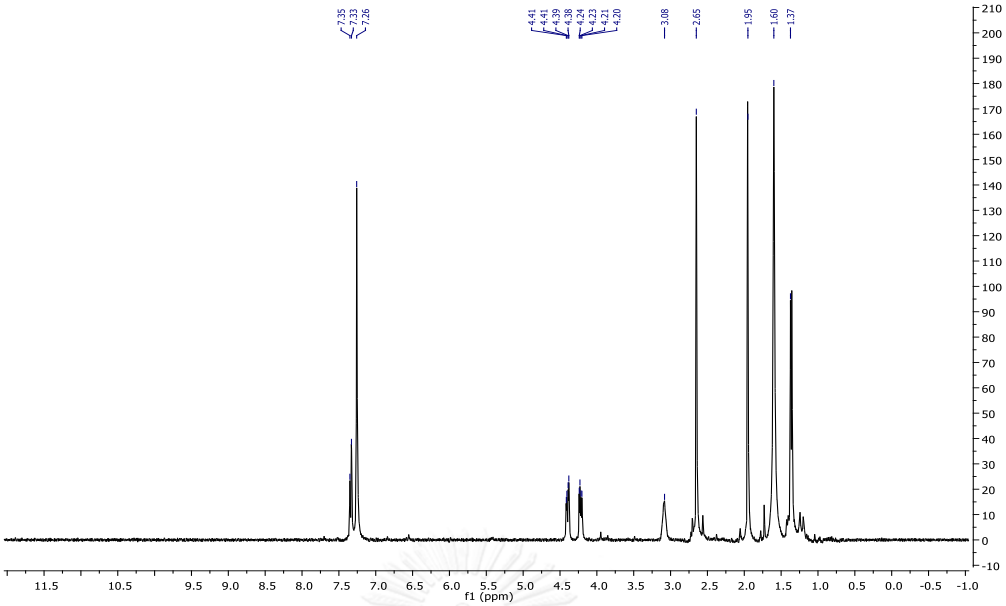

Appendix 5. The ^{1}H NMR spectrum ($CDCl_3$) of mansonone E (**5**)

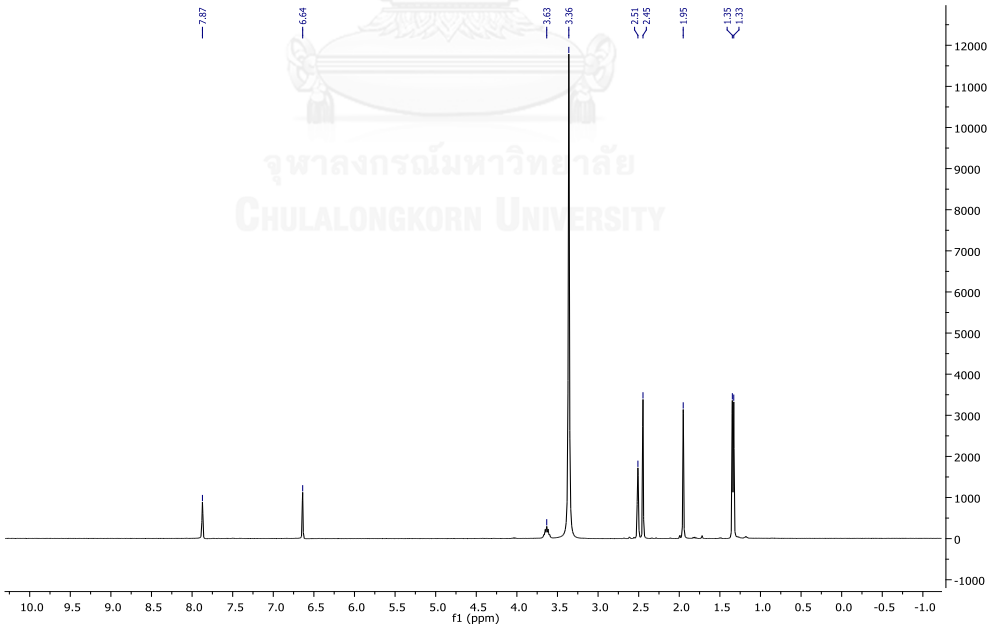

Appendix 6. The ^{1}H NMR spectrum (DMSO) of mansonone G (**6**)

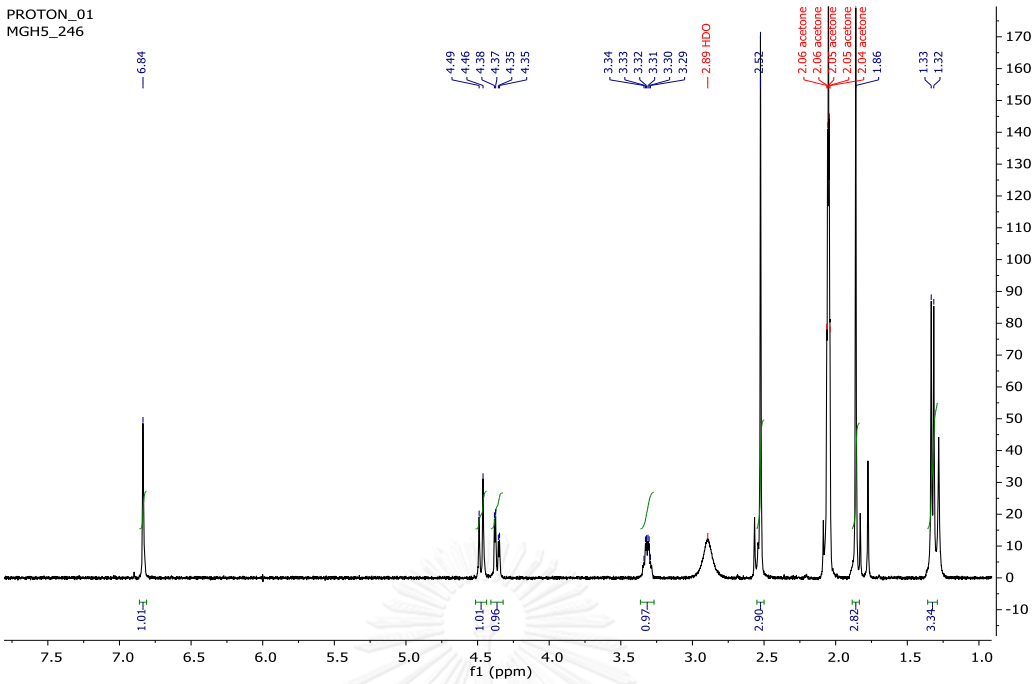

Appendix 7. The ^{1}H NMR spectrum (acetone d_6) of mansonone H (**7**)

Appendix 8. HRMS (ESI) of **G02**

Mass Spectrum List Report

Analysis Info

Analysis Name	OSCU581109001.d	Acquisition Date	11/9/2015 11:24:41 AM
Method	Tune_low_POS_Natee20130403.m	Operator	Administrator
Sample Name	G-02	Instrument	micrOTOF 72
	G-02		

Acquisition Parameter

Source Type	ESI	Ion Polarity	Positive	Set Corrector Fill	50 V
Scan Range	n/a	Capillary Exit	180.0 V	Set Pulsar Pull	337 V
Scan Begin	50 m/z	Hexapole RF	150.0 V	Set Pulsar Push	337 V
Scan End	3000 m/z	Skimmer 1	45.0 V	Set Reflector	1300 V
		Hexapole 1	24.3 V	Set Flight Tube	9000 V
				Set Detector TOF	2093 V

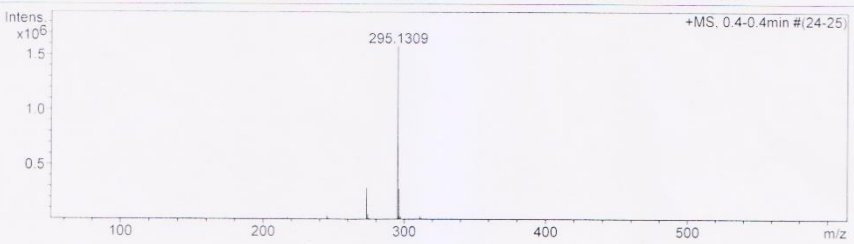

#	m/z	I	I %	S/N	FWHM	Res.
1	217.1232	11418	0.7	104.7	0.0454	4784
2	218.1173	2145	0.1	19.3	0.0539	4049
3	227.1099	2974	0.2	26.9	0.0531	4280
4	245.1240	28330	1.8	260.0	0.0680	3602
5	246.1280	4718	0.3	42.9	0.0696	3534
6	255.1379	2152	0.1	19.3	0.0566	4507
7	273.1485	287951	18.3	2642.1	0.0596	4582
8	274.1517	48574	3.1	445.2	0.0595	4606
9	275.1543	5765	0.4	52.4	0.0601	4574
10	294.9321	4394	0.3	39.7	0.1906	1547
11	295.1309	1576832	100.0	14448.3	0.0676	4366
12	295.5897	3451	0.2	31.1	0.2045	1446
13	295.7817	2449	0.2	21.9	0.2652	1115
14	295.9543	2117	0.1	18.9	0.1073	2759
15	296.1341	279600	17.7	2561.3	0.0625	4736
16	297.1359	28450	1.8	260.1	0.0612	4855
17	298.1384	2910	0.2	26.1	0.0589	5066
18	311.1035	29378	1.9	268.3	0.0643	4837
19	312.1072	5658	0.4	51.2	0.0624	5005
20	313.1153	3439	0.2	30.9	0.0898	3488
21	421.2330	2230	0.1	20.4	0.0925	4554
22	428.1895	5601	0.4	52.6	0.0850	5036
23	428.6918	3243	0.2	30.1	0.0830	5164
24	522.5939	2814	0.2	27.5	0.1001	5220
25	550.6259	2528	0.2	25.0	0.1116	4936
26	567.2714	7723	0.5	79.5	0.1207	4700
27	568.2717	2833	0.2	28.6	0.1236	4599
28	1884.8452	2348	0.1	35.7	0.0286	65836
29	2362.9837	2266	0.1	33.9	0.0317	74461
30	2363.3279	2332	0.1	34.9	0.0332	71267

Appendix 9. HRMS (ESI) of **G03**

Mass Spectrum List Report

Analysis Info

Analysis Name	OSCU581109002.d	Acquisition Date	11/9/2015 11:28:07 AM
Method	Tune_low_POS_Natee20130403.m	Operator	Administrator
Sample Name	G-03	Instrument	micrOTOF 72
	G-03		

Acquisition Parameter

Source Type	ESI	Ion Polarity	Positive	Set Corrector Fill	50 V
Scan Range	n/a	Capillary Exit	180.0 V	Set Pulsar Pull	337 V
Scan Begin	50 m/z	Hexapole RF	150.0 V	Set Pulsar Push	337 V
Scan End	3000 m/z	Skimmer 1	45.0 V	Set Reflector	1300 V
		Hexapole 1	24.3 V	Set Flight Tube	9000 V
				Set Detector TOF	2093 V

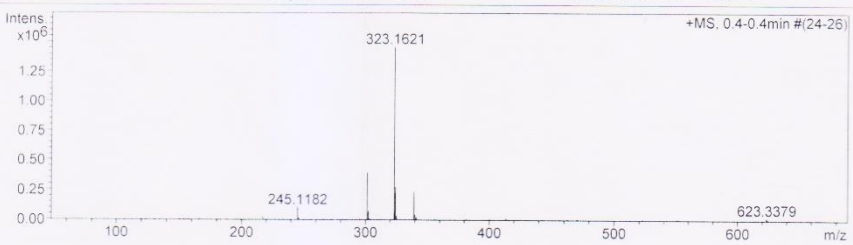

#	m/z	I	I %	S/N	FWHM	Res.
1	202.1013	3957	0.3	30.7	0.0465	4351
2	217.1238	25935	1.8	194.9	0.0477	4556
3	227.1089	5040	0.3	36.3	0.0538	4219
4	245.1182	102135	7.0	711.2	0.0530	4627
5	246.1211	16423	1.1	113.5	0.0518	4754
6	295.1382	7092	0.5	42.8	0.0930	3174
7	301.1796	398625	27.4	2414.2	0.0657	4583
8	302.1831	74688	5.1	450.6	0.0649	4655
9	303.1869	10563	0.7	62.9	0.0769	3943
10	322.9440	4044	0.3	22.4	0.2886	1119
11	323.1621	1454878	100.0	8383.4	0.0726	4450
12	324.1657	271273	18.6	1559.0	0.0695	4667
13	325.1668	32506	2.2	185.6	0.0705	4611
14	339.1356	236050	16.2	1312.9	0.0726	4670
15	340.1388	42462	2.9	234.9	0.0731	4650
16	341.1389	22531	1.5	123.9	0.0781	4368
17	342.1423	4060	0.3	21.5	0.0825	4146
18	372.3455	4796	0.3	25.3	0.0766	4858
19	381.2022	9216	0.6	50.0	0.0965	3949
20	400.3775	7012	0.5	38.5	0.0851	4703
21	413.2570	13631	0.9	76.8	0.0990	4173
22	429.2264	4242	0.3	23.5	0.1333	3220
23	441.2773	4068	0.3	22.7	0.1357	3253
24	470.2366	6732	0.5	39.6	0.1021	4604
25	470.7389	3974	0.3	22.8	0.0921	5114
26	522.5948	8697	0.6	54.7	0.1043	5010
27	550.6253	8397	0.6	54.5	0.1143	4819
28	623.3379	21645	1.5	165.0	0.1278	4877
29	624.3424	8571	0.6	64.6	0.1380	4524
30	641.3460	5351	0.4	41.3	0.1425	4500

Appendix 10. HRMS (ESI) of **G04**

Mass Spectrum List Report

Analysis Info

Analysis Name	OSCU581109003.d	Acquisition Date	11/9/2015 11:31:53 AM
Method	Tune_low_POS_Natee20130403.m	Operator	Administrator
Sample Name	G-04	Instrument	micrOTOF 72
	G-04		

Acquisition Parameter

Source Type	ESI	Ion Polarity	Positive	Set Corrector Fill	50 V
Scan Range	n/a	Capillary Exit	150.0 V	Set Pulsar Pull	337 V
Scan Begin	50 m/z	Hexapole RF	150.0 V	Set Pulsar Push	337 V
Scan End	3000 m/z	Skimmer 1	45.0 V	Set Reflector	1300 V
		Hexapole 1	24.3 V	Set Flight Tube	9000 V
				Set Detector TOF	2093 V

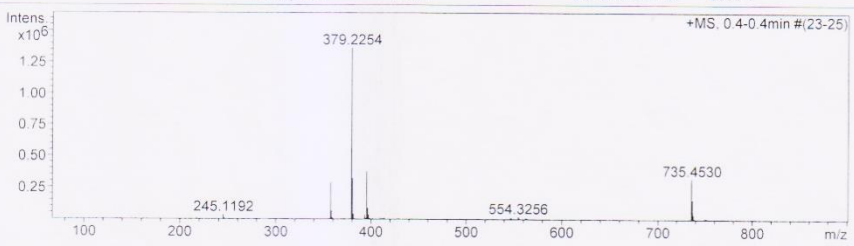

#	m/z	I	I %	S/N	FWHM	Res.
1	217.1240	6908	0.5	55.2	0.0466	4658
2	245.1192	33815	2.5	257.7	0.0519	4719
3	357.2431	290047	21.3	1824.8	0.0757	4718
4	358.2459	65969	4.8	414.7	0.0746	4803
5	359.2455	10582	0.8	65.9	0.0795	4520
6	371.2148	7411	0.5	46.3	0.0868	4278
7	377.2133	7075	0.5	44.3	0.1051	3590
8	379.2254	1364482	100.0	8710.6	0.0835	4542
9	380.2268	323011	23.7	2062.8	0.0777	4895
10	381.2291	41647	3.1	265.4	0.0744	5125
11	393.2029	35445	2.6	227.6	0.0814	4833
12	394.2061	8699	0.6	55.3	0.0818	4819
13	395.1991	378433	27.7	2440.7	0.0848	4662
14	396.2010	88162	6.5	568.3	0.0788	5027
15	397.1996	36798	2.7	236.9	0.0839	4733
16	398.2018	7188	0.5	45.6	0.0890	4476
17	409.1805	10766	0.8	69.3	0.0921	4442
18	411.2073	7585	0.6	48.6	0.0980	4198
19	413.2382	10276	0.8	66.2	0.1089	3794
20	546.3362	12029	0.9	85.0	0.1032	5296
21	546.8395	9806	0.7	69.1	0.1027	5326
22	554.3256	21421	1.6	153.2	0.1018	5447
23	554.8280	16142	1.2	115.1	0.1000	5547
24	555.3275	7264	0.5	51.1	0.1129	4918
25	562.3141	9485	0.7	67.2	0.1050	5357
26	735.4530	324176	23.8	2197.0	0.1554	4734
27	736.4566	156231	11.4	1057.5	0.1512	4871
28	737.4584	38453	2.8	258.8	0.1511	4879
29	738.4597	7464	0.5	48.7	0.1494	4944
30	749.4297	10088	0.7	66.3	0.1611	4651

Appendix 11. HRMS (ESI) of **G05**

Mass Spectrum List Report

Analysis Info

Analysis Name	OSCU581109004.d	Acquisition Date	11/9/2015 11:35:40 AM
Method	Tune_low_POS_Natee20130403.m	Operator	Administrator
Sample Name	G-05	Instrument	micrOTOF 72
	G-05		

Acquisition Parameter

Source Type	ESI	Ion Polarity	Positive	Set Corrector Fill	50 V
Scan Range	n/a	Capillary Exit	250.0 V	Set Pulsar Pull	337 V
Scan Begin	50 m/z	Hexapole RF	150.0 V	Set Pulsar Push	337 V
Scan End	3000 m/z	Skimmer 1	45.0 V	Set Reflector	1300 V
		Hexapole 1	24.3 V	Set Flight Tube	9000 V
				Set Detector TOF	2093 V

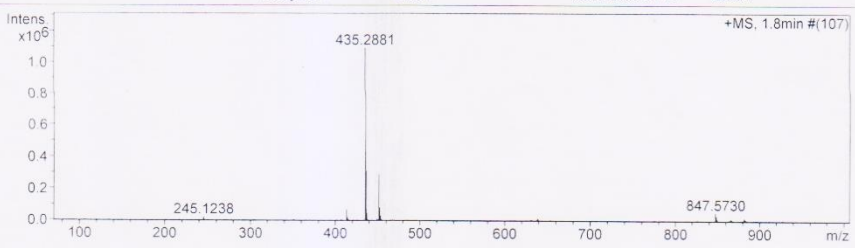

#	m/z	I	I %	S/N	FWHM	Res.
1	217.1283	5051	0.5	43.3	0.0613	3545
2	245.1238	19509	1.8	166.6	0.0663	3695
3	413.3069	65937	6.0	554.4	0.0908	4550
4	414.3104	18717	1.7	156.9	0.0932	4447
5	435.2881	1092111	100.0	9308.8	0.0983	4427
6	435.8448	3689	0.3	30.6	0.2838	1536
7	436.2911	315189	28.9	2687.5	0.0930	4689
8	437.2929	44139	4.0	375.8	0.0883	4952
9	438.2949	5116	0.5	42.8	0.0942	4652
10	449.2652	9350	0.9	79.5	0.1011	4443
11	451.2609	291017	26.6	2502.2	0.0968	4664
12	452.2633	80994	7.4	696.2	0.0925	4889
13	453.2617	29387	2.7	252.2	0.1016	4463
14	454.2631	6930	0.6	58.8	0.0888	5118
15	465.2424	3614	0.3	30.5	0.1085	4288
16	638.4160	12048	1.1	106.9	0.1254	5093
17	638.9197	10233	0.9	90.6	0.1241	5150
18	639.4179	5437	0.5	47.7	0.1321	4841
19	847.5730	51098	4.7	432.3	0.1755	4830
20	848.5756	30112	2.8	254.2	0.1736	4889
21	849.5796	9153	0.8	76.5	0.1756	4838
22	863.5494	5778	0.5	47.7	0.1718	5026
23	864.5508	3596	0.3	29.2	0.1664	5196
24	865.5790	14830	1.4	124.1	0.1811	4781
25	866.5854	8598	0.8	71.5	0.1815	4775
26	867.5762	3862	0.4	31.5	0.1975	4393
27	881.5576	17367	1.6	145.0	0.1923	4583
28	882.5562	10105	0.9	83.9	0.1866	4730
29	883.5568	4784	0.4	39.1	0.1962	4502
30	895.5433	3444	0.3	27.8	0.1964	4561

Appendix 12. HRMS (ESI) of **G06**

Mass Spectrum List Report

Analysis Info

Analysis Name	OSRH590324001.d	Acquisition Date	3/24/2016 1:15:37 PM
Method	Tune_wide_POS_Tawatchai_05Feb2016.m	Operator	Administrator
Sample Name	G-06	Instrument	micrOTOF 72
	G-06		

Acquisition Parameter

Source Type	ESI	Ion Polarity	Positive	Set Corrector Fill	50 V
Scan Range	n/a	Capillary Exit	180.0 V	Set Pulsar Pull	337 V
Scan Begin	50 m/z	Hexapole RF	400.0 V	Set Pulsar Push	337 V
Scan End	3000 m/z	Skimmer 1	70.0 V	Set Reflector	1300 V
		Hexapole 1	25.0 V	Set Flight Tube	9000 V
				Set Detector TOF	2295 V

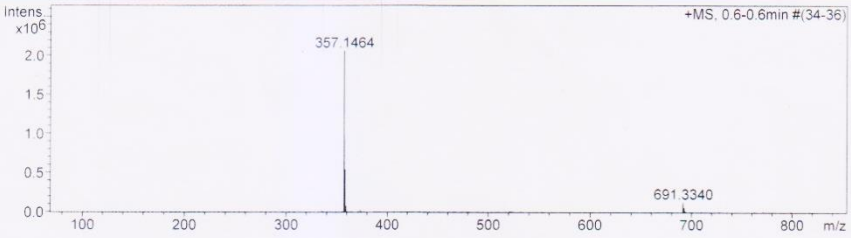

#	m/z	I	I %	S/N	FWHM	Res.
1	144.9775	4225	0.2	10.7	0.0085	17042
2	335.1610	15549	0.8	47.2	0.0627	5348
3	336.1640	4179	0.2	12.3	0.0646	5200
4	355.3191	5543	0.3	16.6	0.1649	2155
5	356.9071	14081	0.7	42.9	0.2095	1704
6	357.1464	2059834	100.0	6352.1	0.0787	4536
7	357.6480	11487	0.6	34.9	0.3802	941
8	357.8573	9658	0.5	29.3	0.3754	953
9	358.1479	540101	26.2	1665.2	0.0678	5280
10	358.4771	5046	0.2	15.1	0.2031	1765
11	359.1504	76704	3.7	236.1	0.0675	5320
12	360.1526	8753	0.4	26.5	0.0713	5054
13	371.1258	8672	0.4	26.2	0.0721	5146
14	373.1201	26301	1.3	80.6	0.0714	5225
15	374.1227	7100	0.3	21.4	0.0721	5186
16	521.2295	8378	0.4	25.2	0.0964	5409
17	521.7278	5691	0.3	16.9	0.0912	5719
18	691.3340	130604	6.3	427.0	0.1425	4852
19	692.3377	63061	3.1	205.9	0.1432	4835
20	693.3400	16285	0.8	52.7	0.1449	4786
21	1075.7154	4200	0.2	13.0	0.0229	46961
22	1443.0525	5625	0.3	16.5	0.0263	54815
23	1443.2741	4371	0.2	12.8	0.0364	39657
24	1920.6318	4294	0.2	12.4	0.0300	64128
25	2339.2694	4935	0.2	13.9	0.0325	71936
26	2531.2518	4242	0.2	12.4	0.0342	74114
27	2596.9527	4849	0.2	14.5	0.0334	77716
28	2799.0710	4195	0.2	12.6	0.0373	75012
29	2868.1574	3960	0.2	11.6	0.0363	79012
30	2938.0561	4042	0.2	11.8	0.0376	78214

Appendix 13. HRMS (ESI) of **G07**

Mass Spectrum List Report

Analysis Info

Analysis Name	OSCURH590508002.d	Acquisition Date	5/8/2016 3:08:33 PM
Method	Tune_low_POS_Natee20130403.m	Operator	Administrator
Sample Name	G-07	Instrument	micrOTOF 72
	G-07		

Acquisition Parameter

Source Type	ESI	Ion Polarity	Positive	Set Corrector Fill	50 V
Scan Range	n/a	Capillary Exit	180.0 V	Set Pulsar Pull	337 V
Scan Begin	50 m/z	Hexapole RF	150.0 V	Set Pulsar Push	337 V
Scan End	3000 m/z	Skimmer 1	45.0 V	Set Reflector	1300 V
		Hexapole 1	24.3 V	Set Flight Tube	9000 V
				Set Detector TOF	2295 V

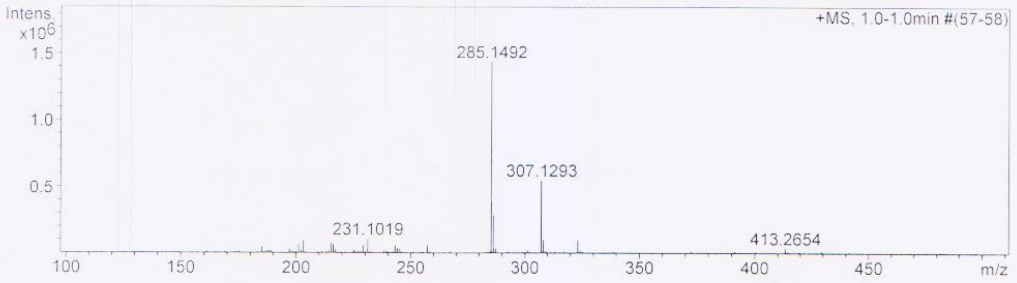

#	m/z	I	I %	S/N	FWHM	Res.
1	185.0940	49433	3.4	69.6	0.0497	3726
2	188.0858	21622	1.5	30.2	0.0642	2928
3	197.0943	32873	2.3	46.4	0.0530	3717
4	201.0909	70337	4.9	99.9	0.0560	3590
5	202.1064	20394	1.4	28.6	0.0806	2507
6	203.1047	95518	6.6	136.0	0.0543	3744
7	215.1061	79931	5.6	114.4	0.0568	3789
8	216.1124	66868	4.6	95.6	0.0557	3879
9	217.1164	29235	2.0	41.5	0.0594	3654
10	225.0933	21073	1.5	29.9	0.0658	3418
11	229.0896	58257	4.0	83.7	0.0672	3408
12	231.1019	108834	7.6	157.0	0.0579	3989
13	238.0398	21688	1.5	30.9	0.0595	4004
14	243.1036	61634	4.3	89.2	0.0640	3798
15	244.1092	37168	2.6	53.5	0.0616	3963
16	245.1171	34300	2.4	49.4	0.0615	3987
17	257.1558	67037	4.7	97.6	0.0645	3987
18	285.1492	1438555	100.0	2137.9	0.0665	4289
19	286.1522	286376	19.9	425.2	0.0624	4584
20	287.1533	36684	2.6	53.8	0.0649	4423
21	301.1404	26026	1.8	38.2	0.0653	4612
22	307.1293	549544	38.2	825.0	0.0651	4720
23	308.1322	103311	7.2	154.5	0.0654	4709
24	323.1032	104344	7.3	157.2	0.0663	4874
25	324.1054	21464	1.5	31.6	0.0644	5035
26	413.2654	39775	2.8	62.4	0.0854	4837
27	622.0312	88366	6.1	157.2	0.1238	5023
28	922.0119	88281	6.1	171.8	0.1817	5073
29	923.0125	19599	1.4	37.2	0.1789	5159
30	1521.9811	31736	2.2	63.4	0.3063	4970

Appendix 14. HRMS (ESI) of **G08**

Mass Spectrum List Report

Analysis Info

Analysis Name	OSRH590324002.d	Acquisition Date	3/24/2016 1:18:34 PM
Method	Tune_wide_POS_Tawatchai_05Feb2016.m	Operator	Administrator
Sample Name	G-08	Instrument	micrOTOF 72
	G-08		

Acquisition Parameter

Source Type	ESI	Ion Polarity	Positive	Set Corrector Fill	50 V
Scan Range	n/a	Capillary Exit	200.0 V	Set Pulsar Pull	337 V
Scan Begin	50 m/z	Hexapole RF	400.0 V	Set Pulsar Push	337 V
Scan End	3000 m/z	Skimmer 1	70.0 V	Set Reflector	1300 V
		Hexapole 1	25.0 V	Set Flight Tube	9000 V
				Set Detector TOF	2295 V

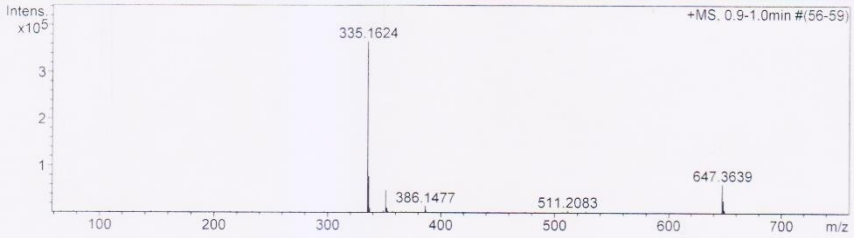

#	m/z	I	I %	S/N	FWHM	Res.
1	145.0541	4038	1.1	9.3	0.0097	14995
2	335.1624	365792	100.0	958.4	0.0670	5004
3	336.1652	78058	21.3	204.3	0.0673	4995
4	337.1679	11828	3.2	30.7	0.0671	5022
5	349.1446	5568	1.5	14.3	0.0757	4613
6	351.1411	48715	13.3	128.1	0.0717	4895
7	352.1440	11304	3.1	29.4	0.0754	4671
8	353.1403	4703	1.3	12.0	0.0802	4404
9	357.1424	4754	1.3	12.1	0.0857	4168
10	386.1477	16274	4.4	42.9	0.0707	5458
11	386.6484	8129	2.2	21.2	0.0842	4591
12	511.2083	6765	1.8	18.0	0.0961	5318
13	527.1886	4480	1.2	11.8	0.1110	4749
14	647.3639	63594	17.4	179.4	0.1343	4820
15	648.3682	27790	7.6	78.1	0.1367	4745
16	649.3714	7346	2.0	20.3	0.1312	4951
17	951.8412	4956	1.4	13.0	0.0209	45473
18	951.9801	3965	1.1	10.3	0.0224	42538
19	1207.1383	4496	1.2	11.8	0.0236	51211
20	1443.0416	5082	1.4	13.1	0.0262	55155
21	1443.2671	3914	1.1	10.1	0.0347	41576
22	1699.9605	3976	1.1	10.4	0.0280	60729
23	1864.2220	4385	1.2	11.4	0.0298	62656
24	1864.4760	4050	1.1	10.5	0.0338	55184
25	2339.2655	5535	1.5	14.5	0.0330	70974
26	2339.4641	3985	1.1	10.4	0.0607	38520
27	2531.2638	4675	1.3	12.4	0.0352	71846
28	2868.4884	4115	1.1	11.0	0.0453	63274
29	2938.0369	4737	1.3	12.6	0.0377	77958
30	2938.2840	3986	1.1	10.6	0.0409	71883

Appendix 15. HRMS (ESI) of **G09**

Mass Spectrum List Report

Analysis Info

Analysis Name	OSCURH590508001.d	Acquisition Date	5/8/2016 3:13:13 PM
Method	Tune_low_POS_Natee20130403.m	Operator	Administrator
Sample Name	G-09	Instrument	micrOTOF 72
	G-09		

Acquisition Parameter

Source Type	ESI	Ion Polarity	Positive	Set Corrector Fill	50 V
Scan Range	n/a	Capillary Exit	180.0 V	Set Pulsar Pull	337 V
Scan Begin	50 m/z	Hexapole RF	150.0 V	Set Pulsar Push	337 V
Scan End	3000 m/z	Skimmer 1	45.0 V	Set Reflector	1300 V
		Hexapole 1	24.3 V	Set Flight Tube	9000 V
				Set Detector TOF	2295 V

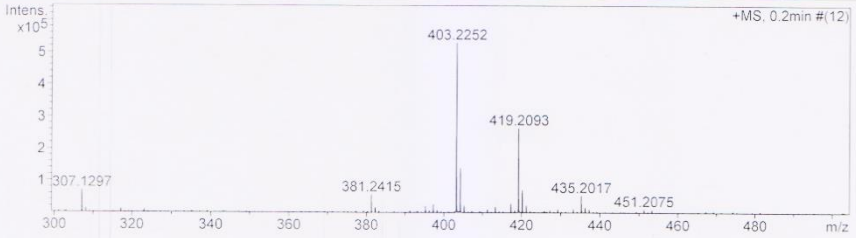

#	m/z	I	I %	S/N	FWHM	Res.
1	307.1297	68940	13.0	110.9	0.0649	4733
2	319.1669	2680	0.5	4.4	0.0988	3232
3	331.1777	1893	0.4	3.1	0.0704	4703
4	343.1863	1553	0.3	2.6	0.1123	3057
5	349.1925	2565	0.5	4.3	0.0773	4519
6	361.1753	1923	0.4	3.2	0.1447	2496
7	367.2229	1970	0.4	3.3	0.0825	4450
8	374.2142	1213	0.2	2.0	0.0269	13933
9	381.2415	56300	10.6	95.6	0.0757	5034
10	383.2439	4617	0.9	7.8	0.0892	4295
11	395.2217	20483	3.9	35.1	0.0786	5030
12	397.2371	25806	4.9	44.3	0.0797	4982
13	403.2252	529352	100.0	912.2	0.0814	4953
14	404.2278	138685	26.2	239.2	0.0819	4937
15	405.2303	22774	4.3	39.3	0.0860	4714
16	411.2155	9446	1.8	16.4	0.0878	4683
17	413.2375	18113	3.4	31.4	0.0966	4280
18	417.2040	28499	5.4	49.6	0.0851	4902
19	419.2093	263834	49.8	459.8	0.0899	4665
20	420.2114	70581	13.3	123.1	0.0877	4791
21	421.2102	23123	4.4	40.4	0.0999	4215
22	429.2279	10972	2.1	19.3	0.0870	4931
23	435.2017	53426	10.1	94.2	0.0917	4748
24	451.2075	10524	2.0	18.8	0.1096	4116
25	453.2204	8702	1.6	15.5	0.1053	4303
26	467.2231	4001	0.8	7.2	0.1777	2630
27	474.2633	2789	0.5	5.1	0.0678	6995
28	488.3013	1957	0.4	3.6	0.0374	13054

Appendix 16. HRMS (ESI) of **G10**

Mass Spectrum List Report

Analysis Info

Analysis Name	OSCURH590508003.d	Acquisition Date	5/8/2016 3:16:58 PM
Method	Tune_low_POS_Natee20130403.m	Operator	Administrator
Sample Name	G-10	Instrument	micrOTOF 72
	G-10		

Acquisition Parameter

Source Type	ESI	Ion Polarity	Positive	Set Corrector Fill	50 V
Scan Range	n/a	Capillary Exit	180.0 V	Set Pulsar Pull	337 V
Scan Begin	50 m/z	Hexapole RF	150.0 V	Set Pulsar Push	337 V
Scan End	3000 m/z	Skimmer 1	45.0 V	Set Reflector	1300 V
		Hexapole 1	24.3 V	Set Flight Tube	9000 V
				Set Detector TOF	2295 V

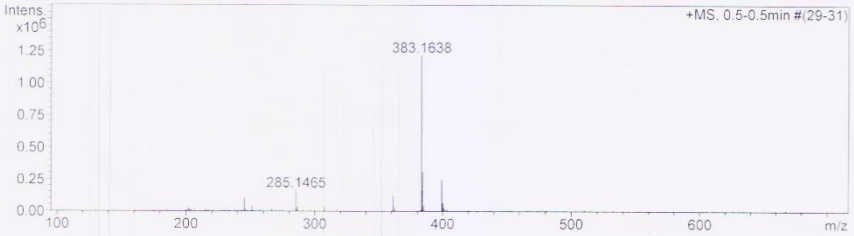

#	m/z	I	I %	S/N	FWHM	Res.
1	201.0998	12743	1.1	21.2	0.0569	3536
2	202.1313	26028	2.1	43.8	0.0499	4052
3	203.1119	11120	0.9	18.5	0.0668	3042
4	217.1213	12267	1.0	20.6	0.0574	3782
5	231.1035	13692	1.1	23.2	0.0565	4089
6	245.1167	103250	8.5	179.6	0.0529	4631
7	246.1205	18941	1.6	32.5	0.0503	4892
8	251.0670	42048	3.5	73.1	0.0552	4550
9	257.1662	13602	1.1	23.4	0.0609	4221
10	266.0897	15079	1.2	26.1	0.0584	4560
11	267.0990	9842	0.8	16.8	0.0668	4001
12	285.1465	159717	13.2	285.0	0.0586	4865
13	286.1497	32434	2.7	57.4	0.0582	4913
14	307.1297	33747	2.8	60.5	0.0646	4752
15	317.1688	10162	0.8	17.9	0.0677	4683
16	361.1801	123060	10.1	230.3	0.0720	5018
17	362.1831	33224	2.7	61.7	0.0725	4995
18	382.9081	8444	0.7	15.3	0.3023	1267
19	383.1638	1213392	100.0	2310.3	0.0796	4815
20	384.1657	305122	25.1	580.8	0.0761	5051
21	385.1686	45570	3.8	86.2	0.0779	4943
22	399.1378	245891	20.3	472.6	0.0810	4926
23	400.1404	64309	5.3	123.1	0.0784	5107
24	401.1412	27356	2.3	52.0	0.0813	4933
25	403.2263	13885	1.1	26.1	0.0818	4929
26	743.3425	340384	28.1	768.5	0.1482	5015
27	744.3458	176693	14.6	398.5	0.1497	4972
28	745.3491	50561	4.2	113.3	0.1485	5018
29	746.3513	10288	0.8	22.2	0.1587	4704
30	763.4035	11657	1.0	25.4	0.1503	5079

Appendix 17. HRMS (ESI) of **G11**

Mass Spectrum List Report

Analysis Info

Analysis Name	OSCURH590508004.d	Acquisition Date	5/8/2016 3:21:56 PM
Method	Tune_low_POS_Natee20130403.m	Operator	Administrator
Sample Name	G-11	Instrument	micrOTOF 72
	G-11		

Acquisition Parameter

Source Type	ESI	Ion Polarity	Positive	Set Corrector Fill	50 V
Scan Range	n/a	Capillary Exit	120.0 V	Set Pulsar Pull	337 V
Scan Begin	50 m/z	Hexapole RF	150.0 V	Set Pulsar Push	337 V
Scan End	3000 m/z	Skimmer 1	45.0 V	Set Reflector	1300 V
		Hexapole 1	24.3 V	Set Flight Tube	9000 V
				Set Detector TOF	2295 V

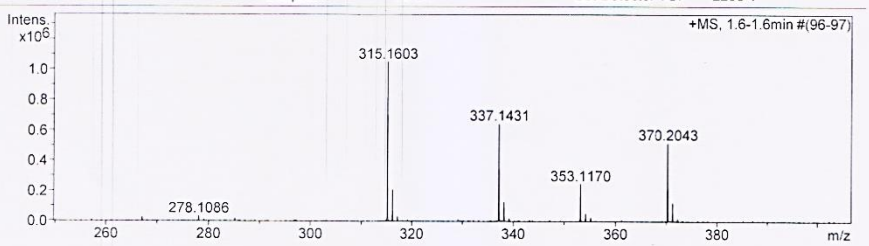

#	m/z	I	I %	S/N	FWHM	Res.
1	255.1596	2946	0.3	5.0	0.0566	4505
2	257.1725	5115	0.5	10.0	0.0523	4921
3	261.1134	4574	0.4	8.9	0.0570	4579
4	267.0983	24946	2.4	49.1	0.0536	4979
5	275.1223	2895	0.3	5.7	0.0563	4890
6	278.1086	32685	3.1	64.9	0.0552	5034
7	285.1476	17448	1.7	34.9	0.0584	4884
8	291.5576	1850	0.2	3.7	0.0132	22147
9	297.1982	3929	0.4	7.9	0.0622	4779
10	303.1553	4093	0.4	8.3	0.0853	3556
11	315.1603	1050683	100.0	2157.5	0.0661	4771
12	316.1633	208792	19.9	429.1	0.0644	4906
13	317.1665	35596	3.4	73.2	0.0641	4947
14	325.1574	1169	0.1	2.4	0.1101	2954
15	332.1831	4773	0.5	10.0	0.0665	4998
16	337.1431	643668	61.3	1348.8	0.0693	4866
17	338.1460	126004	12.0	264.3	0.0684	4943
18	339.1505	19207	1.8	40.3	0.0733	4627
19	347.1659	3725	0.4	7.9	0.0925	3752
20	353.1170	246112	23.4	519.9	0.0714	4949
21	361.1774	6219	0.6	13.2	0.0895	4035
22	363.1848	2717	0.3	5.8	0.0933	3891
23	370.2043	516553	49.2	1097.9	0.0749	4943
24	371.2063	123879	11.8	263.4	0.0746	4974
25	377.1997	2502	0.2	5.3	0.1206	3127
26	387.0729	5658	0.5	12.1	0.1083	3573
27	389.0636	4628	0.4	9.9	0.0878	4431
28	395.1921	1141	0.1	2.4	0.0702	5627
29	399.7438	1500	0.1	3.2	0.0162	24679

Appendix 18. HRMS (ESI) of **G12**

Mass Spectrum List Report

Analysis Info

Analysis Name	OSCURH590508005.d	Acquisition Date	5/8/2016 3:28:39 PM
Method	Tune_wide_POS_Natee20130403.m	Operator	Administrator
Sample Name	G-12	Instrument	micrOTOF 72
	G-12		

Acquisition Parameter

Source Type	ESI	Ion Polarity	Positive	Set Corrector Fill	50 V
Scan Range	n/a	Capillary Exit	150.0 V	Set Pulsar Pull	337 V
Scan Begin	50 m/z	Hexapole RF	400.0 V	Set Pulsar Push	337 V
Scan End	3000 m/z	Skimmer 1	70.0 V	Set Reflector	1300 V
		Hexapole 1	25.0 V	Set Flight Tube	9000 V
				Set Detector TOF	2295 V

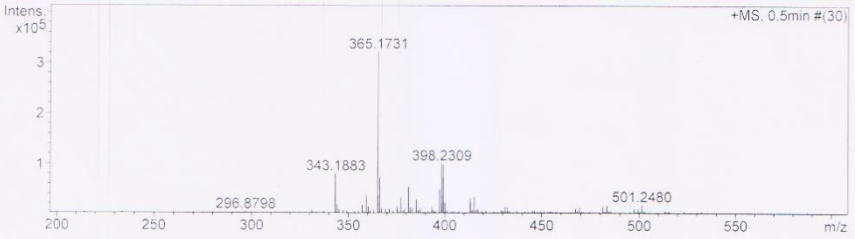

#	m/z	I	I %	S/N	FWHM	Res.
1	343.1883	80713	25.1	148.5	0.0667	5148
2	344.1917	19080	5.9	34.6	0.0646	5327
3	357.1702	19044	5.9	34.6	0.0766	4661
4	359.1847	38821	12.1	71.5	0.0714	5030
5	365.1731	321623	100.0	598.9	0.0690	5292
6	366.1755	73537	22.9	136.4	0.0679	5394
7	377.1968	33768	10.5	62.5	0.0714	5284
8	381.1510	54357	16.9	101.2	0.0735	5185
9	385.1655	29700	9.2	55.0	0.0772	4990
10	397.1661	49088	15.3	91.9	0.0798	4976
11	398.2309	100411	31.2	188.8	0.0771	5166
12	399.1877	98774	30.7	185.8	0.0994	4016
13	400.1873	23091	7.2	42.8	0.0949	4218
14	413.2066	31838	9.9	59.7	0.1517	2723
15	415.1689	35254	11.0	66.2	0.0886	4687
16	481.2632	17355	5.4	33.0	0.0936	5142
17	483.2700	17842	5.5	33.9	0.1000	4832
18	501.2480	18997	5.9	36.4	0.1039	4822
19	685.4017	49926	15.5	89.5	0.1339	5119
20	686.4063	23081	7.2	40.7	0.1368	5019
21	707.3885	83978	26.1	149.4	0.1419	4986
22	708.3915	39620	12.3	69.8	0.1411	5021
23	725.4016	23917	7.4	41.2	0.1604	4522
24	739.4008	22648	7.0	38.9	0.1606	4603
25	740.4289	17734	5.5	30.3	0.1647	4496
26	741.4044	21570	6.7	37.1	0.1660	4466
27	755.4112	17098	5.3	29.7	0.2063	3662
28	758.4565	19874	6.2	34.8	0.1788	4243
29	772.4703	26952	8.4	48.5	0.1743	4431
30	773.4506	17938	5.6	31.9	0.2061	3752

Appendix 19. HRMS (ESI) of **G13**

Mass Spectrum List Report

Analysis Info

Analysis Name	OSRH590324003.d	Acquisition Date	3/24/2016 1:21:51 PM
Method	Tune_wide_POS_Tawatchai_05Feb2016.m	Operator	Administrator
Sample Name	G-13	Instrument	micrOTOF 72
	G-13		

Acquisition Parameter

Source Type	ESI	Ion Polarity	Positive	Set Corrector Fill	50 V
Scan Range	n/a	Capillary Exit	200.0 V	Set Pulsar Pull	337 V
Scan Begin	50 m/z	Hexapole RF	400.0 V	Set Pulsar Push	337 V
Scan End	3000 m/z	Skimmer 1	70.0 V	Set Reflector	1300 V
		Hexapole 1	25.0 V	Set Flight Tube	9000 V
				Set Detector TOF	2295 V

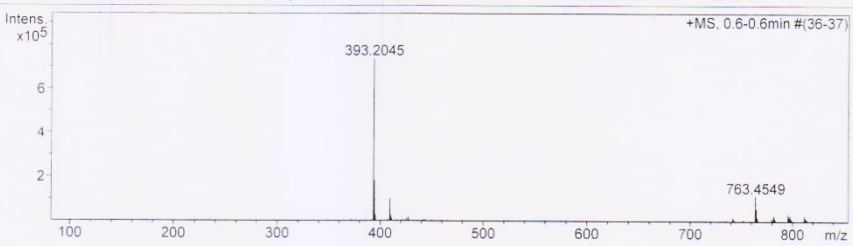

#	m/z	I	I %	S/N	FWHM	Res.
1	371.2186	9451	1.3	25.9	0.0763	4862
2	392.9529	6168	0.8	16.7	0.1229	3198
3	393.2045	737064	100.0	2074.4	0.0765	5141
4	394.2068	184041	25.0	517.5	0.0728	5413
5	395.2096	28792	3.9	80.4	0.0754	5241
6	407.1892	10306	1.4	28.4	0.0962	4234
7	409.1793	102955	14.0	289.8	0.0787	5201
8	410.1818	26660	3.6	74.5	0.0796	5155
9	411.1845	11821	1.6	32.6	0.0917	4485
10	425.2045	13150	1.8	36.4	0.1003	4239
11	427.2095	19033	2.6	53.1	0.0839	5093
12	441.2219	9652	1.3	26.6	0.1256	3512
13	443.1973	7312	1.0	20.0	0.1014	4369
14	741.4674	19295	2.6	50.8	0.1587	4672
15	742.4694	10279	1.4	26.6	0.1511	4914
16	751.4304	6303	0.9	16.0	0.1512	4970
17	763.4549	115391	15.7	316.2	0.1664	4587
18	764.4577	58436	7.9	159.7	0.1664	4595
19	765.4589	16863	2.3	45.3	0.1789	4279
20	779.4350	15698	2.1	42.7	0.1803	4324
21	780.4404	8722	1.2	23.2	0.1808	4317
22	781.4634	26846	3.6	74.0	0.1701	4594
23	782.4659	13900	1.9	37.8	0.1637	4779
24	795.4760	36723	5.0	103.0	0.1780	4469
25	796.4815	19736	2.7	54.9	0.1763	4517
26	797.4537	28020	3.8	78.5	0.1826	4367
27	798.4507	13437	1.8	37.1	0.1789	4463
28	811.4561	28438	3.9	80.8	0.1880	4315
29	812.4595	14627	2.0	41.1	0.1934	4200
30	813.4566	11428	1.6	31.9	0.1948	4176

Bruker Daltonics DataAnalysis 3.3 printed: 3/24/2016 3:44:16 PM Page 1 of 1

Appendix 20. HRMS (ESI) of **G14**

Mass Spectrum List Report

Analysis Info

Analysis Name	OSCURH590508006.d	Acquisition Date	5/8/2016 3:32:33 PM
Method	Tune_wide_POS_Tawatchai_05Feb2016.m	Operator	Administrator
Sample Name	G-14	Instrument	micrOTOF 72
	G-14		

Acquisition Parameter

Source Type	ESI	Ion Polarity	Positive	Set Corrector Fill	50 V
Scan Range	n/a	Capillary Exit	180.0 V	Set Pulsar Pull	337 V
Scan Begin	50 m/z	Hexapole RF	400.0 V	Set Pulsar Push	337 V
Scan End	3000 m/z	Skimmer 1	70.0 V	Set Reflector	1300 V
		Hexapole 1	25.0 V	Set Flight Tube	9000 V
				Set Detector TOF	2295 V

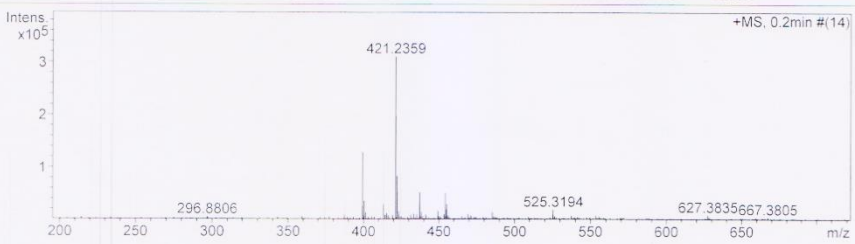

#	m/z	I	I %	S/N	FWHM	Res.
1	387.2479	9770	3.1	17.4	0.0811	4776
2	399.2521	129079	41.5	237.8	0.0759	5260
3	400.2554	36482	11.7	66.8	0.0770	5195
4	401.2439	14335	4.6	25.9	0.0890	4509
5	413.2429	30157	9.7	55.1	0.0979	4223
6	414.2456	9331	3.0	16.6	0.0926	4475
7	415.2478	12833	4.1	23.1	0.1019	4077
8	419.2395	9445	3.0	16.8	0.0871	4813
9	421.2359	310877	100.0	574.8	0.0809	5205
10	422.2388	83309	26.8	153.6	0.0801	5268
11	423.2399	16358	5.3	29.6	0.0812	5211
12	431.2453	9716	3.1	17.3	0.0987	4367
13	433.2567	11692	3.8	21.0	0.0901	4807
14	435.2232	11076	3.6	19.8	0.1004	4334
15	437.2114	52469	16.9	96.6	0.0870	5027
16	438.2160	14987	4.8	27.1	0.0858	5106
17	441.2309	10220	3.3	18.2	0.1073	4113
18	449.2565	17057	5.5	30.9	0.1038	4328
19	453.2363	10781	3.5	19.3	0.1151	3939
20	454.2938	51357	16.5	94.6	0.0905	5021
21	455.2660	30090	9.7	55.1	0.1271	3581
22	469.2635	11565	3.7	20.7	0.1376	3410
23	485.3250	15086	4.9	27.3	0.1021	4755
24	525.3194	19057	6.1	34.8	0.1069	4916
25	627.3835	9116	2.9	16.9	0.1246	5035
26	797.5412	14872	4.8	30.1	0.1804	4421
27	798.5383	8852	2.8	17.6	0.1857	4300
28	819.5252	54052	17.4	111.8	0.1813	4519
29	820.5271	30306	9.7	62.4	0.1765	4650
30	821.5347	8985	2.9	18.0	0.1990	4127

Appendix 21. HRMS (ESI) of **G15**

Mass Spectrum List Report

Analysis Info

Analysis Name	OSRH590324004.d	Acquisition Date	3/24/2016 1:24:51 PM
Method	Tune_wide_POS_Tawatchai_05Feb2016.m	Operator	Administrator
Sample Name	G-15	Instrument	micrOTOF 72
	G-15		

Acquisition Parameter

Source Type	ESI	Ion Polarity	Positive	Set Corrector Fill	50 V
Scan Range	n/a	Capillary Exit	200.0 V	Set Pulsar Pull	337 V
Scan Begin	50 m/z	Hexapole RF	400.0 V	Set Pulsar Push	337 V
Scan End	3000 m/z	Skimmer 1	70.0 V	Set Reflector	1300 V
		Hexapole 1	25.0 V	Set Flight Tube	9000 V
				Set Detector TOF	2295 V

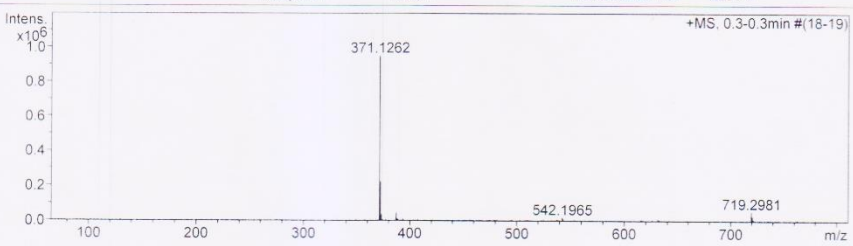

#	m/z	I	I %	S/N	FWHM	Res.
1	357.1460	6626	0.7	16.0	0.0768	4649
2	370.8786	5627	0.6	13.5	0.3074	1207
3	371.1262	948212	100.0	2353.9	0.0729	5094
4	371.6322	5106	0.5	12.2	0.2253	1650
5	372.1287	221887	23.4	550.5	0.0718	5183
6	373.1315	35167	3.7	86.8	0.0722	5165
7	387.1007	45802	4.8	113.5	0.0747	5185
8	388.1027	11687	1.2	28.6	0.0745	5212
9	389.1056	5786	0.6	13.9	0.0872	4463
10	393.2056	8228	0.9	19.9	0.0702	5598
11	421.2195	5102	0.5	12.1	0.1159	3636
12	435.2273	4889	0.5	11.6	0.1064	4090
13	451.2306	4754	0.5	11.3	0.1042	4329
14	456.0650	7784	0.8	18.9	0.0871	5237
15	465.2439	4622	0.5	10.9	0.1254	3709
16	479.2353	4464	0.5	10.5	0.1337	3583
17	495.2519	4614	0.5	10.9	0.1454	3406
18	537.1955	7984	0.8	19.5	0.1077	4989
19	542.1965	17548	1.9	43.9	0.0924	5865
20	542.6991	11967	1.3	29.7	0.0945	5743
21	543.1991	5350	0.6	12.8	0.0984	5519
22	553.1758	5011	0.5	12.0	0.1807	3061
23	615.2452	7055	0.7	17.9	0.1196	5146
24	631.2223	9792	1.0	25.5	0.1227	5144
25	719.2981	52626	5.6	148.0	0.1488	4835
26	720.2999	26022	2.7	72.9	0.1460	4935
27	721.3011	7408	0.8	20.3	0.1463	4930
28	1443.0456	4578	0.5	11.1	0.0269	53591
29	2339.2548	5287	0.6	12.5	0.0342	68313
30	2596.9709	4734	0.5	11.8	0.0349	74455

Appendix 22. HRMS (ESI) of **G16**

Mass Spectrum List Report

Analysis Info

Analysis Name	OSRH590324005.d	Acquisition Date	3/24/2016 1:27:50 PM
Method	Tune_wide_POS_Tawatchai_05Feb2016.m	Operator	Administrator
Sample Name	G-16	Instrument	micrOTOF 72
	G-16		

Acquisition Parameter

Source Type	ESI	Ion Polarity	Positive	Set Corrector Fill	50 V
Scan Range	n/a	Capillary Exit	200.0 V	Set Pulsar Pull	337 V
Scan Begin	50 m/z	Hexapole RF	400.0 V	Set Pulsar Push	337 V
Scan End	3000 m/z	Skimmer 1	70.0 V	Set Reflector	1300 V
		Hexapole 1	25.0 V	Set Flight Tube	9000 V
				Set Detector TOF	2295 V

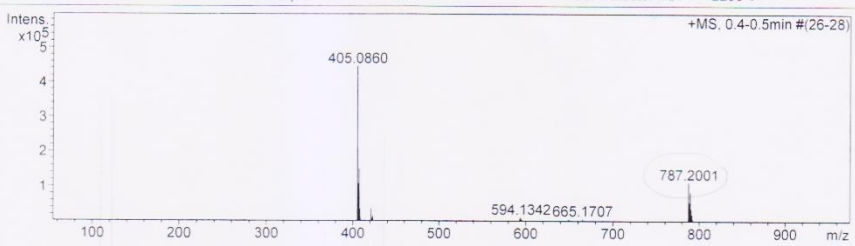

#	m/z	I	I %	S/N	FWHM	Res.
1	393.2053	4791	1.1	11.6	0.1032	3809
2	405.0860	446312	100.0	1126.7	0.0759	5337
3	406.0885	109450	24.5	276.0	0.0728	5580
4	407.0835	150693	33.8	380.3	0.0773	5265
5	408.0862	36134	8.1	90.8	0.0737	5535
6	409.0906	6304	1.4	15.4	0.0760	5384
7	413.2598	5395	1.2	13.1	0.0731	5657
8	421.0590	38228	8.6	96.4	0.0732	5749
9	422.0639	9959	2.2	24.7	0.0729	5791
10	423.0591	16479	3.7	41.3	0.0803	5270
11	495.2591	4810	1.1	11.7	0.1246	3976
12	593.1337	9564	2.1	24.7	0.1053	5635
13	593.6337	6788	1.5	17.2	0.1098	5407
14	594.1342	12290	2.8	32.0	0.0995	5970
15	594.6339	6624	1.5	16.8	0.1084	5485
16	595.1358	6036	1.4	15.2	0.1132	5255
17	649.1901	6865	1.5	17.8	0.1252	5187
18	665.1707	8012	1.8	21.1	0.1306	5093
19	787.2001	113145	25.4	326.0	0.1435	5487
20	788.2017	55260	12.4	158.8	0.1400	5631
21	789.1976	84504	18.9	243.4	0.1439	5484
22	790.1991	37053	8.3	106.3	0.1456	5427
23	791.1988	21657	4.9	61.7	0.1426	5549
24	792.1973	7717	1.7	21.4	0.1435	5521
25	1443.0480	5596	1.3	14.7	0.0269	53716
26	1443.2633	4784	1.1	12.5	0.0335	43119
27	2036.0393	4885	1.1	12.2	0.0298	68371
28	2339.2625	5383	1.2	13.4	0.0338	69199
29	2531.2534	5001	1.1	12.8	0.0344	73504
30	2596.9726	4810	1.1	12.2	0.0360	72147

Appendix 23. HRMS (ESI) of **G17**

Mass Spectrum List Report

Analysis Info

Analysis Name	OSRH590324006.d	Acquisition Date	3/24/2016 1:31:07 PM
Method	Tune_wide_POS_Tawatchai_05Feb2016.m	Operator	Administrator
Sample Name	G-17	Instrument	micrOTOF 72
	G-17		

Acquisition Parameter

Source Type	ESI	Ion Polarity	Positive	Set Corrector Fill	50 V
Scan Range	n/a	Capillary Exit	200.0 V	Set Pulsar Pull	337 V
Scan Begin	50 m/z	Hexapole RF	400.0 V	Set Pulsar Push	337 V
Scan End	3000 m/z	Skimmer 1	70.0 V	Set Reflector	1300 V
		Hexapole 1	25.0 V	Set Flight Tube	9000 V
				Set Detector TOF	2295 V

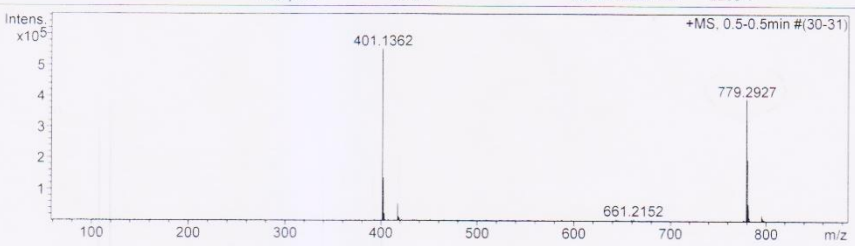

#	m/z	I	I %	S/N	FWHM	Res.
1	145.0582	4615	0.8	9.6	0.0091	15862
2	401.1362	551694	100.0	1382.4	0.0773	5191
3	402.1382	136253	24.7	341.1	0.0735	5473
4	403.1407	23191	4.2	57.7	0.0740	5445
5	417.1099	54875	9.9	137.1	0.0789	5286
6	418.1145	13971	2.5	34.6	0.0805	5192
7	419.1150	8530	1.5	20.9	0.0728	5754
8	495.2609	4518	0.8	10.8	0.1248	3967
9	643.2374	6338	1.1	15.1	0.1294	4973
10	645.2379	4580	0.8	10.7	0.1256	5138
11	659.2181	4904	0.9	11.5	0.1120	5888
12	661.2152	7751	1.4	18.7	0.1174	5632
13	679.2233	5446	1.0	12.8	0.1208	5624
14	776.2837	5845	1.1	14.2	0.1511	5139
15	776.7816	5023	0.9	12.1	0.1394	5573
16	779.2927	391254	70.9	1016.7	0.1434	5434
17	780.2962	198095	35.9	514.6	0.1422	5486
18	781.2978	56037	10.2	145.0	0.1415	5522
19	782.2997	11922	2.2	30.1	0.1423	5497
20	795.2671	19698	3.6	50.8	0.1429	5564
21	796.2706	9830	1.8	24.9	0.1498	5317
22	797.2743	5880	1.1	14.5	0.1551	5141
23	1023.3997	6148	1.1	16.4	0.1857	5510
24	1039.3836	9024	1.6	24.2	0.1931	5381
25	1040.3828	6168	1.1	16.3	0.1840	5653
26	1443.0419	5334	1.0	14.4	0.0269	53693
27	1443.2683	4551	0.8	12.2	0.0357	40418
28	1864.1966	4471	0.8	10.7	0.0293	63586
29	2036.0338	4409	0.8	10.4	0.0298	68309
30	2339.2561	5674	1.0	13.4	0.0339	69023

Appendix 24. HRMS (ESI) of **G18**

Mass Spectrum List Report

Analysis Info

Analysis Name	OSCURH590508007.d	Acquisition Date	5/8/2016 3:35:55 PM
Method	Tune_wide_POS_Tawatchai_05Feb2016.m	Operator	Administrator
Sample Name	G-18	Instrument	micrOTOF 72
	G-18		

Acquisition Parameter

Source Type	ESI	Ion Polarity	Positive	Set Corrector Fill	50 V
Scan Range	n/a	Capillary Exit	180.0 V	Set Pulsar Pull	337 V
Scan Begin	50 m/z	Hexapole RF	400.0 V	Set Pulsar Push	337 V
Scan End	3000 m/z	Skimmer 1	70.0 V	Set Reflector	1300 V
		Hexapole 1	25.0 V	Set Flight Tube	9000 V
				Set Detector TOF	2295 V

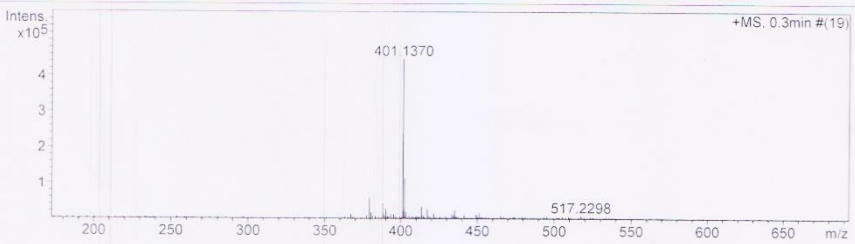

#	m/z	I	I %	S/N	FWHM	Res.
1	367.1562	13761	3.1	23.0	0.0784	4685
2	379.1545	60297	13.5	103.5	0.0742	5111
3	380.1566	17494	3.9	29.6	0.0772	4924
4	381.1598	8893	2.0	14.7	0.0982	3882
5	388.0419	43952	9.8	75.6	0.0751	5170
6	389.0488	10547	2.4	17.6	0.0788	4940
7	390.0403	28434	6.4	48.7	0.0764	5102
8	393.1652	12408	2.8	20.9	0.1291	3046
9	395.1569	12826	2.9	21.7	0.0977	4044
10	401.1370	447513	100.0	781.3	0.0777	5164
11	402.1396	113863	25.4	198.4	0.0749	5372
12	403.1448	19770	4.4	33.9	0.0860	4690
13	413.2661	34189	7.6	59.4	0.0833	4963
14	414.2697	9267	2.1	15.6	0.0837	4949
15	417.1163	26847	6.0	46.6	0.0900	4637
16	421.2266	15955	3.6	27.4	0.0981	4294
17	433.1375	13534	3.0	23.3	0.1000	4332
18	434.1828	11393	2.5	19.5	0.1112	3906
19	435.1526	24349	5.4	42.6	0.1235	3524
20	441.2943	8759	2.0	14.8	0.0982	4493
21	449.1573	9750	2.2	16.7	0.1365	3289
22	449.3555	10883	2.4	18.7	0.1056	4257
23	451.1432	16545	3.7	28.9	0.1135	3974
24	465.2419	9507	2.1	16.4	0.1357	3429
25	757.3369	19905	4.4	39.8	0.1664	4551
26	758.3420	10105	2.3	19.8	0.1653	4587
27	779.3230	51160	11.4	104.0	0.1763	4421
28	780.3284	26744	6.0	53.9	0.1749	4463
29	812.3757	9260	2.1	18.2	0.2093	3881
30	844.4194	12815	2.9	25.5	0.1855	4552

Appendix 25. HRMS (ESI) of **G19**

Mass Spectrum List Report

Analysis Info

Analysis Name	OSRH590324007.d	Acquisition Date	3/24/2016 1:33:51 PM
Method	Tune_wide_POS_Tawatchai_05Feb2016.m	Operator	Administrator
Sample Name	G-19	Instrument	micrOTOF 72
	G-19		

Acquisition Parameter

Source Type	ESI	Ion Polarity	Positive	Set Corrector Fill	50 V
Scan Range	n/a	Capillary Exit	200.0 V	Set Pulsar Pull	337 V
Scan Begin	50 m/z	Hexapole RF	400.0 V	Set Pulsar Push	337 V
Scan End	3000 m/z	Skimmer 1	70.0 V	Set Reflector	1300 V
		Hexapole 1	25.0 V	Set Flight Tube	9000 V
				Set Detector TOF	2295 V

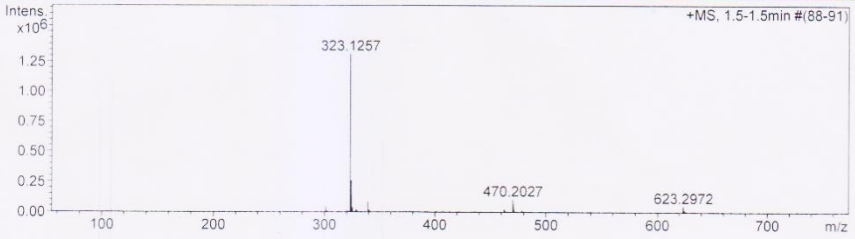

#	m/z	I	I %	S/N	FWHM	Res.
1	301.1424	45552	3.5	103.8	0.0600	5018
2	302.1460	9795	0.7	22.0	0.0591	5115
3	320.1171	14313	1.1	32.4	0.0647	4947
4	321.1316	6935	0.5	15.5	0.0675	4757
5	322.9107	7733	0.6	17.3	0.2301	1403
6	323.1257	1314398	100.0	3021.2	0.0681	4747
7	324.1283	259770	19.8	596.8	0.0637	5088
8	325.1312	37084	2.8	84.8	0.0651	4998
9	328.1043	17917	1.4	40.7	0.0652	5033
10	328.6073	7951	0.6	17.8	0.0694	4738
11	329.1193	18664	1.4	42.5	0.0637	5165
12	329.6213	7156	0.5	16.0	0.0680	4850
13	339.0997	84998	6.5	195.6	0.0656	5168
14	340.1036	17466	1.3	39.8	0.0683	4981
15	341.1040	10374	0.8	23.4	0.0734	4650
16	377.1966	7251	0.6	16.4	0.1020	3699
17	393.1970	6715	0.5	15.3	0.1059	3712
18	401.1413	6288	0.5	14.3	0.0926	4332
19	407.2183	7428	0.6	17.1	0.1023	3980
20	421.2321	7681	0.6	17.8	0.1047	4024
21	462.2124	24222	1.8	58.6	0.0811	5697
22	462.7150	17257	1.3	41.6	0.0822	5628
23	463.2182	11267	0.9	26.9	0.0903	5132
24	470.2027	106541	8.1	261.3	0.0830	5666
25	470.7040	62107	4.7	152.1	0.0859	5477
26	471.2067	23141	1.8	56.2	0.0891	5291
27	478.1920	11733	0.9	28.3	0.0902	5299
28	478.6904	7177	0.5	17.0	0.0830	5769
29	623.2972	50891	3.9	133.2	0.1376	4531
30	624.3009	19834	1.5	51.6	0.1495	4177

Appendix 26. HRMS (ESI) of **G20**

Mass Spectrum List Report

Analysis Info

Analysis Name	OSCURH590508008.d	Acquisition Date	5/8/2016 3:41:01 PM
Method	Tune_low_POS_Natee20130403.m	Operator	Administrator
Sample Name	G-20	Instrument	micrOTOF 72
	G-20		

Acquisition Parameter

Source Type	ESI	Ion Polarity	Positive	Set Corrector Fill	50 V
Scan Range	n/a	Capillary Exit	120.0 V	Set Pulsar Pull	337 V
Scan Begin	50 m/z	Hexapole RF	150.0 V	Set Pulsar Push	337 V
Scan End	3000 m/z	Skimmer 1	45.0 V	Set Reflector	1300 V
		Hexapole 1	24.3 V	Set Flight Tube	9000 V
				Set Detector TOF	2295 V

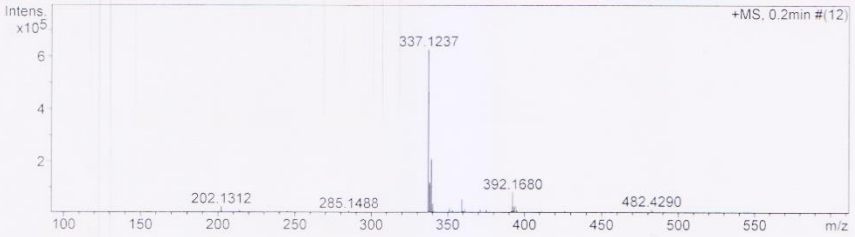

#	m/z	I	I %	S/N	FWHM	Res.
1	202.1312	28531	4.6	44.3	0.0428	4728
2	337.1237	626428	100.0	1040.3	0.0705	4780
3	338.1271	121109	19.3	200.7	0.0688	4917
4	339.1213	209741	33.5	348.2	0.0696	4876
5	340.1241	40316	6.4	66.4	0.0686	4956
6	351.1034	22170	3.5	36.5	0.0761	4613
7	359.1063	55284	8.8	92.5	0.0706	5089
8	361.1056	19195	3.1	31.7	0.0743	4860
9	371.1292	15848	2.5	26.2	0.0750	4950
10	375.0848	15716	2.5	26.1	0.0900	4167
11	392.1680	82540	13.2	141.5	0.0825	4751
12	393.1589	26569	4.2	45.1	0.1067	3683
13	394.1636	31016	5.0	52.8	0.0844	4672
14	482.4290	17845	2.8	32.0	0.0999	4827
15	673.2283	16339	2.6	26.8	0.1459	4613
16	690.2721	17239	2.8	28.0	0.1368	5046
17	692.2708	14968	2.4	24.1	0.1465	4726
18	695.2280	176410	28.2	297.6	0.1399	4970
19	696.2328	71063	11.3	119.0	0.1377	5058
20	697.2272	125780	20.1	211.5	0.1386	5032
21	698.2282	46183	7.4	76.7	0.1411	4949
22	699.2260	29738	4.7	48.9	0.1426	4902
23	711.2059	21998	3.5	35.5	0.1441	4935
24	713.2181	18310	2.9	29.2	0.1485	4802
25	728.2880	73831	11.8	120.8	0.1456	5002
26	729.2819	39850	6.4	64.5	0.1580	4615
27	730.2846	58423	9.3	95.2	0.1480	4935
28	731.2786	27627	4.4	44.2	0.1601	4567
29	732.2810	16019	2.6	25.1	0.1548	4732
30	1051.3570	15033	2.4	27.9	0.2037	5161

VITA

Miss Rita Hairani was born on February 13th, 1984 in Samarinda, Indonesia. She received a Bachelor degree with very satisfactory grade from Chemistry departement at Mulawarman University in 2006. She pursued her master degree at Graduate school of Forestry with very satisfactory grade in 2013. She awarded by Indonesian government scholarship, throughout her master degree course at Mulawarman University. She is a master candidate studying Organic Chemistry at Chulalongkorn Unversity. During the study time, She was awarded by ASEAN Scholarship from Chulalongkorn University and at the end of her study in 2015 she was awarded by “Beasiswa Kaltim cemerlang” scholarship from local government in Indonesia. In April to June 2016, Miss Rita Hairani has opportunity to have research experience at Ewha Womans University in South Korea and was funding by Overseas Research Experience Scholarship from Graduate School Chulalongkorn University.